Quantum Thermodynamic Machines: The Role of Interaction and Information

A thesis

submitted by

George Thomas

in partial fulfillment of

the requirements for the degree of

Doctor of Philosophy

Indian Institute of Science Education and Research (IISER)

Mohali

August, 2014

Declaration

The work presented in this thesis has been carried out by me under the guidance of Dr. Ramandeep S. Johal at the Indian Institute of Science Education and Research Mohali. This work has not been submitted in part or in full for a degree, diploma or a fellowship to any other University or Institute. Whenever contributions of others are involved, every effort has been made to indicate this clearly, with due acknowledgement of collaborative research and discussions. This thesis is a bonafide record of original work done by me and all sources listed within have been detailed in the bibliography.

George Thomas

Place :

Date :

In my capacity as the supervisor of the candidate's PhD thesis work, I certify that the above statements by the candidate are true to the best of my knowledge.

Dr. Ramandeep S. Johal

Associate Professor

Department of Physical Sciences

IISER Mohali

Place :

Date :

Acknowledgements

I would like to thank my supervisor Dr. Ramandeep S. Johal for his unwavering and creative guidance. His academic excellence and outstanding personality were the beacons during this journey.

My sincere gratitude to visionary Director, Prof. N. Sathyamurthy for inspiration. I am thankful to Prof. Sudeshna Sinha, Head of the Department of Physical Sciences, for support and encouragement. I am grateful to my internal monitoring committee members, Dr. Sanjeev Kumar and Dr. K. P. Singh for insightful suggestions and motivation. I thank my group members; Preety for collaboration and Venu Mehta and Harsh Katyayan for encouragement and discussions in the group meetings.

I am grateful to IISER Mohali for providing advanced infrastructure and excellent research environment. I also thank IISER Mohali for financial support and hostel facility. I would like to acknowledge the Computer Center of IISER Mohali and Dr. Paramdeep S. Chandi for much needed support and providing software such as Mathematica for research purposes. My gratitude to the Library facility of IISER Mohali and Dr. P. Visakhi, Deputy Librarian, for providing subscription to various journals, which plays an essential role in research.

I deeply appreciate the help and concern from my friends, Amrita Kumari, Debmalya Das, Ritabrata Sengupta and Harpreet Singh during these years. I also thank my friends, Neha Jain, Shalini Gupta, C. Jebarathinam, Kanika Pasrija, Swagatam Nayak, Mohit Tanga, Jithin Paul and Amol Ratnaparkhe for various memorable moments. Special thanks to Shruti Dogra for constant support, care and useful discussions. I am indebted to my friends, Joshil K. Abraham and Pavithran S. Iyer for their friendship and helping nature.

I also thank the Deans, faculty members, non-teaching staff, research scholars and BS-MS students of IISER Mohali for making the campus an excellent place to pursue research. My deepest gratitude to my parents and family members for their love and kindness.

George Thomas

List of publications

1. **G. Thomas** and R. S. Johal, *Coupled quantum Otto cycle*, Phys. Rev. E **83**, 031135 (2011).

2. **G. Thomas** and R. S. Johal, *Expected behavior of quantum thermodynamic machines with prior information*, Phys. Rev. E **85**, 041146 (2012).

3. **G. Thomas**, P. Aneja and R. S. Johal, *Informative priors and analogy between quantum and classical heat engines*, Phys. Scr. **T151**, 014031 (2012).

4. **G. Thomas** and R. S. Johal, *Friction due to inhomogeneous driving of coupled spins in a quantum heat engine*, Eur. Phys. J. B, (2014) **87**: 166.

5. **G. Thomas**, P. Aneja and R. S. Johal, *Incomplete Information and Expected Performance Characteristics of Heat Engines*, Research and Reviews : Journal of Statistics, special issue on recent statistical methodologies and applications (in press).

6. **G. Thomas** and R. S. Johal, *Estimating performance of Feynman's ratchet from limited information*, arXiv:1410.2140 [cond-mat.stat-mech] (submitted for publication).

Contents

List of Figures

Chapter 1

Introduction

One of the greatest contributions of the twentieth-century science is quantum theory which has revolutionized our understanding about the universe. On the other hand, thermodynamics is one of the pillars of classical science, whose application include wide ranging systems such as black holes [22] and biological systems [54]. Moreover the notion of thermodynamic consistency has played an important role in the progress of science such as the discovery of Planck's law for black-body radiation.

Extension of thermodynamics to quantum regime [47, 1, 74, 58, 111] has attracted a wide attention in recent years. This emerging field is popularly known as quantum thermodynamics. An important motivation to study quantum thermodynamics is the tremendous advancement in the technology at nano-scale. Also the frontier fields of ultra-cold atoms and quantum information are closely related to quantum thermodynamics [102, 89, 29, 74].

1.1 Quantum thermodynamic machines

As the classical models of heat engines played a central role in the development of the field of classical thermodynamics, quantum heat engines are novel tools to probe the underlying thermodynamic properties of quantum systems. It is interesting to understand some of the pioneering steps taken in this direction. In 1959, a paper by H. E. D. Scovil and E. O. Schulz-DuBois discussed a three-level MASER as a quantum heat engine [106]. Here, the working substance is a three-level atom. Two reservoirs (or baths) are connected selectively to the energy levels of the working

substance as shown in Fig. 1.1. As heat flows from hot bath to cold bath through

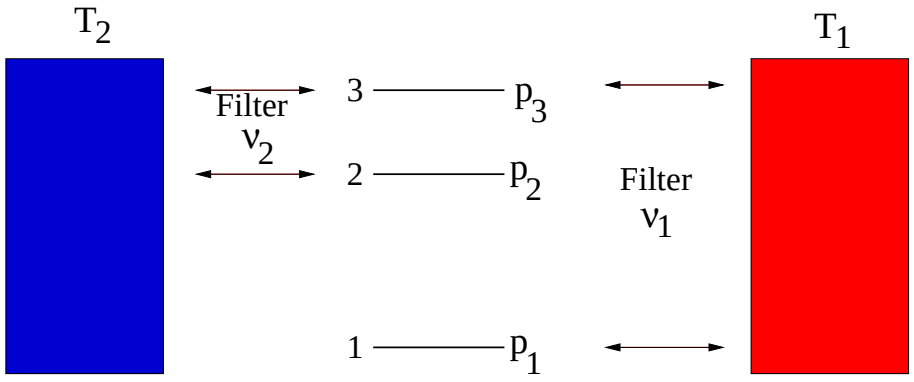

Figure 1.1: MASER as a heat engine: A three-level system is attached to two thermal reservoirs using filters. Here ν_1 and ν_2 are the pump frequency and the idler frequency respectively [106].

the three level system, an amount of work is delivered by the system in the form of photons. For the maser action to prevail, we need $p_2/p_1 \geq 1$, where p_i is the corresponding population for the ith energy level. Further, the condition for the maser action can be written as $\eta \leq \eta_c$, where $\eta = 1 - \nu_2/\nu_1$ and $\eta_c = 1 - T_2/T_1$ are the efficiency of the system and Carnot value, respectively. Hence the model is consistent with the second law of thermodynamics.

When a quantum system is attached with a bath, the total system, i.e. the system and the bath together undergo a unitary process. However the dynamics of the quantum system alone is in general, not unitary. The theory of open quantum systems was developed in the mid-1970s [84, 50]. The quantum evolution of a system in contact with a bath, is given by a master equation and the most general form of this master equation is known as Lindblad equation:

$$\frac{d\rho}{dt} = \frac{-i}{\hbar}[H,\rho] + \sum_{i,j=1}^{N^2-1} a_{ij}\left(F_i\rho F_j^\dagger - \frac{1}{2}(\rho F_j^\dagger F_i + F_j^\dagger F_i\rho)\right). \tag{1.1}$$

Here H is the Hamiltonian and $\{F_i\}$ constitute an orthonormal basis of operators on the system's Hilbert space. This evolution is trace-preserving and completely positive [84]. Further this dynamics helps us to understand the mechanism behind the thermalization of a quantum system when it is attached with a bath. Later, in 1979, an open quantum system attached to different thermal reservoirs was studied as a model of quantum heat engine [7]. Here, the external conditions associated

with the open quantum system are changed in such a way that the system operates as a heat engine. Moreover, the Carnot value as the upper bound for the efficiency is also verified.

The earlier development of thermodynamics was based on classical systems. On the other hand, quantum systems show non-classical features such as superposition of states, entanglement etc. So one of the motivations to study quantum thermodynamics is to understand the scope of thermodynamics to incorporate non-classical features of quantum systems. Even though the second law of thermodynamics is a statistical law, all the successful theories are consistent with it. Besides the idea of Maxwell's demon [80], there were many attempts to understand the implication of second law of thermodynamics [108, 107, 38]. So we discuss some of the important attempts which used non-classical features to overcome the limitations set by the second law of thermodynamics. Further we see the solution by which the consistency of second law of thermodynamics is established in these models.

Scully and his co-workers used quantum coherence to demonstrate an engine which can extract work from a single heat bath [108]. Their model is a quantum photo-Carnot engine where radiation pressure pushes the piston to extract work. Three-level atoms prepared in an initial temperature T_h flow through the engine and keep the driving radiation at $T_{rad} = T_h$. If a small bit of coherence is introduced in the ground doublet, then the field temperature can rise above T_h and the efficiency can surpass Carnot efficiency. This phenomenon can be used to extract work from a single bath. But this apparent contradiction of the second law is resolved if we consider the amount of work needed to prepare the coherence. A similar attempt to outperform the efficiency of classical heat engine with a quantum model is discussed in [38]. In this model, two spin-1/2 particles coupled through XY-Heisenberg interaction is considered and a beam of such correlated pairs constitute a quantum reservoir for a photo-Carnot engine. As these particles pass through the cavity, work is produced by putting the cavity in contact with another reservoir. Depending upon sending one atom or both the atoms of a correlated pair, the effective temperature of the cavity changes. Using this fact, the quantum heat engine can outperform its classical counterpart by attaining efficiency above Carnot efficiency. But preparation of these correlated pairs needs work and hence the apparent

contradiction with the second law, is resolved.

Another study [107] examines the possibility of extracting work from a single bath using quantum negentropy [105]. In this model, the atomic center of mass degrees of freedom act as an internal reservoir which is used as the source of negentropy. Initially, two-level atoms with center of mass wave packet (pulse) with length l_0 runs through the set-up to extract work. Even though the work is derived from a single heat bath, after each cycle the length of the pulse increases. Hence to prepare the center of mass wave-packet to its initial length, work has to be done on the system. One of the important differences between a Maxwell's demon operated Szilard engine (discussed in next subsection) and the above mentioned QHE is that no measurement is involved in this model. The three examples discussed above unveil the profound physics underlying the second law of thermodynamics. Moreover these remarkable designs of heat engines can contribute to future technologies.

Since we are in the domain of quantum systems, it is interesting to understand the implication of the size of quantum thermodynamic machines. A question addressed in Ref. [86] is: how small a thermal machine can be? The size of the system is determined by the dimensions of its Hilbert space. In this work, a model of self contained refrigerator is introduced. It does not need a work source, rather the equivalent energy comes from a thermal bath. Whenever the system (qubit) to be cooled, exceeds a certain temperature, heat is drawn from this bath and the refrigerator cools the system. In this particular set up, three qubits are considered. Here the first qubit is the qubit to be cooled. The second and the third qubits are considered as part of the refrigerator which cools the first qubit. Let E_1, E_2 and E_3 are the energy level spacings of the first, the second and the third qubits respectively. These energy level spacings are chosen in such a way that $E_3 = E_2 - E_1$. Cooling is achieved by a suitable choice of interaction Hamiltonian. The authors argue that the smallest possible self-contained refrigerator to cool a qubit is a three level system. The possibility of realizing a similar model based on four quantum dots is discussed in [122].

Another interesting approach in understanding the thermodynamic behavior of quantum systems is through Brownian motion. A specific example is discussed in Ref. [3], where a quantum Brownian oscillator is considered to model quantum

version of Carnot, Otto and Stirling cycles. Using Wigner phase-space description, the master equation governing the Brownian oscillator [2] attached to a bath with temperature T is transformed into a Fokker-Planck type equation. This description helps to identify heat and work terms explicitly.

1.2 Thermodynamics and information

There is a much debated and subtle relation between the concept of information and thermodynamics, which is still an active area of research [80]. The first striking relation comes in the form of entropy. The thermodynamic entropy and the information-theoretic entropy derived by Shannon have a similar form. But the concrete notion to emphasize the deep relation between thermodynamic and information came from Landauer's erasure principle [76].

The story begins with Maxwell [80] who considered a hypothetical intelligent being, guarding the trap door fixed in the middle of a container. The container is filled with gas molecules at certain temperature T. The demon separates the faster molecules to one side and the slower molecules to the other side by selectively allowing the molecules to pass through the trap door. Hence, a thermal gradient is created and work can be extracted. After the extraction of the work, the system is brought back to the initial state by attaching it with the bath at temperature T.

Later, Szilard came up with an interesting model of engine based on Maxwell's demon [89, 80], that attracted the interest of many workers. The concept of Szilard engine is simple and elegant as shown in Fig. 1.2. A chamber with volume V contains a single particle gas and this system is attached to a bath at temperature T . A demon inserts a partition in the middle of the box and measures the position of the particle to know whether it is in the left side (L) or in the right side (R) of the box. Depending upon the information about the particle, the demon attaches a weight to the partition. The gas is then allowed to expand isothermally by pushing the partition and thereby lifting the weight. The volume of the gas changes from $V/2$ to V and the system comes back to the initial state by doing an amount of work equal to $kT \ln 2$, where k is the Boltzmann constant. So the system needs only a single bath to work like an engine and the entropy of the universe after work extraction

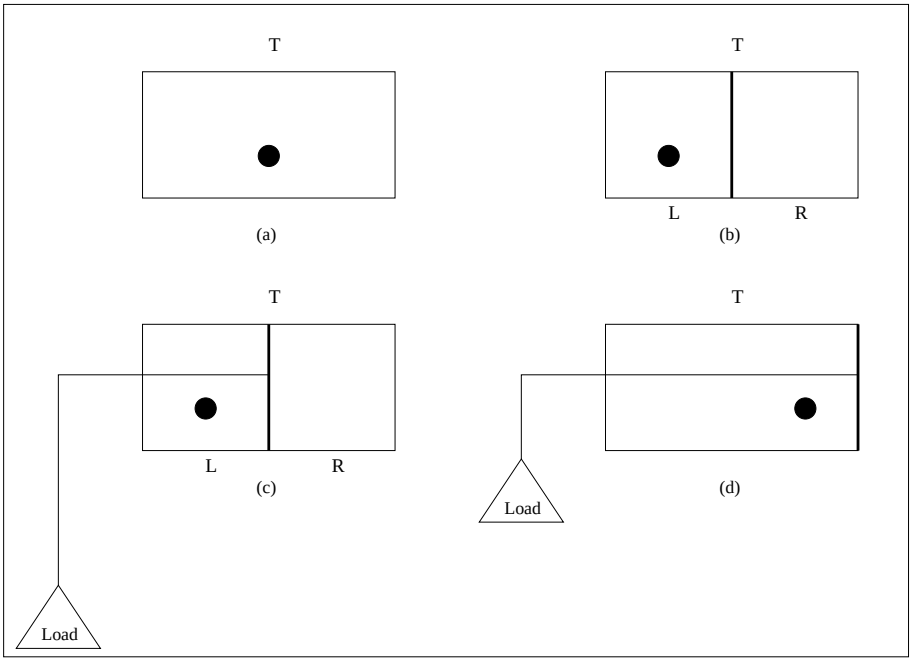

Figure 1.2: Szilard Engine

reduces by an amount $k \ln 2$. So there is an apparent violation of the second law of thermodynamics. Even though many attempts were made by researchers [80], an acceptable solution was proposed by Landauer [76]. He suggested that in order to complete the cycle, the memory of demon must come to its initial state. This has to be done by erasing one bit of information encoded by the demon to locate the position of the particle (L or R). Further it is shown that by erasing this information, the entropy of the universe is increased by an amount $k \ln 2$ and hence the apparent contradiction with the second law is resolved.

1.2.1 Thermodynamics, information and inference

Bayesian inference methods are widely used in physics [98, 39]. Recent applications of Bayesian approach in various fields include network modularity [57], quantum theory [34, 35, 82] and quantum thermodynamics [69, 115]. In Bayesian approach to probability, prior probability distribution or simply called prior plays a crucial role. Prior is assigned based on the prior information before acquiring the experimental data [64]. In the light of new data (D), the prior $P(x)$ is updated to posterior

$P(D|x)$ using Bayes theorem, given as

$$P(x|D)dx = \frac{P(D|x)P(x)dx}{P(D)}, \tag{1.2}$$

where $P(D|x)$ is the probability of D when x is given and $P(D) = \int P(D|x)P(x)dx$ is the normalization constant. Choice of an appropriate prior by quantifying the prior information is a subtle issue [64]. The prior is chosen based on certain arguments such as maximum entropy principle [65, 66] or requirement of invariance [64]. The assignment of prior is not based on any frequencies. It is therefore 'subjective' in the sense that it represents the state knowledge of the observer [64, 67].

Subjective probability is assigned based on the degree of rational belief. Here probability quantifies the state of knowledge of the observer [67] or in other words assesses the information one has about a certain event. At this point, the following question is relevant: What can we learn about a system from a given state of knowledge? So we discuss some of the studies carried out in this direction. In Ref. [69], a model of quantum Otto engine is considered. In this model, the working medium is a two-level system. The energy-level spacing of the spin is unknown. From the given information, a suitable prior distribution is constructed for this uncertain parameter. Further this prior is used to find the expected values of the work and efficiency of the engine. Surprisingly, in a certain limit, the efficiency at maximum work turned out to be the Curzon-Ahlborn (CA) efficiency [36] which is given as

$$\eta_{CA} = 1 - \sqrt{\frac{T_c}{T_h}}, \tag{1.3}$$

where T_h and T_c are the temperatures of hot and cold reservoirs respectively. This efficiency seems to have universal character, because many finite-time models of heat engines at their optimal performance have the efficiency near to this value. When there is no uncertain parameter, the efficiency at maximum work for a quantum Otto engine is above CA value. But for the classical counterpart, the efficiency at maximum work is CA value. So, a suitable choice of prior for given information leads to interesting conclusions such as classical thermodynamic behavior in quantum systems [69, 115].

1.2.2 Thermodynamics and entanglement

From earlier discussions, we have noted the resemblance of information-theoretic entropy and thermodynamic entropy. Now we explore the relation between thermodynamics and entanglement which is purely a quantum feature. For bipartite pure states, the most important measure of entanglement is the entropic measure. Suppose state of the total system ρ_{AB} resides in the Hilbert space $\mathcal{H}_A \otimes \mathcal{H}_B$. Then the measure of entanglement is the von Neumann entropy of the reduced system which is defined as

$$S(\rho_{AB}) = -\mathrm{Tr}(\rho_A \ln \rho_A) = -\mathrm{Tr}(\rho_B \ln \rho_B). \tag{1.4}$$

A detailed description of this entropy is given in Subsection 1.4.2. For separable states, the measure is zero, for maximally entangled states the measure is $\ln N$, where N is the dimension of the reduced state. For all other states, the measure lies in the range $0 \leq S(\rho_{AB}) \leq \ln N$. Also it can be shown that using local operations, i.e. any operation on one of the parties, would not increase entanglement between them [90]. In 1997, Popescu and Rohrlich [93] showed that in a transformation of m non-maximally entangled pure states to n maximally entangled states, the efficiency is maximum for a reversible transformation and n is proportional to m ($m \to \infty$) and the proportionality constant is the entropy of the initial reduced density matrix [23].

Even though we have complete knowledge of the state of the system, i.e. entropy is zero for the pure states, there is lack of knowledge about the subsystem which means that subsystems can be in mixed states (for entangled states). But in classical physics, if we have complete knowledge of the total system that implies the complete knowledge about the subsystems too. Thermal state of the system can be interpreted from this approach [49, 94, 85]. Consider universe (system with a large environment) is in a pure state. Then the explicit derivation in [94] shows that thermalization of the system occurs because of the entanglement of the system with the environment.

We have seen the measure of entanglement for pure states. In quantum thermodynamics, in general, we deal with mixed states. One of the basic measures of entanglement for mixed state is entanglement of formation which quantifies the resources to build up the entangled state [24]. As we have in Eq. (1.4), for pure states

ρ_{AB}, the entanglement is calculated from the entropy of the either of the reduced density matrices. Therefore, in the case of mixed states, entanglement is defined as the average entanglement calculated from its constituent pure states minimized over all decompositions of ρ [124]. In one of the remarkable work [124], Wootter showed how to construct the entanglement minimizing decomposition. For doing it, the first step is to find a spin flipped state.

$$\tilde{\rho} = (\sigma_y \otimes \sigma_y)\rho(\sigma_y \otimes \sigma_y). \tag{1.5}$$

Then find the product of density matrix and its time reversed state, $R = \rho\tilde{\rho}$. Now a quantity called concurrence is defined as

$$C = \max\{0, \lambda_1 - \lambda_2 - \lambda_3 - \lambda_4\}, \tag{1.6}$$

where λ_i is the square root of the ith eigenvalue of the matrix R in decreasing order of magnitude.

The concurrence and the entanglement of formation are having one to one correspondence and hence concurrence can also be used as a useful measure of mixed state entanglement. Interestingly, M. C. Arnesen et al. [17] used this technique to calculate thermal entanglement of ID Heisenberg chain consisting of two spin-1/2 particles attached to a heat bath with temperature T. The Hamiltonian of the system is given as

$$H = J(\vec{\sigma}^{(1)}.\vec{\sigma}^{(2)} + \vec{\sigma}^{(2)}.\vec{\sigma}^{(1)}) + B(\vec{\sigma}_z^{(1)} + \vec{\sigma}_z^{(2)}), \tag{1.7}$$

where $\vec{\sigma}^{(i)} = \{\sigma_x^{(i)}, \sigma_y^{(i)}, \sigma_z^{(i)} | i = 1, 2\}$ are the Pauli matrices, $J = J_x = J_y = J_z$ is the exchange constant and B is the magnetic field along z-axis. Cases $J > 0$ and $J < 0$ correspond to antiferromagnetic and ferromagnetic interactions, respectively. The spins are placed in a magnetic field B. The concurrence calculated for the equilibrium density matrix is given as

$$C = \max\left\{0, \frac{e^{8J/kT} - 3}{1 + e^{8J/kT} + e^{2B/kT} + e^{-2B/kT}}\right\}. \tag{1.8}$$

This work has a special significance when the working medium of an engine consists of spin systems and shows thermal entanglement. One such model is introduced in [127], in which a four-staged quantum Otto engine is considered. The adiabatic process is done by changing the exchange constant. The work and efficiency are

calculated and explored their dependence with concurrence. With this motivation, we have done further studies on this model. We constructed a more experimentally feasible cycle where adiabatic process is done by changing the magnetic field associated with the spins. Further we analyzed the mechanism by which frictional effect arises in the system. Our findings discussed in Chapter 2 and 3 throw more light on the thermodynamics of such quantum systems.

1.3 Quantum thermodynamic processes

In classical thermodynamics, there are four basic thermodynamic processes [33, 43]. They are: Isothermal process, adiabatic process, isochoric process and isobaric process. The corresponding thermodynamic variables kept constant during these processes are temperature, entropy, volume and pressure respectively. With these basic processes, all the main heat cycles such as Carnot cycle, Otto cycle, Stirling cycle and Brayton cycle are constructed. All the processes are considered quasi-static in nature, which means that the process proceeds slow enough that it is an ordered succession of equilibrium states whereas the real process is not quasi-static, rather it is a temporal succession of both equilibrium and non-equilibrium states [33].

The quantum generalization of thermodynamic processes is used in quantum heat cycles [96, 95]. In the following subsections, we briefly review the quantum analogues of the basic thermodynamic processes.

1.3.1 Quantum isothermal process

Consider a particle in a potential well or a spin placed under a magnetic field. The work can be done by/on the system by changing the width of the potential well or changing the magnetic field. Suppose the system is attached to a bath at temperature T while doing the work. In quantum isothermal process [96], the temperature of the system should remain constant during the process as in the classical case. This is possible only if the occupation probability of the energy level changes as the energy level varies. Suppose, in an isothermal process, the energy eigenvalues changes from $\{E_n\}$ to $\{E'_n\}$, where n runs from 1 to N and N is the

dimension of the Hilbert space of the system. Then the corresponding populations change from and $\{P_n\}$ to $\{P'_n\}$ such that

$$\frac{P'_r}{P'_s} = e^{(E'_s - E'_r)/kT}. \tag{1.9}$$

In order to keep the temperature constant throughout the process, the system should be driven quasi-statically.

1.3.2 Quantum adiabatic process

Quantum adiabatic process proceeds slowly enough so that the quantum adiabatic theorem holds. Suppose the system is initially in the nth eigenstate of the initial Hamiltonian and the Hamiltonian is changed gradually. According to quantum adiabatic theorem [28, 71], the system will remain in the nth eigenstate of the instantaneous Hamiltonian during the process. In another words, if the initial system is in a thermal state, then the population in the eigenstates of the Hamiltonian remain unchanged, $dP_n = 0, \forall n$. A detailed description of quantum adiabatic theorem is given in Subsection 3.1.2. In the classical adiabatic process, the necessary condition is the heat exchange $dQ = 0$, but it not necessary that the populations remain unchanged. For example, in a fast process, internal transitions can take place even though no heat is exchanged between the system and the bath. So it is a classical adiabatic process, but not a quantum adiabatic process [96]. Hence classical adiabatic process is more general compared to the quantum adiabatic process [97, 96].

In an adiabatic branch, the internal friction arises when Hamiltonian at different instants of time do not commute [75]. Suppose, we start from a state given as $\rho(t_0)$ and the system undergoes a unitary evolution $\rho(t) = U(t, t_0)\rho(t_0)U(t, t_0)^\dagger$, where U is a function of Hamiltonian. Now we consider a projection of the final state into eignebasis of the final Hamiltonian as in Eq. (1.25). As a result, energy-entropy [75] of the system increases. The increase in the entropy depends upon the rate with which the Hamiltonian is changed. In the adiabatic limit of very slow driving, where the quantum adiabatic theorem holds, the increase in entropy is zero. As a consequence of increase in entropy, the extractable work decreases. This phenomenon is identified as quantum analogue of internal friction.

1.3.3 Quantum isochoric process

Both in quantum and classical isochoric processes, the work done is zero and the system exchanges heat with the bath. At the end of the process, the system equilibrates with the bath. For a spin system, the energy spacing which is analogous to the volume, kept constant throughout the process [73]. During the process, the occupation probability P_n and the entropy (S) change as the system exchanges heat with the bath. The heat exchanged between the system and the bath is equal to the change in the mean energy of the system.

1.3.4 Quantum isobaric process

The mean energy of the system is written as $U = \sum_n P_n E_n$. So the first law of thermodynamics is given as $dU = \sum_n dE_n P_n + \sum_n P_n dE_n$. The first and the second terms of the right hand side are identified as the heat ($đQ$) and the work ($đW$) respectively [73]. So we can write [95]

$$\sum_n dE_n P_n + \sum_n E_n dP_n = TdS + \sum Y_n dy_n, \tag{1.10}$$

where Y_n and y_n are the generalized force and the corresponding generalized coordinate respectively, such that $đW = -Y_n dy_n$. When the generalized coordinate y_n is volume, then the Y_n represents the generalized force-pressure. An interesting model system to demonstrate the isobaric process is a particle in a one-dimensional (1D) potential well [95]. The generalized coordinate can be taken as the width of the potential well L. Since we deal with the 1D well, the pressure is same as the force. To keep the pressure constant throughout the isobaric process, it is shown that the temperature of the system should be proportional to the width of the potential well, $T \propto L$, analogous to the classical process (with ideal gas) where $T \propto V$ [95].

1.4 Review of basic concepts

1.4.1 Pure and mixed ensemble

An ensemble is a collection of systems which are identically prepared. Suppose $|\alpha_1\rangle$ represents a state in Hilbert space $\mathcal{H}$. A collection of such states constitute a

pure ensemble. An example is the silver atoms coming out of Stern-Gerlach filtering apparatus [103]. All the atoms in the beam are having same spin direction and hence represented by the same ket vector $|\alpha_1\rangle$. Now consider a situation in which 1/4 th members of the ensemble are characterized by $|\alpha_1\rangle$ and 3/4th by $|\alpha_2\rangle$, where $|\alpha_2\rangle$ is another state ket defined in $\mathcal{H}$. This type of ensemble is called mixed ensemble and as the name indicates it is a mixture of pure states. To handle such ensemble, in 1927, J. von Neumann introduced the idea of density operators. So the density operator for mixed ensemble is represented as

$$\rho = \frac{1}{4}|\alpha_1\rangle\langle\alpha_1| + \frac{3}{4}|\alpha_2\rangle\langle\alpha_2|. \tag{1.11}$$

The pure ensemble is given as $\rho = |\alpha_1\rangle\langle\alpha_1|$ or $|\alpha_2\rangle\langle\alpha_2|$. In general, density matrix of two level system can be written as

$$\rho = \frac{1}{2}(I + \overrightarrow{r}.\overrightarrow{\sigma}), \tag{1.12}$$

where I is the identity matrix, $\sigma = (\sigma_x, \sigma_y, \sigma_z)$ are the Pauli matrices and $\overrightarrow{r} = (x, y, z)$. The vector $\overrightarrow{r}$ is known as the Bloch vector. So the state of two level system can be represented on Bloch sphere as shown in Fig. 1.3. In the Bloch sphere picture, all the pure states reside on the surface of the sphere. On the other hand, the mixed states reside inside the sphere. Now we consider a special case, when the density matrix is diagonalized, all the diagonal elements are same and equal to $1/N$, where N is the dimension of the Hilbert space. Such mixed states are called maximally mixed states. In a Bloch sphere, the maximally mixed state resides in the origin. Density operator for both pure and mixed states are Hermitian operators of trace 1 ($\mathrm{Tr}(\rho) = 1$). But for pure states, we have

$$\mathrm{Tr}(\rho) = \mathrm{Tr}(\rho^2) = 1, \tag{1.13}$$

and for the mixed states

$$\mathrm{Tr}(\rho) \neq \mathrm{Tr}(\rho^2) < 1. \tag{1.14}$$

1.4.2 Quantum entropies

The quantum entropies are important tools used in quantum information and quantum statistical mechanics. Quantum entropies quantify the information content of

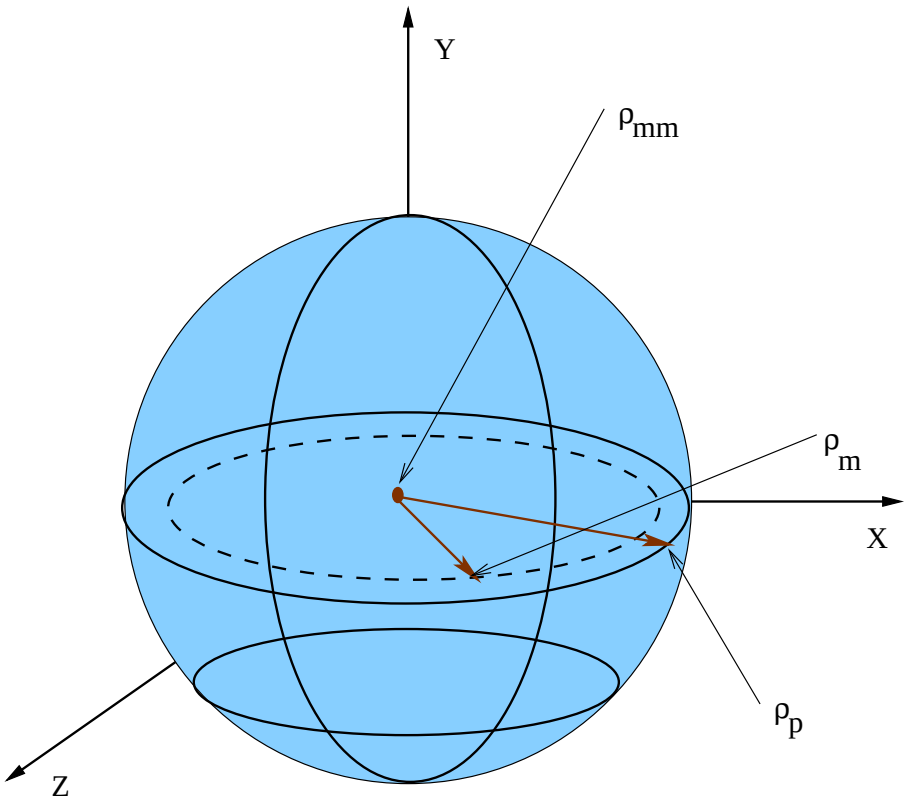

Figure 1.3: A pictorial representation of different states of two-level systems on a Bloch sphere. ρ_p represent a pure state which resides on the surface of the sphere. The mixed states are denoted by ρ_m and they are represented by the points inside the Bloch sphere. A special case is a maximally mixed state ρ_{mm}, which is situated at the center of the sphere.

quantum systems [90]. They are also used to analyze the irreversible nature of the quantum process [30]. The von-Neumann entropy of a system represented by density operator ρ, is defined as

$$S(\rho) = -\mathrm{Tr}[\rho \ln \rho]. \tag{1.15}$$

So for a pure state, the von Neumann entropy is zero. The mixed state is characterized by a non-zero von Neumann entropy. For a maximally mixed state, the von Neumann entropy is equal to $\ln N$. So in general we can write

$$0 \leq S(\rho) \leq \ln N. \tag{1.16}$$

This entropy is invariant under unitary transformation of ρ, which means

$$S(U\rho U^{\dagger}) = S(\rho). \tag{1.17}$$

Now we look into Shannon entropy formulated by Claude E. Shannon in his remarkable paper titled *A Mathematical Theory of Communication* [109]. The Shannon entropy is defined as

$$S_s = -\sum_i p_i \ln p_i, \tag{1.18}$$

where $p_i = \langle\psi_i|\rho|\psi_i\rangle$ and $\{\psi_i\}$ constitute an orthonormal basis. So Shannon entropy is equal to von-Neumann entropy when $\{\psi_i\}$ are the eigenstates of ρ. In general, we can write

$$S_s \geq S(\rho). \tag{1.19}$$

1.4.3 First law of thermodynamics and definition of work and heat

Suppose the state of the system is defined by a density operator ρ. Then the expected value of any observable A is defined as

$$\langle A\rangle = \mathrm{Tr}(\rho A). \tag{1.20}$$

In quantum thermodynamics, one of the important quantities is the internal energy (E), which is defined as the expectation value of the Hamiltonian H. So we have

$$E = \langle H\rangle = \mathrm{Tr}(\rho H). \tag{1.21}$$

In a quantum process, in general H can be time-dependent and does not commute for different times $[H(t'), H(t'')] \neq 0$. We also consider that the system is attached with a bath during the process. So differentiating the above equation, we have

$$\frac{dE}{dt} = \mathrm{Tr}\left(H(t)\frac{d\rho(t)}{dt}\right) + \mathrm{Tr}\left(\frac{dH(t)}{dt}\rho(t)\right), \tag{1.22}$$

Comparing this equation with the first law of thermodynamics, $dE = dQ + dW$, we identify the first term on the right hand side as the rate of heat flow ($\dot{Q}$) and the second term as the power ($\wp$) [7]. Integrating ($\dot{Q}$) and ($\wp$) with respect to time, we get heat (Q) and work (W) involved in the quantum process respectively.

1.4.4 Second law of thermodynamics and majorization

Consider two density matrices ρ and σ corresponding to two different states of a d-dimensional system. The respective eigenvalues of ρ and σ are represented by

$\{\lambda_\rho^i\}$ and $\{\lambda_\sigma^i\}$. We say ρ majorizes σ ($\rho \succ \sigma$) [25, 91, 90], when

$$\sum_i^n \lambda_\rho^i \geq \sum_i^n \lambda_\sigma^i, \tag{1.23}$$

for any n ($1 \leq n \leq d$), when both sets of eigenvalues are written in decreasing order. This means that the Shannon entropy of both the density matrices should obey the relation

$$S(\sigma) \geq S(\rho). \tag{1.24}$$

If the above condition in Eq. (1.23) is satisfied, then we can write

$$\sigma = \sum_n P_n U \rho U^\dagger P_n, \tag{1.25}$$

where U is a unitary operator and $\{P_n\}$ are the projection operators in a certain eigenbasis. Now we state different versions of the second law of thermodynamics [31]:

- Kelvin statement: No process is possible whose sole result is absorption of heat from a reservoir and conversion of this heat into work.
- Clausius statement: No process is possible whose sole result is the transfer heat from a cooler to hotter body.
- Principle of Carathéodory: In every neighborhood of any state S of an adiabatically isolated system there are states inaccessible from S.

Although the above three statements are equivalent, we try to understand the implication of the third statement in the concept of majorization. Eq. (1.25) shows that by unitary evolution followed by a projection operation, one can go from a low entropic state to higher entropic state and not the other way around. This is exactly given by the principle of Carathéodory that from any state S, by adiabatic process (unitary process), a low entropic state cannot be achieved.

1.4.5 Dynamics of open quantum system

A quantum system ($\mathcal{S}$), when it is coupled to an environment (bath) $\mathcal{B}$ is called an open quantum system. We are interested in the dynamics of such systems because when a system is attached to a thermal bath, this dynamics leads the system to

equilibrate with the bath. Suppose the Hilbert spaces of $\mathcal{S}$ and $\mathcal{B}$ are $\mathcal{H}_\mathcal{S}$ and $\mathcal{H}_\mathcal{B}$ respectively. Then the state of the combined system $(\mathcal{S}+\mathcal{B})$ lives in a tensor product space, which is given as $\mathcal{H}=\mathcal{H}_\mathcal{S}\otimes\mathcal{H}_\mathcal{B}$. Let $H_\mathcal{S}$ and $H_\mathcal{B}$ are the Hamiltonian of system and bath respectively and $H_{\mathcal{SB}}$ is the interaction Hamiltonian responsible for the coupling between system and the environment. Then the Hamiltonian of the combined system is given as

$$H = H_\mathcal{S}\otimes I_\mathcal{B} + I_\mathcal{S}\otimes H_\mathcal{B} + H_{\mathcal{SB}}, \tag{1.26}$$

where $I_\mathcal{S}$ and $I_\mathcal{B}$ are the identity operators with dimensions corresponding to the system and the bath respectively. Bath is a system with infinite degrees of freedom. This property of the bath is responsible for the irreversible evolution of open quantum system [30]. Consider $\rho(t_0)$ as the initial density matrix of the combined system. The combined system undergoes a unitary evolution. But we are interested in the state of the open quantum system $\mathcal{S}$, represented as $\rho_\mathcal{S}(t)$ at a given instant of time t. This is obtained by tracing out the bath degrees of freedom and it is given as

$$\rho_\mathcal{S}(t) = \mathrm{Tr}_\mathcal{B}\left[U(t,t_0)\rho(t_0)U(t,t_0)^\dagger\right]. \tag{1.27}$$

The most general form of this evolution is given in Eq. (1.1).

1.4.6 Entropy maximum postulates and definition of temperature in thermodynamics

The first postulate of thermodynamics leads to the definition of equilibrium states. The remaining three postulates are given below and they are generally called entropy maximum postulates [33].

Postulate II: *There exists a function (called the entropy and denoted by S) of the extensive parameters of any composite system, defined for all equilibrium states and having the following property: The values assumed by the extensive parameters in the absence of an internal constraint are those that maximize the entropy over the manifold of constrained equilibrium states.*

Postulate III: *The entropy of a composite system is additive over the constituent subsystems. The entropy is continuous and differentiable and is a monotonically increasing function of the energy.*

Postulate IV: *The entropy of any system is non-negative and vanishes in the state for which* $\left(\frac{\partial U}{\partial S}\right)_{V,N_1,N_2..,N_r} = 0$ *(that is, at zero temperature), where* U *is the internal energy and the* $N_1, .., N_r$ *are the mole numbers.*

Now we go through one of the main implications of the maximum entropy postulate. Here we consider a composite system consisting of two subsystems separated by an impermeable wall which allows only the heat exchange between the subsystems. The volume and the mole numbers of the subsystems are fixed but the energies of the subsystems (U_1 and U_2) are variable. At thermodynamic equilibrium, from the above postulates and by the definition of temperature $T_i = (\partial U_i/\partial S_i)$, where $i = 1, 2$, we get $T_1 = T_2$.

So the entropy is maximum when the temperatures of the two subsystems are equal. Further the above analysis can be extended to understand the relevance of other intensive variables such as pressure and chemical potential in mechanical equilibrium and equilibrium with respect to matter flow respectively.

1.5 Thesis layout

In Chapter 2, we study the 1-d isotropic Heisenberg model of two spin-1/2 systems as a quantum heat engine. The engine undergoes a four-step Otto cycle where the two adiabatic branches involve changing the external magnetic field at a fixed value of the coupling constant. We find conditions for the engine efficiency to be higher than the uncoupled model; in particular, we find an upper bound which is tighter than the Carnot bound. A new domain of parameter values is pointed out which was not feasible in the interaction-free model. Locally, each spin seems to effect the flow of heat in a direction opposite to the global temperature gradient. This seeming contradiction to the second law can be resolved in terms of local effective temperature of the spins.

In Chapter 3, we consider the same model of working medium but with two essential differences: (1) the rate of driving in adiabatic branches is finite, (2) the driving is inhomogeneous. We observe a frictional effect on the adiabatic branches of the heat cycle, which arises because the Hamiltonian does not commute for different times. The frictional effect is characterized by entropy production in the system and

reduction in the work extracted. Corresponding to a sudden and a very slow driving, we find expressions for the lower and upper bounds of work that can be extracted on the adiabatic branches. These bounds are also confirmed with numerical simulations of the corresponding Liouville-von Neumann equation.

In Chapter 4, we estimate the expected behavior of a quantum model of heat engine when we have incomplete information about external macroscopic parameters, like magnetic field controlling the intrinsic energy scales of the working medium. We explicitly derive the prior probability distribution for these unknown parameters, $a_i, (i = 1, 2)$. Based on a few simple assumptions, the prior is found to be of the form $\Pi(a_i) \propto 1/a_i$. By calculating the expected values of various physical quantities related to this engine, we find that the expected behavior of the quantum model exhibits thermodynamic-like features. This leads us to propose that incomplete information quantified as appropriate prior distribution can lead us to expect classical thermodynamic behavior in quantum models. Finally, we study the implications of posterior probabilities obtained through Bayes theorem.

Chapter 5 is devoted to analyzing the efficiency obtained from certain models of heat engines. In the first part of this chapter, we discuss the Curzon-Ahlborn(CA) efficiency which is obtained in many finite-time heat engine models. The leading term of this efficiency in near equilibrium expansion is half of the Carnot value. Further we show that how this efficiency can be obtained through Bayesian Statistics. We also study the optimal performance of Feynman's ratchet as a heat engine and also as a refrigerator when a parameter in the model is uncertain. We assign a prior distribution for the uncertain parameter and the functional form of this prior is identical to Jeffreys prior. For heat engine, the power is optimized and for the refrigerator, we optimized the χ-criterion which is the product of heat-power and coefficient of performance. For both heat engine and refrigerator, we obtain the corresponding Curzon-Ahlborn values, $1 - \sqrt{\theta}$ and $1/\sqrt{1-\theta} - 1$, respectively.

From estimates based on prior information, we also come across a different class of efficiency where the leading term in near-equilibrium expansion is one-third of Carnot efficiency. Similar efficiency is obtained in a model of Brownian heat engine when it operates at maximum power. We also show other examples where the incomplete information leads to $\eta_c/3$ in near equilibrium.

Chapter 6 is devoted to summarizing the content of this thesis and possible extensions of our research work.

Chapter 2

Quantum Otto cycle with coupled spins

2.1 Introduction

Nikolaus Otto was the first person to build a working model of a four-stroke internal combustion engine in 1861. Hence the four-stroke gasoline engines used nowadays are generally called Otto engines. Stroke is the movement of the piston (in or out) in the combustion engine. The four strokes in a gasoline engine are the following. *Intake stroke*: In this stage, the fuel along with the air is pumped into the cylinder so that the piston reaches the bottom. Then the input valve through which the air-fuel mixture entered into the cylinder, closes. *Compression stroke*: The piston moves upward and compresses the air-fuel mixture. *Ignition*: The air-fuel mixture is ignited using the spark plug. The mixture gets heated up increasing the temperature and the pressure. *Power stroke*: The mixture at high temperature and pressure pushes the piston down by giving a power output. *Exhaust stroke*: In this stroke, the exhaust valve opens and the burned air-fuel mixture is pushed out of the combustion chamber.

In this chapter, we briefly review the classical Otto cycle and a simple model of quantum Otto cycle. Then we introduce a coupled quantum system as the working medium of the quantum Otto cycle. The Otto cycle consists of two adiabatic and two isochoric processes. In classical Otto cycle, the volume is changed during the adiabatic processes. Analogously in the quantum cycle described [73, 96], the energy

level spacings are changed during the adiabatic branches of the heat cycle.

2.2 Classical Otto cycle

Unlike Carnot cycle, Otto cycle is not a reversible cycle. So the efficiency of the Otto engine is less than Carnot efficiency. The classical Otto cycle consists of four stages, two isochoric (constant volume) and two adiabatic processes. The working medium of this cycle is classical ideal gas. The four-staged cycle is explained with P-V diagram shown in Fig.2.1.

Stage 1(D $\rightarrow$ A): The system (working medium) is attached to a hot bath with temperature T_1. The volume of the cylinder is V_1. The system attains equilibrium with the bath at constant volume. In this stage, the system absorbs an amount of heat Q_1 from the hot bath.

Stage 2(A $\rightarrow$ B): The system is removed from the bath. It undergoes an adiabatic expansion so that the volume changes from V_1 to V_2. In this stage, work is done by the system and hence the temperature of the system drops to T_1'.

Stage 3(B $\rightarrow$ C): In this stage, the system is kept in contact with a cold bath at temperature T_2. The system releases an amount of heat Q_2 and attains equilibrium with the bath.

Stage 4(C $\rightarrow$ D): The system is isolated from the cold bath and an adiabatic compression is carried out such that the volume is changed from V_2 to its initial value V_1. Since work is done on the system, the temperature of the system rises to T_2'. To complete the cycle, the system is again attached to hot bath.

Now we analyze the heat exchanged between the system and the bath. In stage 1, the temperature of the system before attaching with the hot bath is T_2'. Since the working medium is a classical ideal gas, the internal energy of the system at that point is CT_2'. Similarly, at the end of stage 1, the mean energy of the system is CT_1. So the heat absorbed by the system during the isochoric process is given by $Q_1 = C(T_1 - T_2')$. In the same way, the heat rejected to the cold bath is $Q_2 = C(T_2 - T_1')$. So the work done by the system is

$$W = Q_1 + Q_2 = C(T_1 + T_2 - T_2' - T_1'). \tag{2.1}$$

Because of the adiabatic process, we can write $T_1 V_1^{(\gamma-1)} = T_1' V_2^{(\gamma-1)}$ and $T_2 V_2^{(\gamma-1)} =$

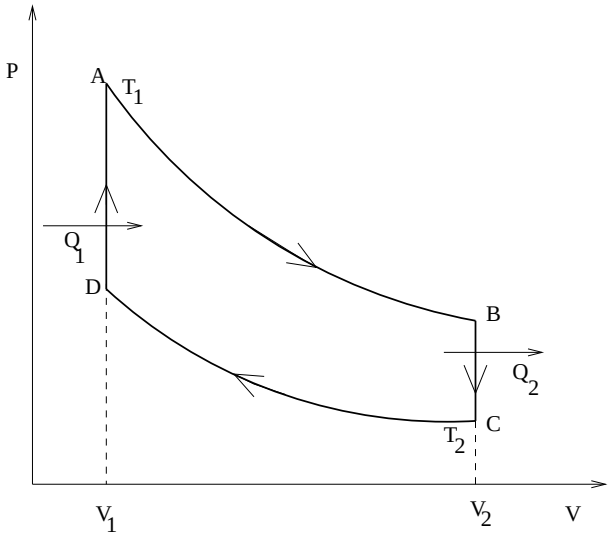

Figure 2.1: P-V diagram representing classical Otto cycle.

$T_2' V_1^{(\gamma-1)}$, where $\gamma = C_p/C_v$. So the efficiency of the Otto engine $\eta = W/Q_1$, can be written as

$$\eta = 1 - \left(\frac{V_1}{V_2}\right)^{(\gamma-1)} \tag{2.2}$$

$$= 1 - \frac{T_1'}{T_1} = 1 - \frac{T_2}{T_2'}. \tag{2.3}$$

2.3 A model of a quantum Otto cycle

Analogous to the classical Otto cycle, a quantum Otto cycle can be constructed [73, 96]. Here, the working medium can be a few particle quantum system. In Ref. [73], a two level system is considered as the working substance of quantum heat engine. In the adiabatic branch, the system is uncoupled from the bath and the the energy spacing is varied. The quantum analogue of isochoric process is done by attaching the system with the bath keeping the energy spacing constant throughout the process. Consider a two level system with energy eigenvalues $(0, a_1)$ and in equilibrium with a hot bath at temperature T_1. Let the canonical probability for the system to be in the upper and lower energy levels be p_1 and $1 - p_1$ respectively, where $p_1 = (1 + \exp(a_1/kT_1))^{-1}$.

Now consider an adiabatic process in which the energy level spacing is changed from a_1 to a_2 adiabatically and hence the population in each energy level is un-

changed. This is analogous to the first adiabatic process discussed in the classical cycle where volume changes from V_1 to V_2. In the next step, the system is attached to a cold bath with temperature T_2. The occupation probabilities of the upper and lower energy levels become p_1' and $1-p_1'$ respectively, where $p_1' = (1+\exp(a_2/kT_2))^{-1}$. For the second adiabatic process, the energy spacing changes from a_2 to a_1 adiabatically. To complete the cycle, the system is again attached to the hot bath. A pictorial representation of the cycle is given in the Figure 2.2. Work is done on or

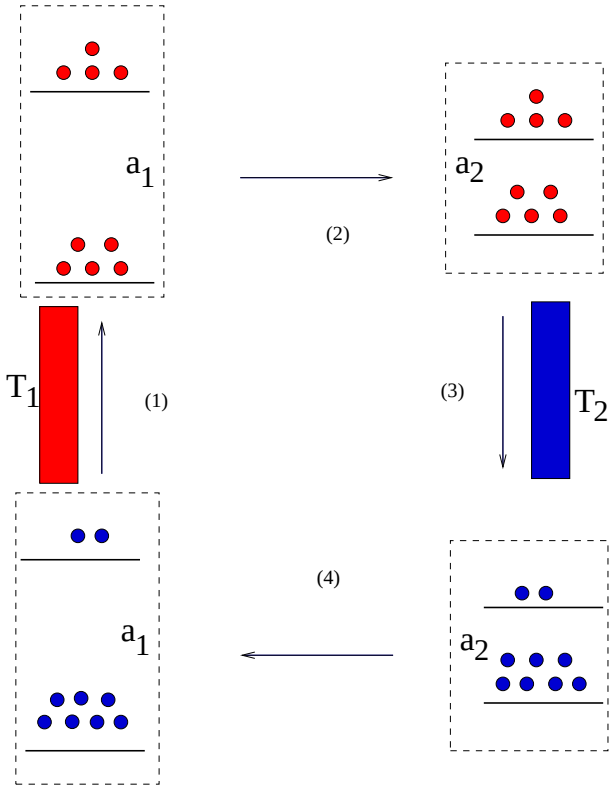

Figure 2.2: A pictorial representation of the cycle undergone by the system.

by the system during the adiabatic process and a heat exchange takes place during the thermalization branch. The heat absorbed from the hot bath is

$$Q_1 = a_1 p_1 - a_1 p_1' = a_1 \left(\frac{1}{1+\exp(a_1/T_1)} - \frac{1}{1+\exp(a_2/T_2)} \right). \tag{2.4}$$

We set $k = 1$. Similarly the heat rejected to the cold bath is

$$Q_2 = a_2 \left(\frac{1}{1+\exp(a_2/T_2)} - \frac{1}{1+\exp(a_1/T_1)} \right). \tag{2.5}$$

The work done by the system $W = Q_1 + Q_2$, is

$$W = (a_1 - a_2) \left(\frac{1}{1+\exp(a_1/T_1)} - \frac{1}{1+\exp(a_2/T_2)} \right). \tag{2.6}$$

The positive work condition (net work is done by the system) demands,

$$\frac{a_2}{T_2} \geq \frac{a_1}{T_1}, \tag{2.7}$$

provided $a_1 > a_2$. The efficiency of the engine is given as

$$\eta = 1 + \frac{Q_2}{Q_1} = 1 - \frac{a_2}{a_1}. \tag{2.8}$$

Thus the efficiency is bounded from above by Carnot limit.

2.4 Coupled quantum heat engine

2.4.1 Motivation

As we have seen in Chapter 1, heat engines are suitable candidates to investigate thermodynamic behavior in quantum systems. Here we introduce a coupled quantum heat engine and study its thermodynamic behavior. Some authors have studied the role of different kinds of interactions between spin-1/2 particles in a Quantum Otto cycle [127, 126, 123]. In particular, the role of quantum entanglement has been conjectured using measure like concurrence and the second law has been shown to hold in such models. The importance of this work was discussed in detail in the first chapter. Motivated from this work, we also investigate a coupled Otto engine using a 1-d Heisenberg model with isotropic exchange interactions between two spin-1/2 particles (see Eq. (2.9) below). In Ref. [127], the same model was analyzed, where during the adiabatic steps, the exchange constant J was altered between two chosen values ($J_1 \rightarrow J_2 \rightarrow J_1$), while keeping the external magnetic field at a fixed value. From an experimental point of view, it is also interesting to investigate a cycle where the exchange constant is fixed and only the magnetic field is varied during the adiabatic steps. Further, the uncoupled model cycles considered earlier in literature where the magnetic field is varied, can be taken as a benchmark with which to compare the engine performance of the coupled model.

There is some limitation to consider a Carnot cycle in similar models. For a Carnot cycle, one should be able to assign a temperature for the system at the end of the adiabatic process. This is possible only if all the energy level spacings are changed with the same ratio [96] and hence in a Carnot cycle one has to change both J and B.

2.4.2 Model

In this model, the working medium for the QHE consists of two spin-1/2 particles within the 1D isotropic Heisenberg model [127, 17]. The Hamiltonian is given by

$$H = J(\vec{\sigma}^{(1)}.\vec{\sigma}^{(2)} + \vec{\sigma}^{(2)}.\vec{\sigma}^{(1)}) + B(\vec{\sigma}_z^{(1)} + \vec{\sigma}_z^{(2)}), \tag{2.9}$$

where $\vec{\sigma}^{(i)} = \{\sigma_x^{(i)}, \sigma_y^{(i)}, \sigma_z^{(i)} | i = 1, 2\}$ are the Pauli matrices. $J = J_x = J_y = J_z$ is the exchange constant and B is the external magnetic field along z-axis. Cases $J > 0$ and $J < 0$ correspond to antiferromagnetic and ferromagnetic interactions, respectively. In this chapter, we consider the antiferromagnetic case only. The energy eigenvalues of H are $-6J$, $(2J - 2B)$, $2J$ and $(2J + 2B)$ and the eigenstates are $|\psi_-\rangle$, $|00\rangle$, $|\psi_+\rangle$ and $|11\rangle$ respectively, where $|\psi_\pm\rangle = (|10\rangle \pm |01\rangle)/\sqrt{2}$ are the maximally entangled Bell states (see Fig. 2.3). If $|0\rangle$ and $|1\rangle$ represent the state of the spin along and opposite to the direction of the magnetic field respectively, then in the natural basis $\{|11\rangle, |10\rangle, |01\rangle, |00\rangle\}$, we can write the density matrix as

$$\rho = P_1|\psi_-\rangle\langle\psi_-| + P_2|00\rangle\langle 00| + P_3|\psi_+\rangle\langle\psi_+| + P_4|11\rangle\langle 11| \tag{2.10}$$

The occupation probabilities of the system in the thermal state at temperature T are given by

$$P_1 = \frac{e^{8J/T}}{Z}, \tag{2.11}$$

$$P_2 = \frac{e^{2B/T}}{Z}, \tag{2.12}$$

$$P_3 = \frac{1}{Z}, \tag{2.13}$$

$$P_4 = \frac{e^{-2B/T}}{Z}. \tag{2.14}$$

where, $Z = (1 + e^{8J/T} + e^{2B/T} + e^{-2B/T})$ is the normalization constant.

2.4.3 The heat cycle

The four stages involved in our quantum Otto cycle are described below:
Stage 1. The system with the external magnetic field at B_1 attains thermal equilibrium with a bath at temperature T_1. Let occupation probabilities be p_1, p_2, p_3, and p_4 as tabulated above with $T = T_1$ and $B = B_1$. *Stage 2.* The system is isolated from the hot bath and the magnetic field is changed from B_1 to B_2 by quantum

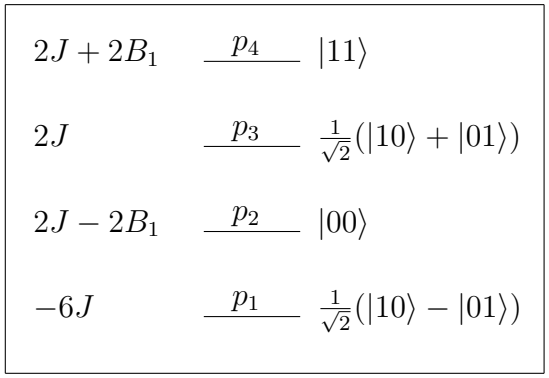

Figure 2.3: Energy level diagram

adiabatic process. According to quantum adiabatic theorem, the process should be slow enough to maintain the individual occupation probability of each energy level. *Stage 3.* The system is brought in thermal contact with a cold bath at temperature T_2. Upon attaining equilibrium with the bath, the occupation probabilities become p'_1, p'_2, p'_3, and p'_4 corresponding to the thermal state with $T = T_2$ and $B = B_2$. On the average, the system gives off heat to the bath. *Stage 4.* The system is removed from the cold bath and undergoes another quantum adiabatic process which changes the magnetic field from B_2 to B_1, but keeps the probabilities p'_1, p'_2, p'_3, and p'_4 unaffected. Finally, the system is brought back in contact with the hot bath. On the average, heat is absorbed from the bath and the system returns to its initial state.

The heat transfered in *Stage 1* and in *Stage 3* of the cycle respectively is

$$Q_1 = \sum_i E_i(p_i - p'_i) \tag{2.15}$$

$$= 8J(p'_1 - p_1) + 2B_1(p'_2 - p_2 + p_4 - p'_4), \tag{2.16}$$

and

$$Q_2 = \sum_i E'_i(p'_i - p_i) \tag{2.17}$$

$$= -8J(p'_1 - p_1) - 2B_2(p'_2 - p_2 + p_4 - p'_4). \tag{2.18}$$

In the above, E_i and E'_i $(i = 1, 2, 3, 4)$ are the energy eigenvalues of the system in *Stage 1* and *Stage 3* respectively. $Q_1 > 0$ and $Q_2 < 0$ corresponds to absorption of heat from hot bath and release of heat to cold bath respectively. Comparing the equations for heat transfer between the system and the reservoirs, Eqs. (2.16) and (2.18), the term $8J(p'_1 - p_1)$ appears in both the equations. Obviously, this term is absent in the uncoupled case for which $J = 0$. As will be shown below, the sign $(\pm)$

of this term determines whether the efficiency in the coupled case will be higher or lower than the uncoupled case.

The work is done in *Stage 2* and *Stage 4* when the energy levels are changed at fixed occupation probabilities. The net work done by the QHE is

$$W = Q_1 + Q_2 = 2(B_1 - B_2)(p_2' - p_2 + p_4 - p_4'), \tag{2.19}$$

which is required to be positive for an engine.

2.5 The local description

In this section, we discuss how the individual spins in the system undergo the cycle. Again, let ϱ_{12} and ϱ_{12}' represent the thermal states in the natural basis when the system is in equilibrium in *Stage 1* and *Stage 3* respectively. Explicitly, the density matrices are

$$\varrho_{12} = \begin{pmatrix} p_4 & 0 & 0 & 0 \\ 0 & \frac{p_1+p_3}{2} & \frac{p_3-p_1}{2} & 0 \\ 0 & \frac{p_3-p_1}{2} & \frac{p_1+p_3}{2} & 0 \\ 0 & 0 & 0 & p_2 \end{pmatrix}, \tag{2.20}$$

$$\varrho_{12}' = \begin{pmatrix} p_4' & 0 & 0 & 0 \\ 0 & \frac{p_1'+p_3'}{2} & \frac{p_3'-p_1'}{2} & 0 \\ 0 & \frac{p_3'-p_1'}{2} & \frac{p_1'+p_3'}{2} & 0 \\ 0 & 0 & 0 & p_2' \end{pmatrix}. \tag{2.21}$$

Let ϱ_1 and ϱ_2 be the reduced density matrices in *Stage 1* for the first and the second spin, respectively. Then from the normalization constraints, $\Sigma_i p_i = \Sigma_i p_i' = 1$, we get

$$\varrho_1 = \varrho_2 = \begin{pmatrix} \frac{1}{2} - \frac{(p_2-p_4)}{2} & 0 \\ 0 & \frac{1}{2} + \frac{(p_2-p_4)}{2} \end{pmatrix}. \tag{2.22}$$

Similarly in *Stage 3*, the reduced density matrices for the first and second spin are

$$\varrho_1' = \varrho_2' = \begin{pmatrix} \frac{1}{2} - \frac{(p_2'-p_4')}{2} & 0 \\ 0 & \frac{1}{2} + \frac{(p_2'-p_4')}{2} \end{pmatrix}. \tag{2.23}$$

Since the applied magnetic field is the same for each spin, their local Hamiltonian is also same. Let H_l and H_l' be the local Hamiltonians for individual spins with

eigenvalues $(B_1, -B_1)$ and $(B_2, -B_2)$ in *Stage 1* and *Stage 3* respectively. The heat transferred locally between *one* spin and a reservoir is defined as $q_1 = \mathrm{Tr}[(\varrho_1 - \varrho_1')H_l]$ and $q_2 = \mathrm{Tr}[(\varrho_1' - \varrho_1)H_l']$. The explicit expressions are given as

$$q_1 = B_1(p_2' - p_2 + p_4 - p_4'), \tag{2.24}$$

$$q_2 = -B_2(p_2' - p_2 + p_4 - p_4'), \tag{2.25}$$

for the hot and the cold reservoir, respectively. So we get the net work done by an individual spin $w = q_1 + q_2$, as

$$w = (B_1 - B_2)(p_2' - p_2 + p_4 - p_4'). \tag{2.26}$$

From Eqs. (2.26) and (2.19), we note that

$$W = 2w. \tag{2.27}$$

Thus the total work performed is the sum of work obtained from the two spins locally. Further, the total heat absorbed by the system can be written as

$$Q_1 = 8J(p_1' - p_1) + 2q_1, \tag{2.28}$$

and similarly for the heat released to the cold bath is

$$Q_2 = -8J(p_1' - p_1) + 2q_2. \tag{2.29}$$

Now it can be seen that because the work is done only due to change in local Hamiltonians, so only the part of the heat which is absorbed locally by a spin can be converted into heat. The part $8J(p_1' - p_1)$ cannot potentially be converted into work, due to the nature of the adiabatic process involved and is transferred directly between the reservoirs. But it may not be transfered only from the hot to the cold bath, in which case it may be regarded like a heat leakage term. In fact, the flow of this heat can be in the opposite direction which is directly related to the enhancement of efficiency due to coupling, as shown below.

In the following, we consider two cases whereby magnetic field may be decreased or alternately, increased in Stage 2. It will be seen that the second case is feasible only in the presence of interactions, $J \neq 0$. In the first case when $J = 0$, the above equations go back to the model discussed in Section 2.3, with two uncoupled spins where an engine operation is obtained for $T_1 > T_2$ and $B_1 > B_2$ with the additional condition $B_2/T_2 > B_1/T_1$.

2.5.1 The case $B_1 > B_2$

From Eq. (2.19), the condition that the work performed be positive ($W > 0$) is given by

$$(p_2' - p_4') > (p_2 - p_4). \tag{2.30}$$

This also implies $q_1 > 0$ in Eq. (2.24). So now, for heat to be absorbed from the hot bath ($Q_1 > 0$), from Eq. (2.28) we have one of the following two possibilities: (i) $p_1' > p_1$ or (ii) $p_1' < p_1$. Alongwith the possibility (ii), we must also have from Eq. (2.16), $(p_2' - p_2 + p_4 - p_4') > (4J/B_1)(p_1 - p_1')$. Now we rewrite Eq. (2.16) as

$$Q_1 = 8J(p_1' - p_1) + \frac{WB_1}{(B_1 - B_2)}, \tag{2.31}$$

or $8J(p_1' - p_1) = Q_1(1 - \eta/\eta_0)$, where $\eta = W/Q_1$ is the efficiency of the coupled engine and $\eta_0 = (B_1 - B_2)/B_1$ is the efficiency of the uncoupled i.e. $J = 0$ case. Thus for $J > 0$, if $p_1' > p_1$, then $\eta < \eta_0$, or the presence of coupling between the spins decreases the efficiency from its value η_0. The global efficiency is equal to the local efficiency in two situations, when $J = 0$ or $p_1 = p_1'$.

On the other hand, if $p_1' < p_1$, then it is possible that the efficiency of the coupled engine can be higher than the uncoupled case. Using the latter condition with Eq. (2.30), we have

$$\frac{(p_2' - p_4')}{p_1'} > \frac{(p_2 - p_4)}{p_1}. \tag{2.32}$$

From the explicit expressions for the probabilities, the above inequality can be simplified to give

$$\frac{B_2}{T_2} > \frac{B_1}{T_1}. \tag{2.33}$$

Thus we see that the above condition which is necessary to extract work in the $J = 0$ model is *also* the condition for the coupled case to obtain an efficiency higher than η_0. But additionally, for a set of given values of T_1, T_2, B_1 and B_2, there is a maximum value of J beyond which the efficiency drops below the η_0 value. See Fig. 2.4.

The reason for the lowering of efficiency when $p_1 < p_1'$, is that the term $8J(p_1' - p_1)$ is positive and it acts like heat leakage term which reduces the efficiency. On the other hand, when $p_1 > p_1'$, this term is negative which means that although each spin locally absorbs heat equal to q_1 from the hot bath, due to interaction the

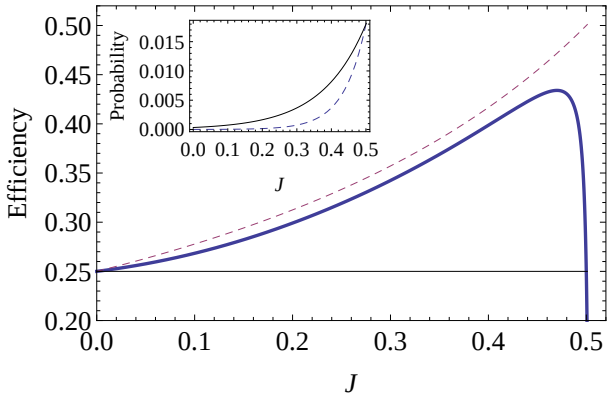

Figure 2.4: Efficiency versus the coupling constant J, for $B_1 > B_2$ case, for values $B_1 = 4$, $B_2 = 3$, $T_1 = 1$ and $T_2 = 0.5$. The uncoupled case corresponds to $\eta_0 = 1 - B_2/B_1 = 0.25$, which is shown as the reference horizontal line. Case (i) $p_1' > p_1$, corresponds to efficiency below this line, while case (ii) $p_1 > p_1'$ gives a higher efficiency. The upper curve denotes the bound for efficiency from Eq. (2.34). The inset shows the behavior of p_1 (solid line) and p_1' (dashed line) vs J.

effective total heat absorbed by the two-spin system is less than $2q_1$, which raises the efficiency for a given quantity of the work performed. It is interesting to know how much maximum gain in efficiency is possible for a given set of parameters. We have proved an upper bound for the global efficiency, given by

$$\eta \leq \frac{1 - B_2/B_1}{1 - 4J/B_1} < \eta_c, \tag{2.34}$$

where $\eta_c = 1 - T_2/T_1$ is the Carnot bound. Also for $\eta > \eta_0$, we have the condition $B_1 > 4J$. This implies that the ordering of energy levels which gives an enhancement of efficiency (over the uncoupled model) is:

$$(2J - 2B_1) < -6J < 2J < (2J + 2B_1), \tag{2.35}$$

and which after the first quantum adiabatic process, becomes

$$(2J - 2B_2) < -6J < 2J < (2J + 2B_2). \tag{2.36}$$

The proof of Eq. (2.34) is given in Section 2.6.

2.5.2 The case $B_2 > B_1$

In this case, during the first quantum adiabatic process, the magnetic field is *increased* from its value B_1 to B_2. If there is no interaction between the spins, the

system cannot work as an engine in this case because the condition $W > 0$ will not be satisfied [73]. The conditions $T_1 > T_2$ and $B_2 > B_1$ directly lead to

$$p_4 > p_4', \tag{2.37}$$

$$p_3 > p_3'. \tag{2.38}$$

Further, the positive work condition implies Eq. (2.30), alongwith Eq. (2.37) gives

$$p_2 > p_2'. \tag{2.39}$$

The normalization of probabilities and the above three conditions together imply

$$p_1' > p_1. \tag{2.40}$$

These are the necessary conditions for the system to work as an engine given that $T_1 > T_2$ and $B_2 > B_1$. According to Eq. (2.26), the local work should be positive. This surprisingly yields, $q_1 < 0$ and $q_2 > 0$ in Eqs. (2.24) and (2.25). This means locally the heat is absorbed from the cold bath and given to the hot bath. Also the local efficiency is

$$\frac{w}{q_2} = 1 - \frac{B_1}{B_2}. \tag{2.41}$$

Thus locally, the spins operate counter to the global temperature gradient present due to $T_1 > T_2$. But globally we do have $Q_1 > 0$ and $Q_2 < 0$. Thus the function of the two-spin engine is consistent with the second law of thermodynamics, although locally we seem to have a violation of the same. This apparent contradiction is resolved below using the concept of local effective temperatures.

2.5.3 Local temperatures

Now each spin in the 2-spin system can be assigned an effective local temperature, corresponding to its local thermal state or the reduced density matrix [46, 47, 52]. This is true regardless of the state of the total system. Particularly, at the end of stages 1 and 3 of the cycle, from Eqs. (2.22-2.23) alongwith local Hamiltonian, we get the local temperatures as

$$T_1' = 2B_1 \left(\ln \left[\frac{2}{(1 + p_4 - p_2)} - 1 \right] \right)^{-1}, \tag{2.42}$$

$$T_2' = 2B_2 \left(\ln \left[\frac{2}{(1 + p_4' - p_2')} - 1 \right] \right)^{-1}. \tag{2.43}$$

The important fact is that in the presence of interactions, the local temperatures are different from the corresponding bath temperatures. Thus $T_1' \neq T_1$ and $T_2' \neq T_2$ if $J \neq 0$. Further, since the work in our heat cycle is done only locally, the total work by the system can be regarded as equal to the work by two independent spins operating between their effective temperatures (see Fig. 2.5).

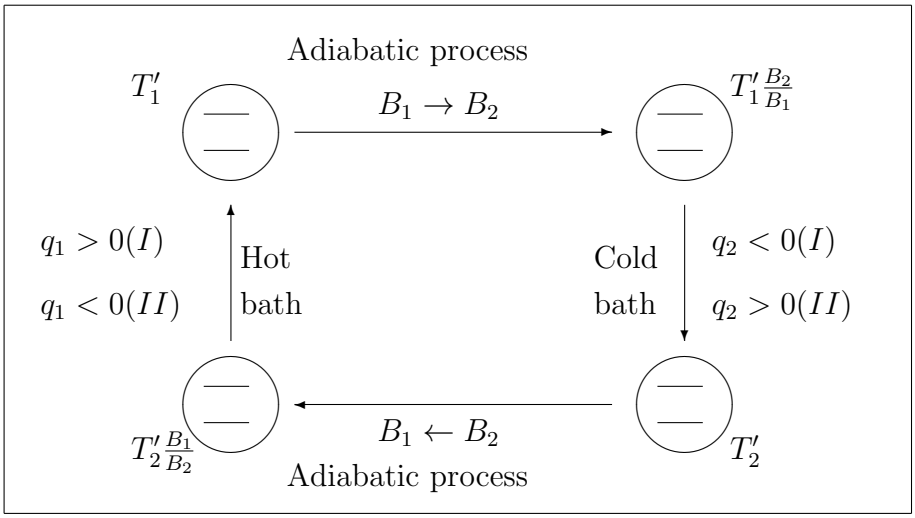

Figure 2.5: Local effective temperatures of a spin (shown as a circle with two levels) during various stages of the heat cycle. Case (I) implies $B_1 > B_2$, while case (II) implies $B_1 < B_2$. Note that, in either case, the opposite signs of heat are exchanged locally upon contact with hot or cold baths.

(I) Engine working in $B_1 > B_2$: the positive work condition for a single spin is given by

$$\frac{B_2}{T_2'} > \frac{B_1}{T_1'}. \tag{2.44}$$

Since $B_1 > B_2$, we get

$$T_1' > T_2'. \tag{2.45}$$

At $J = 0$, $T_1' = T_1$ and $T_2' = T_2$.

(II) Engine working in $B_2 > B_1$: in this model, the positive work condition is satisfied only when

$$\frac{B_1}{T_1'} > \frac{B_2}{T_2'}. \tag{2.46}$$

Thus in this case $T_2' > T_1'$. Moreover, it can be shown from the definitions (2.42) and (2.43) that for both the cases, $T_1' > T_1$ and $T_2' > T_2$. Finally, based on local temperatures, the counter-intuitive mechanism which leads in case (II) to $q_1 < 0$ and $q_2 > 0$ can be justified as follows. For $B_2 > B_1$, due to the first adiabatic process, the local temperature *increases* from T_1' to $T_1'(B_2/B_1)$. After contact with the cold bath, the local temperature becomes T_2', which due to condition (2.46) is more than $T_1'(B_2/B_1)$. Thus heat should flow from the cold bath to the spin or $q_2 > 0$. Similar considerations lead to rejection of heat by the spin at the hot bath or $q_1 < 0$.

2.6 Upper bound for global efficiency ($B_1 > B_2$)

We consider the case of the engine working in the range $B_1 > B_2$. The condition to get a *higher* efficiency as compared to the uncoupled model is the case (ii) discussed in Section 2.5.1 and is given by

$$p_1 > p_1'. \tag{2.47}$$

From the condition $B_2/T_2 > B_1/T_1$ (Eq. (2.33)), we get

$$p_3 > p_3', \tag{2.48}$$

$$p_4 > p_4'. \tag{2.49}$$

Then normalisation of the probabilities gives

$$p_2' > p_2. \tag{2.50}$$

From Eqs. (2.47) and (2.50), we have

$$\frac{p_2'}{p_1'} > \frac{p_2}{p_1}, \tag{2.51}$$

which simplifies to

$$e^{(B_2-4J)/T_2} > e^{(B_1-4J)/T_1}. \tag{2.52}$$

Fig. 2.6 shows three possible ways of arranging the energy levels $(2J-2B_1)$ and $-6J$ relative to the level $(2J-2B_2)$ resulting from the first quantum adiabatic process. Equivalently, Eq. (2.52) is of the form $e^x > e^y$, which may be satisfied in one of the following three ways: Case (a) represents $y > 0$, $x > 0$ and so $x > y$. This implies, $B_1 > 4J$ and $B_2 > 4J$.

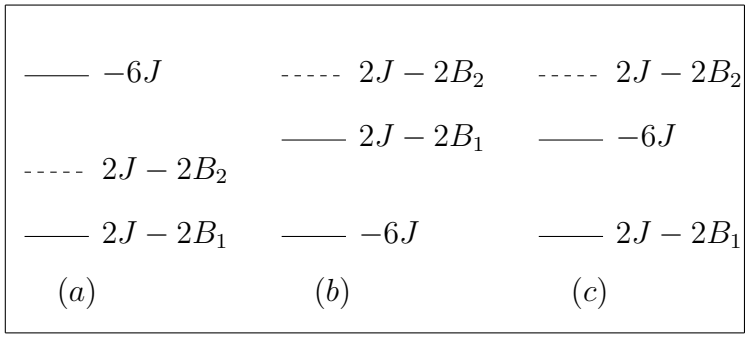

Figure 2.6: Three possible configurations of energy levels with eigenvalues $-6J$, $(2J-2B_1)$ and the level $(2J-2B_2)$ resulting from the first quantum adiabatic process whereby B_1 is changed to a lower value B_2. Only case (a) is possible as discussed in the Section 2.6.

Case (b) represents $x<0$, $y<0$ and $|x|<|y|$. This implies $B_1<4J$, $B_2<4J$, but due to the fact $T_2/T_1<1$, we obtain $B_1<B_2$ which leads to a contradiction.

Case (c) represents $y<0$ and $x>0$. This possibility is also similarly ruled out.

So the only possibility is case (a) representing the fact that the energy levels $(2J-2B_1)$ and $(2J-2B_2)$ lie below the level $-6J$ when the coupled engine gives a *higher* efficiency than the uncoupled case.

When the inequality (2.52) holds, we can write

$$\frac{B_2-4J}{T_2}>\frac{B_1-4J}{T_1}. \tag{2.53}$$

Since $B_1>4J$, $B_2>4J$ and $T_1>T_2$, we get

$$\frac{\eta_0}{1-4J/B_1}<\eta_c=1-\frac{T_2}{T_1}, \tag{2.54}$$

where $\eta_0=1-B_2/B_1$. Now the global efficiency defined as $\eta=W/Q_1$, can be written as

$$\eta=\frac{\eta_0}{1-\frac{4J(p_1-p_1')}{B_1(p_4-p_4'+p_2'-p_2)}}. \tag{2.55}$$

From the inequalities between the probabilities (Eqs. (2.47),(2.49) and (2.50)), it follows that $(p_1-p_1')<(p_4-p_4'+p_2'-p_2)$. Therefore, we finally obtain that when the efficiency is higher than the uncoupled case (or the lower bound is η_0), then an upper bound for efficiency is given by

$$\eta<\frac{\eta_0}{1-4J/B_1}<\eta_c. \tag{2.56}$$

When $J = 0$, we have $\eta = \eta_0$. The upper bound for the efficiency in the case of $B_2 > B_1$ is discussed in the following subsection. Interestingly, we get the same expression for the upper bound as shown in Eq. (2.56).

2.6.1 Upper bound for global efficiency ($B_2 > B_1$)

In Section 2.6, we have derived the upper bound for the efficiency of the engine working in the regime $B_1 > B_2$. We can construct a similar proof to show that the upper bound for the efficiency of the engine operating in the regime $B_2 > B_1$, is less than Carnot efficiency and the expression of the upper bound is same as the expression obtained in the case of $B_1 > B_2$ (Eq. (2.56)). From Eqs. (2.39) and (2.40), we get

$$\frac{p_1'}{p_2'} > \frac{p_1}{p_2}. \tag{2.57}$$

This can be expressed as

$$\exp\left(8J - 2B_2\right)/T_2 > \exp\left(8J - 2B_1\right)/T_1. \tag{2.58}$$

This inequality is satisfied only when $4J > 2B_1$ and $4J > 2B_2$. So it can be shown that the energy levels $2J - 2B_1$ and $2J - 2B_2$ should lie above the energy level $-6J$. When the inequality is satisfied in Eq. (2.58), we can write,

$$\frac{4J - B_2}{4J - B_1} > \frac{T_2}{T_1}. \tag{2.59}$$

Each side of the above equation is less than one. So subtracting both the sides from 1 and re-arranging the equation we can write

$$1 - \frac{T_2}{T_1} > \frac{1 - B_2/B_1}{1 - 4J/B_1}. \tag{2.60}$$

The global efficiency (η) for both the cases $B_1 > B_2$ and $B_2 > B_1$ is given in Eq. (2.55).

Applying the conditions of probabilities, we have $(p_1' - p_1) > (p_4' - p_4 + p_2 - p_2')$. So considering Eqs. (2.55) and (2.60), we can write

$$1 - \frac{T_2}{T_1} > \frac{1 - B_2/B_1}{1 - 4J/B_1} > \eta. \tag{2.61}$$

2.7 Extensions

One can study the Otto cycle for different Heisenberg models and also with higher number of spins. A general program for n-spin system for both isotropic and anisotropic Heisenberg models with homogeneous as well as inhomogeneous magnetic field is given in Appendix A.1.

Our work on quantum Otto cycle influenced some of the recent studies. In Ref. [61], a quantum Brayton cycle is considered. Brayton cycle consists of two isobaric process and two adiabatic processes. The working substance in this model is two spins coupled via Heisenberg XX interaction. The Hamiltonian is given as

$$H = J(\sigma_+^{(1)}.\sigma_-^{(2)} + \sigma_-^{(1)}.\sigma_+^{(2)}) + B(\sigma_z^{(1)} + \sigma_z^{(2)}), \tag{2.62}$$

where $\sigma_+^{(i)}$ and $\sigma_-^{(i)}$ are the raising and the lowering operators for the ith spin. If p_i and E_i are the occupation probability and energy of the ith energy eigenstate respectively, then the pressure is defined as

$$F = \sum_i p_i \frac{dE_i}{dL}. \tag{2.63}$$

Here L is the generalized coordinate of the system. In this model, two generalized coordinates $L_x = 1/B$ and $L_y = 1/J$ are considered. The corresponding pressures for L_x and L_y are F_x and F_y. In the cycle, one possibility is to keep F_y and L_x as constants during the isobaric processes. The cycle constructed with these conditions along with a suitable choice of the parameters shows interesting behavior such as the subsystems operate as refrigerators while the total system works as a heat engine. A similar counter-intuitive behavior is discussed in our model in Section 2.5.2. Recently, a similar observation is also made in a special quantum Otto cycle [60] where both magnetic field and the exchange constant are changed during the adiabatic branch. Following our model, an Otto engine using coupled spins with the Hamiltonian given in Eq. (2.62) was also studied [55].

2.8 Summary

A pair of coupled spin-1/2 particles is used as a working medium to realize a quantum Otto engine. The conditions for the efficiency to be higher than the non-interacting

case are found. The antiferromagnetic interaction between the spins allows a fraction of the total heat to flow from cold bath to hot bath provided the total heat should flow in a direction suggested by global temperature gradient. This mechanism increases the efficiency of the system compared to the case of non-interacting spins. A tighter upper bound for efficiency is found below the Carnot value. The system can also work as a heat engine even if it undergoes an adiabatic compression ($B_2 > B_1$) in the second stage of the cycle. Here we have observed an interesting mode of operation using the reduced density matrix whereby each spin absorbs heat from the cold bath and rejects some heat to the hot bath while performing net work. This feature is also confirmed from the analysis of local effective temperatures of the spins. Recent developments in this field show similar observations in other models of heat engines [61, 60].

Chapter 3

Friction in quantum heat engines

3.1 Introduction

In finite-time heat engines, friction is one of the major causes for the loss of useful energy. Frictional effect in classical heat engines has been studied in [13, 26, 27]. In this chapter, we focus on quantum analogue of internal friction observed in finite-time quantum heat engines [75, 41, 74, 99]. This effect arises when the non-commutativity of the internal and the external part of the Hamiltonian leads to the non-commutativity of the total Hamiltonians at different times, $[H(t), H(t')] \neq 0$. The model of the heat engine [117] considered in this chapter is similar to the one discussed in Chapter 2, but there is an explicit difference in the driving of the system during the adiabatic branches. Here the driving is finite-time and inhomogeneous, i.e. one of the spins of the coupled system is driven at a finite-rate and thereby a frictional effect arises. An interesting analogy to this observation is the frictional effect arises when the parts of a system move with different relative rates. The origin of friction in certain models of QHEs was first reported in [75, 41]. Further to reduce this friction, quantum lubrication has also been proposed [42]. In order to better understand intrinsic friction and its relevance for the analysis of dissipation in driven quantum systems, it seems interesting to look for this effect in other similar models. Before discussing our mechanism of internal friction, we briefly go through an interesting model introduced in [75]. The working medium in this model consists of two spin-1/2 systems coupled via anisotropic Heisenberg interaction

$$H = 2^{-3/2}\omega(t)(\sigma_z^{(1)} \otimes I^{(2)} + I^{(1)} \otimes \sigma_z^{(2)}) + 2^{-3/2}J(\sigma_x\sigma_x - \sigma_y\sigma_y), \tag{3.1}$$

where $\omega(t)$ is the external control field. The first term on the right hand side is the external part of the Hamiltonian and the second term is the internal part of the Hamiltonian. These two terms do not commute and hence changing the externally controlled field $\omega(t)$ leads to non-commutativity of the Hamiltonian at different instants. The Hamiltonian of the working medium can also be written as

$$H = \sum_j h_j B_j, \tag{3.2}$$

where $\{B_j\}$ are the minimal set of operators. In this model, the performance of the engine is estimated by evaluating the equation of motion of this set of operators and the corresponding observables ($\{\langle B_j \rangle\}$). In this particular model, the operators are chosen in such a way that they form a Lie algebra, such that $[B_i, B_j] = \sum_k C_{ij}^k B_k$, where the coefficients C_{ij}^k are called the structure factors of the Lie algebra. Hence these operators are closed under the unitary evolution [6]. In general, these operators undergo evolution such that $\partial B_j/\partial t = \mathcal{L}_H^* B_j + \mathcal{L}_D^* B_j$, where $\mathcal{L}_H^*$ and $\mathcal{L}_D^*$ represent the unitary and the non-unitary part of the evolution respectively. During the adiabatic process, only the unitary part contributes, which is given as $\mathcal{L}_H^* B_j = i[H, B_j]$. Since the $\{B_j\}$ form a Lie algebra, these operators are closed under the operation $\mathcal{L}_H^*$ [6]. On the other hand, when the system is in contact with a bath, the non-unitary part also contributes in the evolution of the system. In this particular model of the quantum heat engine, a particular set of operators are found so that these are closed under both $\mathcal{L}_H^*$ and $\mathcal{L}_D^*$. Further the thermodynamic quantities pertaining to the system are calculated and the performance of the engine under friction is studied. But to understand different mechanisms from which friction arises, further studies on different models are necessary.

In the quantum heat engine that we discuss below, the working medium (system) consists of two spin-half particles with isotropic Heisenberg interaction, kept in an external magnetic field, similar to the model discussed in Chapter 2. But the difference in driving is that it is finite-time and selective. The system is driven by selectively changing the external field applied over one of the spins. This inhomogeneous driving causes frictional effect. But if the field on both the spins remains homogeneous, then friction is absent. As expected, we find that if the driving that creates inhomogeneity of fields on the spins, is performed very slowly, the friction effect is again absent. An analogous system under an inhomogeneous magnetic field

plays important role in quantum computing [59]. Thermal entanglement of such spin system [18] and similar models [5] have also been studied.

Internal friction is observed only when the Hamiltonian is time dependent. So we first discuss the evolution of the system under the time-dependent Hamiltonian. Even so, the system does not exhibit friction if it is driven slowly enough. This is because in slow driving, the quantum adiabatic theorem holds and the system will always be in the instantaneous eigenstate of the Hamiltonian. We also discuss the consequence of quantum adiabatic theorem in the evolution of the system. Subsequently, we introduce our model in which the friction arises due to the inhomogeneous driving. To characterize friction, we study the dynamics, the entropy production and the work characteristics in the finite-time driving.

3.1.1 Time evolution with time-dependent Hamiltonian

The Schroedinger equation for the time evolution operator is given as

$$i\hbar\frac{\partial}{\partial t}U(t,t_0) = H(t)U(t,t_0). \tag{3.3}$$

This fundamental equation [103] leads to the time dependent Schroedinger equation for the state ket, which is given as

$$i\hbar\frac{\partial\psi(t)}{\partial t} = H(t)\psi(t). \tag{3.4}$$

Depending upon different physical situations, there are mainly three cases, for which the solution for Eq. (3.3) has to be derived. Here we are interested in a situation where the Hamiltonian is time-dependent and Hamiltonians for different times do not commute, $[H(t'), H(t'')] \neq 0$. So the general solution for Eq. (3.3), subject to the initial condition

$$U(t,t_0)|_{t=t_0} = I, \tag{3.5}$$

is given as

$$U(t,t_0) = I - \frac{i}{\hbar}\int_{t_0}^{t} H(t_1)U(t_1,t_0)dt_1. \tag{3.6}$$

This can be expanded by iteration as

$$U(t,t_0) = I - \frac{i}{\hbar}\int_{t_0}^{t} H(t_1)\left[I - \frac{i}{\hbar}\int_{t_0}^{t_1} H(t_2)U(t_2,t_0)dt_2\right]dt_1. \tag{3.7}$$

The series followed by such iterations is written as

$$\begin{aligned} U(t,t_0) = \quad I \quad & -\frac{i}{\hbar}\int_{t_0}^{t} H(t_1)dt_1 \\ & +\left(\frac{-i}{\hbar}\right)^2 \int_{t_0}^{t} dt_1 \int_{t_0}^{t_1} dt_2 H(t_1)H(t_2) \\ & +\left(\frac{-i}{\hbar}\right)^3 \int_{t_0}^{t} dt_1 \int_{t_0}^{t_1} dt_2 \int_{t_0}^{t_2} dt_3 H(t_1)H(t_2)H(t_3) \\ & +\cdots \end{aligned} \tag{3.8}$$

This series is known as Dyson series. Here the Hamiltonians at different times are placed in order such that the ones later in time, are in the left. Using the property of the integral, we can write

$$\int_{t_0}^{t} dt_1 \int_{t_0}^{t_1} dt_2 ... \int_{t_0}^{t_2} dt_n H(t_1)H(t_2)..H(t_n) \tag{3.9}$$

$$= \frac{1}{n!}\int_{t_0}^{t} dt_1 \int_{t_0}^{t} dt_2 ... \int_{t_0}^{t} dt_n \mathcal{T}\{H(t_1)H(t_2)..H(t_n)\}. \tag{3.10}$$

The geometrical interpretation for this identity is discussed in [92]. Now the series in Eq. (3.8) corresponding to the time evolution operator can be written in a more compact form as

$$U(t,t_0) = \mathcal{T} e^{(-i/\hbar)\int_{t_0}^{t}(H(t')dt'}. \tag{3.11}$$

In this chapter, we discuss the application of this unitary operator in an adiabatic branch to explore frictional effect observed in a quantum heat engine.

3.1.2 Quantum adiabatic theorem

In 1929, M. Born and V. Fock came up with an elegant property of time evolution of a quantum system called quantum adiabatic theorem [28]. This theorem plays an important role in the quantum heat cycles discussed herein. An interesting description of the quantum adiabatic process is given in [51]. Suppose the system is initially in the nth eigenstate of the initial Hamiltonian (H_{ini}). Then the Hamiltonian is changed gradually from H_{ini} to H_{fin}. According to quantum adiabatic theorem, the system will remain in the nth eigenstate of the final Hamiltonian.

Consider a Hamiltonian which changes with time and suppose the Hamiltonians at different instants do not commute. This implies that the Hamiltonian at two different times may not have a common set of eigenstates. Hence the eigenfunctions

and eigenvalues are time-dependent. But, at any instant, there exists an orthonormal set $\{\phi_n\}$ such that

$$H(t)\phi_n(t) = E_n(t)\phi(t), \tag{3.12}$$

where $E_n(t)$ is the eigenvalue corresponds to the eigenfunction ϕ_n of $H(t)$. Here we consider the non-degenerate and discrete eigenvalue spectrum throughout the evolution. The general solution to the time-dependent Schroedinger equation (Eq. (3.3)) can be written as a linear combination of the eigenfunctions of the Hamiltonian at time t.

$$\psi(t) = \sum_n c_n(t)\phi_n(t)e^{i\alpha_n(t)}, \tag{3.13}$$

where

$$\alpha_n(t) = -\frac{1}{\hbar}\int_0^t E_n(t')dt'. \tag{3.14}$$

Substituting Eq. (3.13) in Eq. (3.3) and canceling the relevant terms according to Eq. (3.12), we get

$$\sum_n \dot{c}_n(t)\phi_n(t)e^{i\alpha_n(t)} = -\sum_n \dot{c}_n(t)\dot{\phi}_n(t)e^{i\alpha_n(t)}. \tag{3.15}$$

Taking the inner product with ϕ_m, we obtain

$$\dot{c}_m = -\sum_n \dot{c}_n(t)\langle\phi_m|\dot{\phi_n}\rangle(t)e^{i(\alpha_n-\alpha_m)}. \tag{3.16}$$

Differentiating Eq. (3.12) with time and then taking inner product with ϕ_m, we get

$$\langle\phi_m|\dot{H}|\phi_n\rangle + \langle\phi_m|H|\dot{\phi}_n\rangle = E_n\langle\phi_m|\dot{\phi}_n\rangle, \tag{3.17}$$

for $n \neq m$. Now we can write

$$\langle\phi_m|\dot{\phi}_n\rangle = \frac{\langle\phi_m|\dot{H}|\phi_n\rangle}{E_n - E_m}. \tag{3.18}$$

Substituting this in Eq. (3.16), we get

$$\dot{c}_m = -c_m\langle\phi_m|\dot{\phi}_m\rangle - \sum_{n\neq m} c_n\frac{\langle\phi_m|\dot{H}|\phi_n\rangle}{E_n - E_m}e^{(-i/\hbar)\int_0^t(E_n(t')-E_m(t'))dt'}. \tag{3.19}$$

Now consider the adiabatic approximation which demands that $\dot{H}$ is extremely small, so that we can neglect the second term in the above equation. Therefore we get

$$\dot{c}_m = -c_m\langle\phi_m|\dot{\phi}_m\rangle, \tag{3.20}$$

which yields a solution

$$c_m(t) = c_m(0)e^{i\gamma_m(t)}, \tag{3.21}$$

where

$$\gamma_m = i\int_0^t \left\langle \phi_m(t')|\frac{\partial}{\partial t'}\phi_m(t')\right\rangle dt'. \tag{3.22}$$

This suggests that if the system starts in an eigenstate of the Hamiltonian ($\psi(0) = \phi_k(0)$), i.e. $c_k(0) = 1$, then from Eq. (3.13), the final state is given as

$$\psi(t) = e^{i\alpha_k(t)}e^{i\gamma_k(t)}\phi_k(t). \tag{3.23}$$

So the system remains in the instantaneous eigenstate of the Hamiltonian with additional phase factors.

3.2 Model

We consider two spin-half particles with isotropic exchange interaction, as the working substance for a quantum Otto cycle. In general, the Hamiltonian is written as $H = H_{\text{int}} + H_{\text{ext}}$, where H_{ext} is the external Hamiltonian which can be controlled and H_{int} is the internal Hamiltonian. In our model, we control in time, the magnetic field applied to particle labeled 2. So we have [117]

$$H_{\text{int}} = J(\sigma^{(1)}.\sigma^{(2)} + \sigma^{(2)}.\sigma^{(1)}), \tag{3.24}$$

$$H_{\text{ext}} = B_1\sigma_z^{(1)} + B_2(t)\sigma_z^{(2)}, \tag{3.25}$$

where $\sigma^{(i)} = (\sigma_x^{(i)}, \sigma_y^{(i)}, \sigma_z^{(i)})$ are the Pauli matrices, J is the isotropic exchange constant and B_1, $B_2(t)$ are the magnetic fields applied along z-axis to the first and the second spin respectively. So the magnetic field applied to the individual spins are not always equal during the adiabatic branch which results in $[H_{\text{ext}}, H_{\text{int}}] \neq 0$. This non-commutativity of the external and the internal Hamiltonian when leading to non-commutativity of the Hamiltonian at different times, is the cause of internal friction in our model [75, 41]. As a special case, we show in Section V that the non-commutative property of external and the internal Hamiltonian by itself is not a sufficient condition for friction.

Now we analyse the system under an inhomogeneous magnetic field in more detail. In this case the eigenbasis of the Hamiltonian is $\{|\psi_i\rangle; i = 1, .., 4\} \equiv \{|\psi_1\rangle,$

$|00\rangle$, $|\psi_3\rangle$, $|11\rangle\}$, where $|\psi_1\rangle$ and $|\psi_3\rangle$ are given by $b|10\rangle - a|01\rangle$ and $a|10\rangle + b|01\rangle$ respectively and $\{|00\rangle, |10\rangle, |01\rangle, |11\rangle\}$ forms the computational basis. Here $a = (y + \sqrt{1+y^2})/N$ and $b = 1/N$, where $N = \sqrt{1 + (y + \sqrt{1+y^2})^2}$ and $y = (B_1 - B_2(t))/4J$. The corresponding eigenvalues are $\{-2J-K, 2J-B_1-B_2(t), -2J+K, 2J + B_1 + B_2(t)\}$, where $K = 4J(\sqrt{1+y^2})$. The equilibrium density matrix when the system is attached to a bath at temperature T_e, is given by $\rho = \exp(-H/T_e)/Z$, where $Z = \mathrm{Tr}(\exp(-H/T_e))$ is partition function of the system, and we have set Boltzmann's constant to unity. The eigenvalues of ρ, or the occupation probabilities of the energy levels, are given by

$$\begin{aligned} P_1 &= e^{-(-2J-K)/T_e}/Z, \\ P_2 &= e^{-(2J-B_1-B_2(t))/T_e}/Z, \\ P_3 &= e^{-(-2J+K)/T_e}/Z, \\ P_4 &= e^{-(2J+B_1+B_2(t))/T_e}/Z. \end{aligned} \tag{3.26}$$

Now we are ready to discuss the quantum heat cycle, which consists of the following four stages:

Stage 1: The magnetic field applied to the first and second spins are identical ($B_1 = B_2$). The coupled-spins system is attached to a cold bath with temperature T_1. The system attains equilibrium with the bath. The density matrix is diagonal in the Hamiltonian's eigenbasis. Because of the homogeneous magnetic field, the eigenstates $|\psi_1\rangle$ and $|\psi_3\rangle$ are maximally entangled Bell states, with $a = b = 1/\sqrt{2}$. The occupation probability $\{p_j\}$ for the state with energy eigenvalue $\{E_j\}$ is calculated from Eq. (3.26) by setting $T_e = T_1$ and $B_2 = B_1$. So the mean energy at the end of the first stage is $\mathrm{Tr}(\rho H) = \sum_j E_j p_j$.

Stage 2: In this stage, the system is isolated from the bath and it can only exchange work with the surroundings. The magnetic field applied to the second spin is changed from $B_2(0) = B_1$ to $B_2(t) = B_3$ in finite time and the system may undergo a non-adiabatic evolution. By non-adiabatic evolution, we mean that the system may be driven fast enough so that the quantum adiabatic theorem does not hold [28, 71]. The density matrix undergoes a unitary evolution. The eigenstates of $H(t)$ are also time dependent. In general, the eigenstates of $\rho(t)$ are not the same as $H(t)$. In the infinitely slow limit ($t \to \infty$), the adiabatic theorem holds and

eigenstates of the density matrix are identical to the eigenstates of the instantaneous Hamiltonian.

So in the case of a fast driving, the final state of the system may not be diagonal in the eigenbasis of the final Hamiltonian. When we project the final density matrix onto the eigenbasis of the Hamiltonian, the corresponding occupation probability of the eigenstate of the Hamiltonian with eigenvalue E'_j is given as $p'_i = \mathrm{Tr}\left(|\psi'_i\rangle\langle\psi'_i|\rho(t)\right)$, where $|\psi'_i\rangle$ is the eigenstate of the final Hamiltonian. In our model, we have assumed that the energy levels do not cross [11, 12]. A pictorial representation is shown in Fig. 3.1. At the end of the second stage, the mean energy can be written as $\mathrm{Tr}(\rho(t)H(t)) = \sum_j E'_j p'_j$. The difference of the initial and the final mean energy is equal to the work performed during the adiabatic process: $W_I = \sum_j E_j p_j - \sum_j E'_j p'_j$.

Stage 3: The system under an inhomogeneous magnetic field is attached to a hot bath with temperature T_2 and it attains equilibrium by absorbing net heat from the bath. The occupation probabilities (q_j) are calculated from Eq. (3.26) by putting $B_2 = B_3$ and $T_e = T_2$. At the end of the third stage, the system is in a thermal state with mean energy $\sum_j E'_j q_j$.

Stage 4: The system again undergoes a unitary evolution by a change of the magnetic field of the second spin from B_3 to B_1, whereby the energy levels change from E'_j back to E_j. The occupation probabilities q'_j in the eigenstates of the Hamiltonian are calculated by projecting the density matrix onto the eigenbasis of the Hamiltonian. So the mean energy at the end of the process is $\sum_j E_j q'_j$. The difference in the mean energy due to this process is $W_{II} = \sum_j E'_j q_j - \sum_j E_j q'_j$.

To close the cycle, the system is again brought in contact with the cold bath. The system on average releases an amount of heat to cold bath. As we show below, W_I and W_{II} are the work done *by* and *on* the system, respectively.

3.3 Dynamics on the adiabatic branch and entropy production

Now we analyse the irreversibility associated with the adiabatic branch by quantifying the entropy production. The adiabatic process is represented by a unitary

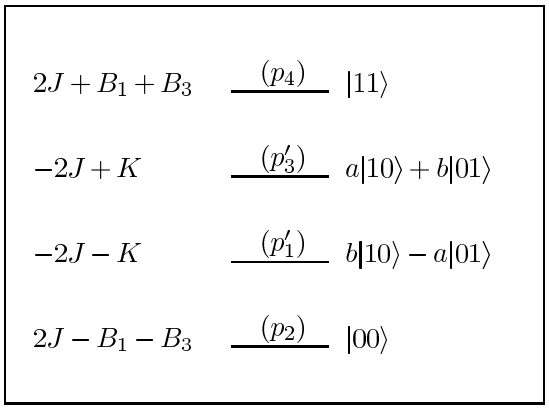

Figure 3.1: A pictorial representation of eigenvalues and eigenstates of the Hamiltonian at the end of first adiabatic process (stage 2). The $\{p'_i\}$ represent the populations in the energy eigenbasis $\{|\psi'_i\rangle\}$. In the infinite time limit, we get $p'_i = p_i$ and the eigenstates of the density matrix are same as that of the Hamiltonian.

process so that after a time t, the system-state evolves to $\rho(t) = U(t,0)\rho(0)U^\dagger(t,0)$, where $U = \mathcal{T}\exp\left(-i\int_0^t H(t')dt'\right)$. The von Neumann entropy S_v remains constant throughout the process. But energy-entropy S_e, defined with the occupational probabilities of the energy levels, changes. S_e in the initial state is given by $-\sum_i p_i \ln p_i$, where $p_i = \mathrm{Tr}(|\psi_i\rangle\langle\psi_i|\rho(0))$. Since the initial state is a thermal state, we have $S_e = S_v$. But after the finite-time adiabatic step, S_e increases where as S_v remains unchanged. Initially, we have $[H(0), \rho(0)] = 0$. Two of the eigenstates $|00\rangle$ and $|11\rangle$ of the Hamiltonian are not functions of the applied magnetic field and hence are independent of time. So if the system is in any of these *two* eigenstates, it will remain there during the process. Thus the initial population in theses states remains constant throughout the adiabatic process.

But the eigenstates $|\psi_1\rangle$ and $|\psi_3\rangle$ of the Hamiltonian depend on the magnetic field and hence are time dependent. So if the system is initially in one of these states, then changing the Hamiltonian with a finite rate results in a non-adiabatic evolution. In other words, the final state of the system is then not an eigenstate of the final Hamiltonian. Let the eigenstates of the final Hamiltonian be given as $\{|\psi'_1\rangle, |00\rangle, |\psi'_3\rangle, |11\rangle\}$ and the set of the eigenstates of the final density matrix is $\{|\phi'_1\rangle, |00\rangle, |\phi'_3\rangle, |11\rangle\}$. Since $|\phi'_1\rangle$ and $|\phi'_3\rangle$ are orthogonal to each other as well as to $|00\rangle$ and $|11\rangle$, we can express the kets $|\phi'_1\rangle$ and $|\phi'_3\rangle$ as linear combinations of $|\psi'_1\rangle$

and $|\psi_3'\rangle$ as

$$\begin{aligned} |\phi_1'\rangle &= \cos(\delta/2)|\psi_1'\rangle - \sin(\delta/2)|\psi_3'\rangle, \\ |\phi_3'\rangle &= \sin(\delta/2)|\psi_1'\rangle + \cos(\delta/2)|\psi_3'\rangle, \end{aligned} \tag{3.27}$$

where $0 \leq \delta \leq \pi$. Now consider a projection of the system-state on to the eigenbasis of Hamiltonian. Two of the populations remain unchanged such that $p_2' = p_2$ and $p_4' = p_4$. The occupation probabilities for the eigenstates $|\phi_1'\rangle$ and $|\phi_3'\rangle$ are p_1 and p_3 respectively. Now project the density matrix onto the eigenbasis $\{|\psi_i'\rangle\}$ of the final Hamiltonian. From Eq. (3.27), we get the occupation probabilities corresponding to $|\psi_1'\rangle$ and $|\psi_3'\rangle$ as

$$\begin{aligned} p_1' &= p_1 \cos^2(\delta/2) + p_3 \sin^2(\delta/2), \\ p_3' &= p_1 \sin^2(\delta/2) + p_3 \cos^2(\delta/2). \end{aligned} \tag{3.28}$$

Due to $p_1 > p_3$, we can write

$$\begin{aligned} p_1 \geq p_1' \geq p_3, \\ p_1 \geq p_3' \geq p_3. \end{aligned} \tag{3.29}$$

As the difference between p_1' and p_3' gets reduced as compared to the one between p_1 and p_3, and recalling that $p_2' = p_2$ and $p_4' = p_4$, the distribution $\{p_i'\}$ is more uniform than $\{p_i\}$, so we have

$$-\sum_{i=1}^{4} p_i' \ln p_i' \geq -\sum_{i=1}^{4} p_i \ln p_i, \tag{3.30}$$

which signifies that the energy-entropy S_e increases during the finite-time adiabatic process. In the infinite time process ($t \to \infty$), the system undergoes quantum adiabatic evolution and in this limit S_e remains unchanged. The total entropy production versus the total time allocated to adiabatic branch will be discussed in Section V.

3.4 Work

The work is performed by or on the system only during the adiabatic branches i.e. in stages 2 and 4, when the evolution of the system is governed by Liouville-von

Neumann equation (with $\hbar = 1$)

$$\frac{d\rho(t)}{dt} = -i\left[H(t), \rho(t)\right]. \tag{3.31}$$

The instantaneous mean energy of the system is given by $\mathrm{Tr}(\rho(t)H(t))$. Differentiating with respect to time we get

$$\mathrm{Tr}\left(\frac{d(H(t)\rho(t))}{dt}\right) = \mathrm{Tr}\left(H(t)\frac{d\rho(t)}{dt}\right) + \mathrm{Tr}\left(\frac{dH(t)}{dt}\rho(t)\right), \tag{3.32}$$

In general, comparing with the first law of thermodynamics, we identify [7] the first term on the right hand side as the rate of heat flow ($\dot{Q}$) and the second term as the power ($\wp$). For an adiabatic process, the first term above on the right hand side vanishes due to Eq. (3.31).

Upon integrating the power, we get the expression for work as

$$\begin{aligned} W = \int_0^t \wp dt &= \int_0^t \mathrm{Tr}\left(\frac{dH(t')}{dt'}\rho(t')\right)dt', \\ &= \int_0^t \mathrm{Tr}\left(\frac{d(H(t')\rho(t'))}{dt'}\right)dt'. \end{aligned} \tag{3.33}$$

Thus the work performed during the adiabatic process lasting for a time interval t, is equal to the change in the mean energy of the system.

3.4.1 Local work

We are changing the magnetic field associated with the second spin, so it is interesting to follow the temporal behavior of individual spins. The Hamiltonian of our system $H(t) = H_1 \otimes I_2 + I_1 \otimes H_2(t) + H_{\mathrm{int}}$, where subscript 1 and 2 indicates the first and second spin respectively and I_1 and I_2 are the 2×2 identity matrices. Here only H_2 depends on time. So we can write

$$\mathrm{Tr}\left(\frac{dH(t)}{dt}\rho(t)\right) = \mathrm{Tr}\left(I_1 \otimes \frac{dH_2(t)}{dt}\rho(t)\right). \tag{3.34}$$

Using $\mathrm{Tr}_1(\rho(t)) = \rho_2(t)$, we can write

$$\begin{aligned} \mathrm{Tr}\left(\frac{dH(t)}{dt}\rho(t)\right) &= \mathrm{Tr}_2\mathrm{Tr}_1\left(I \otimes \frac{dH_2(t)}{dt}\rho(t)\right) \\ &= \mathrm{Tr}_2\left(\frac{dH_2(t)}{dt}\rho_2(t)\right). \end{aligned} \tag{3.35}$$

This is the instantaneous local power. Integrating the local power with respect to time we get the local work. Substituting Eq.(3.35) in Eq. (3.33), we get

$$W = w_2(t) = \int_0^t \mathrm{Tr}_2 \left(\frac{dH_2(t')}{dt'} \rho_2(t') \right) dt', \tag{3.36}$$

where w_2 is the work obtained from the second spin. Since we are not changing the magnetic field associated with the first spin the work obtained from the first spin is zero. So in general we can show that if we change the magnetic field of both the spins with different rates, then the total work will be the sum of local work ($W = w_1 + w_2$). This is similar to the expression obtained in Section 2.5, where the magnetic field associated with the both the spins varies together. The above proof holds if only H_1 and/or H_2 are functions of time and H_{int} is assumed to be independent of time. If for instance, we change the parameter J during an adiabatic branch [127] instead of the magnetic field, then H_{int} becomes a function of time and in this case, the total work cannot be written as the sum of the individual contributions.

3.4.2 Work done in slow and fast process

It can be shown that the work done in a infinitely slow process is always higher than the work done in a finite-time process. Thus the lower bound for work extracted is obtained for an extremely fast process ($t \to 0$). To evaluate the lower bound, we assume that the density matrix of the system remains unchanged. In case of equilibrium with the cold bath, the initial density matrix is given as

$$\rho = p_1 |\phi_1\rangle\langle\phi_1| + p_2 |00\rangle\langle 00| + p_3 |\phi_3\rangle\langle\phi_3| + p_4 |11\rangle\langle 11|, \tag{3.37}$$

where $|\phi_1\rangle = (|10\rangle - |01\rangle)/\sqrt{2}$ and $|\phi_3\rangle = (|10\rangle + |01\rangle)/\sqrt{2}$. Since the system is in thermal state, the initial Hamiltonian commutes with the density matrix and both have the same set of eigenvectors. In the sudden limit ($t \to 0$), the density matrix remains the same as the initial, because $U(0,0) = I$. But the Hamiltonian is changed to

$$\begin{aligned} H = & - (2J + K)|\psi_1'\rangle\langle\psi_1'| + (2J - B_1 - B_3)|00\rangle\langle 00| \\ & + (-2J + K)|\psi_3'\rangle\langle\psi_3'| + (2J + B_1 + B_3)|11\rangle\langle 11|, \end{aligned} \tag{3.38}$$

where $|\psi_1'\rangle = b|10\rangle - a|01\rangle$ and $|\psi_3'\rangle = a|10\rangle + b|01\rangle$. Now we find the population of the corresponding eigenstates of the Hamiltonian by projecting the density matrix onto the eigenbasis of final Hamiltonian as

$$p_1' = \langle\psi_1'|\rho|\psi_1'\rangle = \frac{(p_1+p_3)}{2} - ab(p_3-p_1), \tag{3.39}$$

$$p_3' = \langle\psi_3'|\rho|\psi_3'\rangle = \frac{(p_1+p_3)}{2} + ab(p_3-p_1), \tag{3.40}$$

while $p_2' = p_2$ and $p_4' = p_4$. Similarly for the second adiabatic process where the Hamiltonian is returned to its initial form with eigenbasis $\{|\psi_i\rangle\}$, we obtain upon projecting the density matrix $\tilde{\rho}$ for this process, as

$$q_1' = \langle\psi_1|\tilde{\rho}|\psi_1\rangle = \frac{(q_1+q_3)}{2} - ab(q_3-q_1), \tag{3.41}$$

$$q_3' = \langle\psi_3|\tilde{\rho}|\psi_3\rangle = \frac{(q_1+q_3)}{2} + ab(q_3-q_1), \tag{3.42}$$

with $q_2' = q_2$ and $q_4' = q_4$. Now the work extracted in a complete cycle ($W = W_I + W_{II}$) with fast adiabatic processes is given by

$$W^{\text{fast}} = \sum_i p_i E_i - \sum_i p_i' E_i' + \sum_i q_i E_i' - \sum_i q_i' E_i. \tag{3.43}$$

Using the probabilities calculated above for extremely fast (sudden) processes, we get the lower bound of work

$$\begin{aligned} W_{\text{lb}} = \quad & (B_3 - B_1)(q_4 - q_2 + p_2 - p_4) \\ & + (q_3 - q_1)(K - 8Jab). \end{aligned} \tag{3.44}$$

Note that this is the lower bound (lb) for the work extractable from this system with the Otto cycle. Here we assumed that the system reaches thermal equilibrium with the baths during the thermalization stages. If instead, a partial equilibration is allowed, then the results for extractable work will be different. Further, a necessary condition to extract work can be obtained by requiring $W_{\text{lb}} > 0$. We assume that $B_3 > B_1$. Now the second term in equation (3.44) is negative, since $q_1 > q_3$ and $(K - 8Jab) > 0$ because of $K > 4J$ and $ab < 1/2$. This requires that the following condition be satisfied for the engine operation: $(p_2 - p_4) > (q_2 - q_4)$.

The upper bound for work is obtained for the slow process ($t \to \infty$). According to quantum adiabatic theorem, the system remains in the instantaneous eigenstate

of the Hamiltonian. The work expression is in general written as

$$W^{\text{slow}} = \sum_i p_i E_i - \sum_i p_i E_i' + \sum_i q_i E_i' - \sum_i q_i E_i, \tag{3.45}$$

and yields the upper bound for the extractable work,

$$\begin{aligned} W_{\text{ub}} = \quad & (B_3 - B_1)(q_4 - q_2 + p_2 - p_4) \\ & + (q_3 - q_1 + p_1 - p_3)(K - 4J). \end{aligned} \tag{3.46}$$

These bounds are compared with the finite-time work in Fig. (3.2).

3.5 Local dynamics of spins with slow driving

In the following, we study the local dynamics of the individual spins in a slow adiabatic branch, using the reduced density matrix. When an individual spin is considered, it is no more an isolated system as it interacts with the neighboring spin. In case of the first spin, the local Hamiltonian remains unchanged during the process but the density matrix changes with time. So there is only heat flow (Q_1^{loc}) associated with the first spin. But for the case of second spin both the density matrix and local Hamiltonian change with time. This suggests that the second spin is doing work (w_2) as well as it exchanges heat (Q_2^{loc}) with its environment. To analyse this situation, we consider the local dynamics of the first adiabatic process. The initial local Hamiltonian $H_1^{\text{ini}} = H_2^{\text{ini}} = B_1.\sigma_z$ is same for the both the spins. $H_2(t)$ changes with time, the final Hamiltonian for the second spin is $H_2^{\text{fin}} = B_3.\sigma_z$. The initial density matrix, identical for both the spins, is given as

$$\varrho_1^{\text{ini}} = \varrho_2^{\text{ini}} = \begin{pmatrix} p_4 + \frac{(p_1+p_3)}{2} & 0 \\ 0 & p_2 + \frac{(p_1+p_3)}{2} \end{pmatrix}. \tag{3.47}$$

Final density matrix of the first spin is

$$\varrho_1^{\text{fin}} = \begin{pmatrix} p_4 + a^2 p_3 + b^2 p_1 & 0 \\ 0 & p_2 + b^2 p_3 + a^2 p_1 \end{pmatrix}. \tag{3.48}$$

Similarly the reduced density matrix of the second spin is

$$\varrho_2^{\text{fin}} = \begin{pmatrix} p_4 + b^2 p_3 + a^2 p_1 & 0 \\ 0 & p_2 + a^2 p_3 + b^2 p_1 \end{pmatrix}. \tag{3.49}$$

Since no work is done by the first spin, the difference in the mean energy is the heat exchanged. So we have

$$\begin{aligned} Q_1^{\rm loc} &= {\rm Tr}\left[H_1^{\rm ini}.(\varrho_1^{\rm ini}-\varrho_1^{\rm fin})\right] \\ &= (p_3-p_1)(b^2-a^2)B_1. \end{aligned} \tag{3.50}$$

In the case of the second spin, the difference in the mean energy is the sum of heat and work done by the system, $\Delta U_2 = Q_2^{\rm loc} + w_2$. From Eqs. (3.33) and (3.36), we have shown that the work done by the second spin is equal to the mean energy difference of the global system. So we have

$$\begin{aligned} Q_2^{\rm loc} &= {\rm Tr}\left(H_2^{\rm ini}\varrho_2^{\rm ini} - H_2^{\rm fin}.\varrho_2^{\rm fin}\right) - \sum_i (p_i E_i - p_i E_i') \\ &= (p_1-p_3)\left[(b^2-a^2)B_3 - (K-4J)\right]. \end{aligned} \tag{3.51}$$

3.6 Discussion

Analytic expressions for work have been derived both in the case of a very slow driving and a sudden one. To estimate the finite-time evolution of the system on the adiabatic branch, we have to integrate the Liouville-von Neumann equation, Eq. (3.31). We accomplish this using the fourth-order Runge-Kutta method [56]. In the first adiabatic process, $B(t)$ changes from $B_2(0)$ to B_3. This is modeled by applying a pulse $B_2(t) = B_2(0) + (B_3 - B_2(0))\sin(\pi t/\tau)$ for a time $t = \tau/2$, where τ is half of the time period. Similarly the second adiabatic process is done by applying a pulse $B_2(t) = B_3 + (B_2(0) - B_3)\sin(\pi t/\tau)$ for the same time interval. Thus we allot equal time intervals to both the adiabatic branches. The total work performed and the total entropy production due to the finite-time process are plotted in Fig. (3.2). As discussed in the previous section, the work extracted decreases monotonically with a finite rate of driving. This is also reflected in the corresponding entropy production in the finite-time case.

Let us consider a cycle in which the magnetic fields applied to the first and second spins in stage 1 have different values, $B_1(0)$ and $B_2(0)$ respectively. In this case the internal and external part of the Hamiltonian do not commute with each other. Now suppose that during the first adiabatic process, B_1 and B_2 vary at equal rates so that the difference ($\Delta B = B_1(t) - B_2(t)$) keeps constant during the process. As

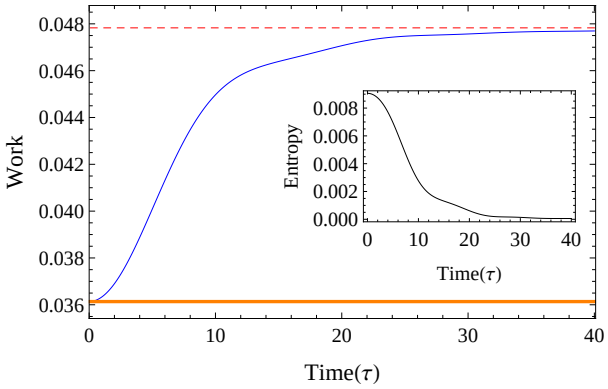

Figure 3.2: Work obtained in a cycle versus the total time (τ) allocated for both the adiabatic processes. Here we use $B_1 = B_2(0) = 3$, $B_3 = 4$, $J = 0.1$, $T_2 = 2$ and $T_1 = 1$. The work is bounded above by $W_{\rm ub}$ (Eq. (3.46), dashed line). The thick horizontal line depicts the lower bound $W_{\rm lb}$, Eq. (3.44), obtained for a sudden adiabatic process ($\tau \to 0$). The inset shows total entropy production on the adiabatic branches versus total time (τ). As τ is increased, the total entropy production reduces monotonically to zero and the frictional effect vanishes.

we have seen in Section 3.2, the parameters a and b appearing in the eigenbasis of the Hamiltonian, are functions of J and ΔB. Since ΔB remains constant during the adiabatic process, the energy eigenstates of the Hamiltonian become time independent which implies that Hamiltonians at different times commute with each other and so friction is absent in this case. Using a similar argument, no friction is expected on the second adiabatic process, when the magnetic fields are restored to their initial values $B_1(0)$ and $B_2(0)$. This serves as an example to appreciate that the non-commutative property of the internal and external Hamiltonian caused by the inhomogeneous magnetic fields may not always lead to non commutativity of Hamiltonian at different times to cause friction. Rather the inhomogeneous driving in which ΔB changes with time leads to the non-commutative property of the Hamiltonian at different times and thereby to frictional effect.

The basic mechanism of intrinsic friction can be argued from the case of a single spin-1/2 system. First consider the Hamiltonian $H = B_z(t)\sigma_z$. In this case, the Hamiltonians at different instants commute. Next, if instead the Hamiltonian is $H = B_z(t)\sigma_z + B_x\sigma_x$, with B_x fixed, then the Hamiltonians at different instants do not commute and a friction-like effect can be seen. Related Hamiltonians are used

in NMR experiments, see, for example [72]. However, in the two-spins model that we consider, intrinsic friction is observed when a part of the system (only one spin) is driven externally at a finite rate. This accords with our intuitive sense of intrinsic friction whereby the effect arises from moving the parts at different relative rates.

In fact, when the magnetic fields on both the spins are changed at the same rate (uniform driving), the extracted work is independent of the driving rate, because friction is absent in this case. To further compare the work characteristics of uniform versus non-uniform driving, we consider, for simplicity, only one adiabatic process, in which the initial state is a thermal state, and the field on one/both the spins is changed from the initial value B_1 to final value B_3 . With uniform driving, the expression for work is the same as derived in the quantum adiabatic limit (very slow driving) [114], and is given by:

$$W_u = 2(B_3 - B_1)(p_2 - p_4). \tag{3.52}$$

In this case, the contribution towards work from each spin is equal, as can be easily seen by using the local description for the spins. With a non-uniform, slow driving, the same transformation from (B_1, B_1) to (B_3, B_3) can be performed in two steps. First, we change the configuration from (B_1, B_1) to (B_3, B_1) . The work performed in this step is:

$$W_{nu} = (B_3 - B_1)(p_2 - p_4) + (K - 4J)(p_1 - p_3). \tag{3.53}$$

Then, we can transform from (B_3, B_1) to (B_3, B_3). The corresponding work is given by:

$$W'_{nu} = (B_3 - B_1)(p_2 - p_4) - (K - 4J)(p_1 - p_3), \tag{3.54}$$

so that the sum $W_{nu} + W'_{nu} = W_u$, holds. Note that the work performed by each spin in the case of non-uniform, adiabatic driving is not equal. On the other hand, it is interesting to note that in the case of sudden, non-uniform driving, the work performed by each spin is the same and is given by $(B_3 - B_1)(p_2 - p_4)$. This can be understood by analysing the reduced density matrices; the latter do not change under sudden driving, while for a slow, non-uniform driving, the reduced density matrices also get transformed.

To conclude, we have studied a model of quantum heat engine where the inhomogeneous driving at a finite rate, of the quantum working medium leads to a frictional

effect. This effect is characterized by increase in the energy-entropy of the system. As expected of a thermodynamic system, the entropy production leads to decrease in the work obtained from a cycle. The work is plotted versus the time allotted for the adiabatic branches. The upper bound for extractable work is obtained for a slow process where the frictional effect vanishes and quantum adiabatic theorem holds, while the lower bound is obtained for a sudden process. Some interesting future problems include the study of frictional effect on models with anisotropic interactions and with systems using higher number of spins. The possibility of quantum lubrication [42] to reduce the intrinsic friction can also be studied.

Chapter 4

Quantum thermodynamic machines with prior information: Subjective approach

4.1 Introduction

The assignment of subjective probability to an event is based on the degree of personal belief. It can be understood from the concept of coherent bet [48, 62]. Suppose a person believes that the occurrence of an event has 50% chance. Then he/she should be ready to bet in either way, i.e. for the event to happen or not to happen. If he/she is ready to bet only in one way, then his/her equal-probability assessment for occurrence and nonoccurence of the event is incoherent. Here the degree of belief should not be confused with imagination and fantasy [62]. In this manner, the term 'subjective' means a state of knowledge of the observer [67].

In the subjective approach, rational people with the same information make similar probability assignment for a particular event. Thus the ideal of objectivity can be recovered from intersubjectivity [48]. Bayesian analysis is widely used as an effective inference method [100]. The methods of probabilistic inference show how to estimate the probability density function for an unknown parameter based on the data available. Thomas Bayes in his work titled *An Essay towards Solving a Problem in the Doctrine of Chances* [21], suggested a method of updating the degree of belief of certain event based on the data. This theorem is known as Bayes theorem and it

plays an important role in inference problems. The theorem involves the concept of prior probability distribution.

4.1.1 Prior probability and Bayes theorem

Prior probability distribution (or prior) $P(x)$ is the probability distribution assigned to an uncertain quantity by taking the prior information into account. Here the prior information is the information available before acquiring the data (D). Once the data (new information) is available, the prior is updated to the posterior probability using Bayes theorem as

$$P(x|D)dx = \frac{P(D|x)P(x)dx}{P(D)}, \tag{4.1}$$

where $P(D|x)$, also known as the likelihood, is the probability of D when x is given and $P(D) = \int P(D|x)P(x)dx$ is the normalization constant. So Bayes theorem serves as a mathematical tool to incorporate the new information and update the probability assignment. One of the crucial points in Bayesian statistics is the assignment of the prior based on initial knowledge. Once data is available, the prior is updated to the posterior. This posterior can be considered as a prior afterwards and for further updating in the light of further data [48]. The importance of the prior probability distribution in the physics problems is discussed in many works [16, 64, 98].

4.1.2 Partial information versus complete ignorance

When only partial information is available in terms of certain mean values, the prior probability is assigned according to maximum entropy principle [65, 64]. Consider a random variable x which can take values from the set $\{x_1, x_2.....x_n\}$. Here n can be finite or countably infinite. The goal is to assign probability $P(x_i|I)$ with respect to the available information (I). According to maximum entropy principle, this is done by maximizing the function S, where

$$S = -\sum_i P(x_i|I) \ln P(x_i|I), \tag{4.2}$$

subject to the constraints imposed by the available information. An extreme situation is the case of complete ignorance or the absence of information. If we are dealing

with discrete random variable, then uniform distribution is acceptable as a suitable choice in this particular case. But the assignment of probability for continuous random variable for complete ignorance is non-trivial. Jeffreys [68] suggested prior probability dx/x for a continuous and positive variable x in the range $[x, x+dx]$. This is chosen on the ground that with the prior we say the same thing if we use x or x^n. This can be understood by the following example [69]. Suppose x is the length of a container and volume V scales with length, $V \sim x^d$, where d is the dimension of the space. But the volume can be changed by changing the length keeping the cross-sectional area fixed. So the consistency demands $P(V)dV = P(x)dx$, which has a solution $P(x) \propto 1/x$.

4.2 Quantum model for work extraction

Consider a pair of two-level systems labeled R and S, with Hamiltonians H_R and H_S having energy eigenvalues $(0, a_1)$ and $(0, a_2)$, respectively. The Hamiltonian of the composite system is given by $H = H_R \otimes I + I \otimes H_S$. The initial state is $\rho_{\rm ini} = \rho_R \otimes \rho_S$, where ρ_R and ρ_S are thermal states corresponding to temperatures T_1 and T_2 ($< T_1$), respectively. Let (r_1, r_2) and (s_1, s_2) be the occupation probabilities of each system, where

$$r_1 = \frac{1}{(1+e^{-a_1/T_1})}, \qquad s_1 = \frac{1}{(1+e^{-a_2/T_2})}, \tag{4.3}$$

with $r_2 = (1 - r_1)$ and $s_2 = (1 - s_1)$. We have set Boltzmann's constant $k_{\rm B} = 1$. The initial mean energy of each system is

$$E_{ini}^{(i)} = \frac{a_i}{(1+e^{a_i/T_i})}, \tag{4.4}$$

where $i = 1, 2$ denote the system R and S, respectively. Within the approach based on quantum thermodynamics [53, 8, 10], the process of maximum work extraction is identified as a quantum unitary process on the thermally isolated composite system. It has been shown in these works that for $a_1 > a_2$, such a process minimises the final energy if the final state is given by $\rho_{\rm fin} = \rho_S \otimes \rho_R$. Effectively, it means that in the final state the two systems *swap* between themselves their initial probability distributions. The cycle is completed by putting the respective systems in contact

with heat baths again. The unitary which does the swap operation is given as

$$U = \begin{pmatrix} 1 & 0 & 0 & 0 \\ 0 & 0 & 1 & 0 \\ 0 & 1 & 0 & 0 \\ 0 & 0 & 0 & 1 \end{pmatrix}. \tag{4.5}$$

The swap-gate plays an important role in quantum computation [45]. In usual practice, the swap operation is done by decomposing the above unitary into elementary gates [45]. But a swap-gate without the composition of elementary gates is also constructed [104]. The swap-operation preserves not just the magnitude of von Neumann entropy of the composite system, but also all eigenvalues of its density matrix. The final energy of each system at the end of work extracting transformation is

$$E_{fin}^{(i)} = \frac{a_i}{(1 + e^{a_j/T_j})}. \tag{4.6}$$

where $i \neq j$. The average work per cycle defined as $W \equiv \mathrm{Tr}[(\rho_{\mathrm{ini}} - \rho_{\mathrm{fin}})H] = E_{ini} - E_{fin}$, is given by

$$W(a_1, a_2) = (a_1 - a_2)\left[\frac{1}{(1 + e^{a_1/T_1})} - \frac{1}{(1 + e^{a_2/T_2})}\right]. \tag{4.7}$$

In this cycle, the heat extracted from the hot reservoir is

$$Q_1 = a_1\left[\frac{1}{(1 + e^{a_1/T_1})} - \frac{1}{(1 + e^{a_2/T_2})}\right]. \tag{4.8}$$

The efficiency of this engine $\eta = W/Q_1$ is

$$\eta = 1 - \frac{a_2}{a_1}. \tag{4.9}$$

Note that for $a_2 = a_1, W = 0, Q_1 > 0$ and $\eta = 0$; for $a_2 = a_1(T_2/T_1)$, we have the limiting values of $W = 0$ and $Q_1 = 0$ and $\eta = 1 - (T_2/T_1)$. The operation of the machine as a heat engine ($W \geq 0$ and $Q_1 \geq 0$), is satisfied if

$$a_1(T_2/T_1) \leq a_2 \leq a_1. \tag{4.10}$$

4.3 Bayesian Approach

Now consider a situation in which the temperatures of the reservoirs are given a priori such that $T_1 > T_2$, but about the parameters a_1 and a_2 we only know that

- a_1 and a_2 represent the same physical quantity, which is the level spacing for system R and S respectively, and so a_1 and a_2 can only take positive real values.

- If the set-up of R+S has to work as an engine, then criterion in Eq. (4.10) must hold, whereby if one parameter is specified, then it fixes the range of the other parameter.

Apart from the above conditions, we assume to have no information about a_1 and a_2. The question we address in the following is: What can we then infer about the expected behavior of physical quantities for this heat engine (such as work per cycle, efficiency and so on) ? We shall follow a subjective approach to probability to address this question. This implies that an uncertain parameter is assigned a prior distribution, which quantifies our preliminary expectation about the parameter to take a certain value. We denote the prior distribution function for our problem by $\Pi(a_1, a_2)$. The prior should take into account the prior knowledge we possess about the parameters. For example, if a_1 is specified, then the prior distribution for a_2, $\pi(a_2|a_1)$ is conditioned on the specified value of a_1, and is defined in the range $[a_1\theta, a_1]$, where $\theta = T_2/T_1$, because we know the set-up works like an engine if we implement Eq. (4.10).

The expected value of any physical quantity X which may be function of a_1 and a_2, is defined as follows:

$$\overline{X} = \int\int X\,\Pi(a_1, a_2)\,da_1 da_2. \tag{4.11}$$

4.3.1 Assignment of the prior

In Bayesian probability theory, the assignment of an appropriate prior is a central issue [64]. It should quantify not only the prior knowledge about the parameter in the particular context, but should meet a consistency criterion according to which different observers in possession of equivalent information should assign similar priors. Suppose, one knows only the range within which the parameter takes its values, then intuition suggests that a uniform distribution may reflect the state of our knowledge. But such a choice is not invariant under reparameterizations. Our aim in the following is to motivate the assignment of prior distributions for level spacings a_1

and a_2, when the physical problem at hand is a heat engine as described in Section (4.2).

It seems convenient to speak in terms of the two observers A and B, who wish to assign priors for a_1 and a_2. The assignment is based on the following assumptions:

(a) Same functional form of the prior is assigned to a_1 and a_2 in the *initial state*, denoted by $\Pi(a_1)$ and $\Pi(a_2)$ respectively. Further, we assume that the prior can be expressed as $\Pi(a_i) \propto df(a_i)/da_i$, using a continuous differentiable function $f(a_i)$ $(i = 1, 2)$.

(b) The conditional prior distributions $p(a_j|a_i)$, implying distribution for a_j given a value of a_i, or $p(a_i|a_j)$ for the converse case, have the same functional form as above, and we assume that $p(a_j|a_i) \propto df(a_j)/da_j$, where the dependence on the given a_i may be present in the normalisation factor. Similarly, we assume $p(a_i|a_j) \propto df(a_i)/da_i$.

Assumption (a) is reasonable since both a_1 and a_2 represent the same physical quantity, and the state of knowledge of A and B about them is the same, which is the fact that their values *in the initial state* lie in a preassigned range $[a_{\min}, a_{\max}]$. For simplicity and symmetry, we take this range to be identical for a_1 and a_2. Presumably, this range depends on the experimental setup, and we assume similar apparatus for controlling the level spacings of the systems R and S.

Now if one of the parameters is specified to an observer, say a_1 to A, then A knows that the machine works as an engine only if the range of a_2 is $[a_1\theta, a_1]$, where a_1 here represents some fixed value. Even so, assumption (b) states that A must assign the same functional form to the prior for a_2 as it used for assigning to a_1. Although this does not represent the general case, we assume this for simplicity and in the following, analyse the consequences of these assumptions.

Thus from (a), we have

$$\Pi(a_i) = \frac{1}{M}\frac{df(a_i)}{da_i}, \tag{4.12}$$

where the normalization constant is determined as

$$\begin{aligned} M &= \int_{a_{\min}}^{a_{\max}} \frac{df(a_i)}{da_i} da_i \\ &= f(a_{\max}) - f(a_{\min}). \end{aligned} \tag{4.13}$$

Following assumption (b), the conditional probability distributions are given by

$$\Pi(a_2|a_1) = \frac{1}{N_1}\frac{df(a_2)}{da_2}, \tag{4.14}$$

and

$$\Pi(a_1|a_2) = \frac{1}{N_2}\frac{df(a_1)}{da_1}, \tag{4.15}$$

where

$$\begin{aligned} N_1 &= \int_{a_1\theta}^{a_1} \frac{df(a_2)}{da_2} da_2 \\ &= f(a_1) - f(a_1\theta), \end{aligned} \tag{4.16}$$

and

$$\begin{aligned} N_2 &= \int_{a_2}^{a_2/\theta} \frac{df(a_1)}{da_1} da_1 \\ &= f(a_2/\theta) - f(a_2), \end{aligned} \tag{4.17}$$

are the respective normalization constants. Now using the product law of probabilities, the joint prior $\Pi(a_1, a_2)$ as expressed by observer A is given by

$$\begin{aligned} \Pi(a_1, a_2) &= \Pi(a_2|a_1) \cdot \Pi(a_1) \\ &= \frac{df(a_2)/da_2}{[f(a_1) - f(a_1\theta)]} \cdot \frac{df(a_1)/da_1}{[f(a_{\max}) - f(a_{\min})]}, \end{aligned} \tag{4.18}$$

or equivalently in terms of B,

$$\begin{aligned} \Pi(a_1, a_2) &= \Pi(a_1|a_2) \cdot \Pi(a_2) \\ &= \frac{df(a_1)/da_1}{[f(a_2/\theta) - f(a_2)]} \cdot \frac{df(a_2)/da_2}{[f(a_{\max}) - f(a_{\min})]}. \end{aligned} \tag{4.19}$$

As shown in the Fig. 4.1, each observer assigns different ranges of values to a_1 and a_2. Each can use its own joint prior to make estimates about a certain quantity. Now since either approach is equivalent, so consistency would require that each makes similar estimates for a given quantity. Also it is reasonable to assume that for some given pair of values (a_1, a_2), which are in the allowed range of each observer, each of them should assign the same probability for choosing a_1 within the small interval da_1 around the given value a_1, as well as of choosing a_2 within the small interval da_2, around the given value a_2. Clearly, for such a pair, both a_1 and a_2 have to lie in the interval $[a_{\min}, a_{\max}]$. One such pair of values, which is definitely common to

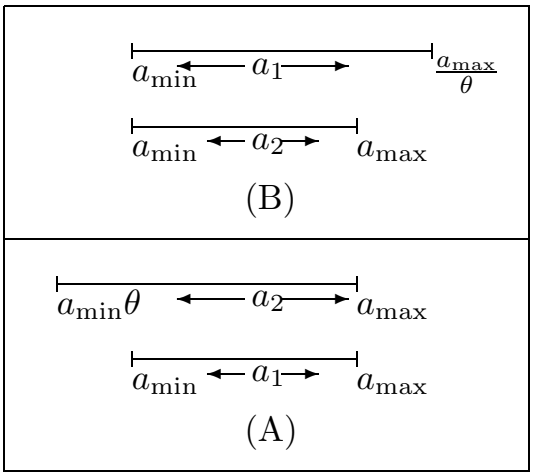

Figure 4.1: Observer A (B) assigns the same range of values for a_1 (a_2) in the initial state of spin R (S). But the range assigned for the other parameter a_2 (a_1), conditional on the operation as an engine, is different. This fact manifests such that A and B in general arrive at different estimates for physical quantities.

both A and B would be (a_1, a_1) i.e. when $a_2 = a_1$. Thus equating the probabilities assigned by A and B for this case, we obtain from Eqs. (4.18) and (4.19),

$$f(a_1) - f(a_1\theta) = f(a_1/\theta) - f(a_1), \tag{4.20}$$

which can be rewritten as

$$2f(a_1) = f(a_1\theta) + f(a_1/\theta). \tag{4.21}$$

This functional equation has a unique solution, $f(x) = \lambda \ln x$, up to an additive constant. Thus we find the explicit form of prior (Eq. (4.12)) as

$$\Pi(a_i) = \frac{1}{\ln\left(\frac{a_{\max}}{a_{\min}}\right)} \frac{1}{a_i}, \tag{4.22}$$

which is functionally the same as Jeffreys' choice [68], also employed in a previous study [69]. The joint prior is then given by

$$\Pi(a_1, a_2) = \frac{1}{\ln\left(\frac{1}{\theta}\right) \ln\left(\frac{a_{\max}}{a_{\min}}\right)} \frac{1}{(a_1 a_2)}. \tag{4.23}$$

The joint prior derived above is relevant only with regard to the final states of R and S. As discussed in the previous section, the initial state of system R (S) depends only on parameter a_1 (a_2). This fact will be used in the following in calculations on the expected values of quantities.

4.4 Expected Values of Physical Quantities

In this section, we use the priors assigned above, to find expected values for various physical quantities related to the engine. For this purpose, we employ the definition in Eq. (4.11). These expected values reflect the estimates by an observer who is assigning the priors. As observed in Eqs. (4.18) and (4.19), there are two methods of writing the joint prior. So in principle, there are two ways to calculate the expected value of some quantity and its value will depend, in general, on the method used.

The expected value of a function estimated by method A can be written as

$$\overline{f_A} \;=\; K\int_{a_{\min}}^{a_{\max}}\frac{da_1}{a_1}\int_{a_1\theta}^{a_1}\frac{f(a_1,a_2)}{a_2}da_2, \tag{4.24}$$

where $K=[\ln(1/\theta)\ln(a_{\max}/a_{\min})]^{-1}$.

Similarly the expected value of the function calculated by method B is given as

$$\overline{f_B} \;=\; K\int_{a_{\min}}^{a_{\max}}\frac{da_2}{a_2}\int_{a_2}^{a_2/\theta}\frac{f(a_1,a_2)}{a_1}da_1,$$

4.4.1 Internal energy

We calculate the expected values of internal energies for systems R and S. These values can then be used to find the expected work per cycle, heat exchanged and so on.

(i) **Initial state**: For a given a_i, the internal energy $E^{(i)}_{ini}$ is given by (4.4). The expected initial energy is defined as

$$\overline{E}^{(i)}_{ini}=\int_{a_{\min}}^{a_{\max}}E^{(i)}_{ini}\Pi(a_i)da_i, \tag{4.25}$$

where $i=1,2$. Note that $E^{(i)}_{ini}$ depends only on a_i, so we need to average over the prior for a_i only. Thus we obtain

$$\overline{E}^{(i)}_{ini}=\left[\ln\left(\frac{a_{\max}}{a_{\min}}\right)\right]^{-1}\int_{a_{\min}}^{a_{\max}}\frac{da_i}{(1+e^{a_i/T_i})}, \tag{4.26}$$

or explicitly

$$\overline{E}^{(i)}_{ini}=\left[\ln\left(\frac{a_{\max}}{a_{\min}}\right)\right]^{-1}\left[(a_{\max}-a_{\min})+T_i\ln\left(\frac{1+e^{a_{\min}/T_i}}{1+e^{a_{\max}/T_i}}\right)\right]. \tag{4.27}$$

(ii) **Final state** : In this case, the internal energy of R as well as S, is function of both a_1 and a_2 (see Eq. (4.6)) and so the expected values are obtained by averaging

over the joint prior, $\Pi(a_1, a_2)$. For instance, the expected final energy of system S (denoted by superscript (2)) as calculated by A,

$$\begin{aligned}\overline{E}^{(2)}_{fin}(\mathrm{A}) &= K\int_{a_{\min}}^{a_{\max}} \frac{1}{(1+e^{a_1/T_1})a_1} da_1 \int_{a_1\theta}^{a_1} da_2, \\ &= K\,(1-\theta)\left[(a_{\max}-a_{\min}) + T_1 \ln\left(\frac{1+e^{a_{\min}/T_1}}{1+e^{a_{\max}/T_1}}\right)\right]. \end{aligned} \tag{4.28}$$

Similarly if calculated by B,

$$\overline{E}^{(2)}_{fin}(\mathrm{B}) = K\int_{a_{\min}}^{a_{\max}} da_2 \int_{a_2}^{a_2/\theta} \frac{da_1}{(1+e^{a_1/T_1})a_1}. \tag{4.29}$$

The latter integral cannot be solved analytically. To simplify, we rewrite it as

$$\overline{E}^{(2)}_{fin}(\mathrm{B}) = K\int_{a_{\min}}^{a_{\max}} da_2 \left[\int_{a_2}^{a_2/\theta} \frac{da_1}{(1+e^{a_1/T_1})a_1}\cdot 1\right]. \tag{4.30}$$

Considering the inner integral as the first function and unity as the second function and integrating by parts, leads to

$$\begin{aligned}\overline{E}^{(2)}_{fin}(\mathrm{B}) &= Ka_2\int_{a_2}^{a_2/\theta} \frac{da_1}{(1+e^{a_1/T_1})a_1}\Bigg|_{a_2=a_{\min}}^{a_2=a_{\max}} \\ &\quad -K\int_{a_{\min}}^{a_{\max}} a_2\left[\frac{d}{da_2}\int_{a_2}^{a_2/\theta} \frac{da_1}{(1+e^{a_1/T_1})a_1}\right] da_2. \end{aligned} \tag{4.31}$$

Here we use Leibniz integral rule

$$\frac{d}{dy}\int_{g(y)}^{h(y)} f(x)dx = \frac{dh(y)}{dy}f(h(y)) - \frac{dg(y)}{dy}f(g(y)), \tag{4.32}$$

to solve the second term of the Eq. (4.31) and to finally obtain

$$\begin{aligned}\overline{E}^{(2)}_{fin}(\mathrm{B}) &= Ka_2\int_{a_2}^{a_2/\theta} \frac{da_1}{(1+e^{a_1/T_1})a_1}\Bigg|_{a_2=a_{\min}}^{a_2=a_{\max}} \\ &\quad -K\left[T_2\ln\left(\frac{1+e^{a_{\min}/T_2}}{1+e^{a_{\max}/T_2}}\right) - T_1\ln\left(\frac{1+e^{a_{\min}/T_1}}{1+e^{a_{\max}/T_1}}\right)\right]. \end{aligned} \tag{4.33}$$

In general, the expected final energies of S, as given by Eqs. (4.28) and (4.33) according to A and B, respectively, are not equal. One would expect that if the state of knowledge of A and B is similar, then they should arrive at similar estimates for a given quantity. However, the difference in the values expected by A and B is not so surprising in light of the fact that different ranges for variables a_1 and a_2 are being employed by them, as shown in Fig. 4.1.

A similar feature is also observed in the expressions for the expected energy of system R (superscript (1)), which we provide below for sake of completeness:

$$\overline{E}^{(1)}_{fin}(\mathrm{A}) = \int\int E^{(1)}_{fin}\Pi(a_2|a_1)\Pi(a_1)\,da_2\,da_1, \tag{4.34}$$

which implies

$$\overline{E}^{(1)}_{fin}(\mathrm{A}) = K \int_{a_{\min}}^{a_{\max}} da_1 \int_{a_1\theta}^{a_1} \frac{da_2}{(1+e^{a_2/T_2})a_2}. \tag{4.35}$$

It is interesting to observe that the above integral is *identical* to the one in Eq. (4.29),

$$\overline{E}^{(1)}_{fin}(\mathrm{A}) = \overline{E}^{(2)}_{fin}(\mathrm{B}). \tag{4.36}$$

The second method however, yields

$$\begin{aligned} \overline{E}^{(1)}_{fin}(\mathrm{B}) &= K \int_{a_{\min}}^{a_{\max}} \frac{da_2}{(1+e^{a_2/T_2})a_2} \int_{a_2}^{a_2/\theta} da_1, \\ &= K\left(\frac{1}{\theta}-1\right)\left[(a_{\max}-a_{\min}) + T_2 \ln\left(\frac{1+e^{a_{\min}/T_2}}{1+e^{a_{\max}/T_2}}\right)\right]. \end{aligned} \tag{4.37}$$

In the next section, we look at these expressions in a particular limit in which the expected values obtained by the two observers yield similar results, so that a meaningful analysis can be carried out in this limit.

4.5 Asymptotic Limit

As remarked above, the observers A and B are supposed to arrive at similar estimates for physical quantities using their respective priors. This happens in the limit, when $a_{\min} << T_2$ and $a_{\max} >> T_1$. In this limit, Eq. (4.27) is approximated as

$$\overline{E}^{(i)}_{ini} \approx \frac{\ln 2}{\ln(\frac{a_{\max}}{a_{\min}})} T_i. \tag{4.38}$$

The ratio $(a_{\max}/a_{\min})$ in the above may be large in magnitude, but is assumed to be finite.

Similarly, it is remarkable to note that in this limit, not only the expected final energy of a system (R or S) calculated by either of the methods (A or B), is the same but also its value for system R or S is also equal. In particular, the first term of Eq. (4.33) can be shown to be negligible in this limit. Thus we have (omitting the observer index)

$$\overline{E}^{(i)}_{fin} \approx \frac{\ln 2}{\ln(\frac{a_{\max}}{a_{\min}})} \frac{(1-\theta)T_1}{\ln(\frac{1}{\theta})}, \tag{4.39}$$

where $i = 1, 2$. Further insight into this may be obtained if we estimate the final temperatures of systems R and S after the work extraction process. Now if values

of both a_1 and a_2 are specified, the temperatures (T_i') of the two systems after work extraction, are given by [10]

$$T_1' = T_2 \frac{a_1}{a_2}, \quad \text{and} \quad T_2' = T_1 \frac{a_2}{a_1}. \tag{4.40}$$

In general, the two final temperatures are different from each other. Within the present framework, when we look at the expected values of the final temperatures as calculated by A or B, we find

$$\overline{T}_1' = \overline{T}_2' = T_1 \frac{(1-\theta)}{\ln(1/\theta)}. \tag{4.41}$$

It is interesting to find that the assignment of the prior is such that the two systems are expected to finally arrive at a common temperature. Going back to Eqs. (4.38) and (4.39) for the energies, we see that they satisfy a simple relation $\overline{E}_{ini}^{(i)} \propto T_i$ and $\overline{E}_{fin}^{(i)} \propto \overline{T}_i'$. This is reminiscent of the thermodynamic behavior of a classical ideal gas.

Next, the heat exchanged between system i and the corresponding reservoir is given by $\overline{Q}_i = \overline{E}_{ini}^{(i)} - \overline{E}_{fin}^{(i)}$. $\overline{Q}_i > 0$ ($\overline{Q}_i < 0$) represents heat absorbed (released) by the system. Then the expressions for the heat exchanged with the reservoirs in the said limit, are as follows:

$$\overline{Q}_1 \approx \frac{\ln 2}{\ln\left(\frac{a_{\max}}{a_{\min}}\right)} \left(1 + \frac{(1-\theta)}{\ln\theta}\right) T_1, \tag{4.42}$$

and

$$\overline{Q}_2 \approx \frac{\ln 2}{\ln\left(\frac{a_{\max}}{a_{\min}}\right)} \left(1 + \frac{(1-\theta)}{\theta\ln\theta}\right) T_2. \tag{4.43}$$

Now the expected work per cycle is defined as: $\overline{W} = \overline{Q}_1 + \overline{Q}_2$. Thus the efficiency is $\eta = 1 + \overline{Q}_2/\overline{Q}_1$. Explicitly, using Eqs. (4.42) and (4.43) we get

$$\eta = 1 + \frac{\theta\ln\theta + (1-\theta)}{\ln\theta + (1-\theta)}. \tag{4.44}$$

This is the efficiency at which the engine is expected to operate. A detailed analysis of this efficiency is given in Chapter 5. Before closing this section, we note that the constant of proportionality in Eqs. (4.38) and (4.39), which is $\ln 2 \cdot (\ln(a_{\max}/a_{\min}))^{-1}$, can be related with heat capacity. The expected value of initial heat capacity of system i, defined as

$$\overline{C}_i = \int_{a_{\min}}^{a_{\max}} C_i \Pi(a_i) da_i, \tag{4.45}$$

where we know that for a two-level system

$$C_i = \left(\frac{a_i}{T_i}\right)^2 \frac{e^{a_i/T_i}}{(1+e^{a_i/T_i})^2}. \tag{4.46}$$

Upon solving, the expected heat capacity in the initial state of the system is given exactly by

$$\overline{C}_i = \left[\ln\left(\frac{a_{\max}}{a_{\min}}\right)\right]^{-1} \left[\frac{a_{\max}\, e^{a_{\max}/T_i}}{T_i(1+e^{a_{\max}/T_i})} - \frac{a_{\min}\, e^{a_{\min}/T_i}}{T_i(1+e^{a_{\min}/T_i})} + \ln\left(\frac{1+e^{a_{\min}/T_i}}{1+e^{a_{\max}/T_i}}\right)\right]. \tag{4.47}$$

Then in the asymptotic limit, the leading term yields

$$\overline{C}_i \equiv \overline{C} \approx \frac{\ln 2}{\ln\left(\frac{a_{\max}}{a_{\min}}\right)}. \tag{4.48}$$

This limiting value is independent of temperature of the system and thus indicates an analogy with the constant heat capacity thermodynamic system.

Finally, we note that the requirement of consistency between the results of A and B implies, in an asymptotic limit, that the behavior expected from minimal prior information is the one which shows simple thermodynamic features such as constant heat capacity and equality of subsystem temperatures upon maximum work extraction. In the next section, we revisit the above analysis, but in a simplified form by considering an additional constraint.

4.6 Analysis at a given thermal efficiency

Let us impose an additional constraint by fixing the value of the engine efficiency η. Then there is essentially one energy scale say a_1, to be specified in the model, because the other scale a_2 is determined from the ratio $a_2/a_1 = (1-\eta)$. Let observer A treat a_1 as the uncertain parameter and denote the prior as $\pi(a_1)$. The second observer B chooses a_2 as the uncertain parameter and the corresponding prior as $\pi^*(a_2)$. In other words, the uncertain parameter of B, differ from a_1 by a scale factor $(1-\eta)$. The probabilities assigned by A and B for a given choice of a_1 and a_2, must satisfy

$$\pi(a_1)da_1 = \pi^*(a_2)da_2. \tag{4.49}$$

On the other hand, one should expect the same functional form for the prior in both cases, which is saying essentially that both A and B are in an identical state

of knowledge, implying $\pi \sim \pi^*$ [64]. Thus relation (4.49) is rewritten as

$$\pi(a_1) = (1-\eta)\,\pi(a_1(1-\eta)), \tag{4.50}$$

a functional equation whose solution is given by $\pi(x) \propto 1/x$. Thus with the additional constraint of a given efficiency, the prior assigned is the Jeffreys' prior.

Let us now illustrate the calculation for observer A. The appropriate normalised prior we have to consider is $\pi(a_1) = [\ln(a_{\max}/a_{\min})]^{-1}(1/a_1)$. From Eq. (4.7), the average work per cycle rewritten as function of a_1 and η is given by

$$W(a_1,\eta) = a_1\eta\left[\frac{1}{(1+e^{a_1/T_1})} - \frac{1}{(1+e^{a_1(1-\eta)/T_2})}\right]. \tag{4.51}$$

The expected work estimated by A is defined as $\overline{W}(A) = \int W(a_1,\eta)\pi(a_1)da_1$. After calculation we have,

$$\overline{W}(A) = \left[\ln\left(\frac{a_{\max}}{a_{\min}}\right)\right]^{-1}\eta\left[\frac{T_2}{(1-\eta)}\ln\left(\frac{1+e^{a_{\max}(1-\eta)/T_2}}{1+e^{a_{\min}(1-\eta)/T_2}}\right) - T_1\ln\left(\frac{1+e^{a_{\max}/T_1}}{1+e^{a_{\min}/T_1}}\right)\right]. \tag{4.52}$$

On the other hand, from the perspective of observer B who treats a_2 as the unknown parameter, the corresponding prior is $\pi(a_2) = [\ln(a_{\max}/a_{\min})]^{-1}(1/a_2)$. Upon writing the work per cycle as $W(a_2,\eta)$, i.e. function of a_2 and η, we define $\overline{W}(B) = \int W(a_2,\eta)\pi(a_2)da_2$, which is explicitly given by

$$\overline{W}(B) = \left[\ln\left(\frac{a_{\max}}{a_{\min}}\right)\right]^{-1}\eta\left[\frac{T_2}{(1-\eta)}\ln\left(\frac{1+e^{a_{\max}/T_2}}{1+e^{a_{\min}/T_2}}\right) - T_1\ln\left(\frac{1+e^{a_{\max}/(1-\eta)T_1}}{1+e^{a_{\min}/(1-\eta)T_1}}\right)\right]. \tag{4.53}$$

In this case also, we see a difference in the average work expected by A and B, which is at variance with our assumption that A and B are in an equivalent state of knowledge. But again, we observe that in the asymptotic limit as considered in Section (4.5), both the expressions for work get reduced to the following simpler form

$$\overline{W}(A) \approx \overline{W}(B) \approx \frac{\ln 2}{\ln\left(\frac{a_{\max}}{a_{\min}}\right)}\eta\left(T_1 - \frac{T_2}{(1-\eta)}\right). \tag{4.54}$$

It is interesting to observe that the expected work in the asymptotic limit attains its optimal value at the well known Curzon-Ahlborn efficiency, $\eta = 1-\sqrt{T_2/T_1}$.

Finally, we may compare the amount of work expected in the general case (as calculated from Eqs. (4.42) and (4.43)) when both a_1 and a_2 are uncertain, with the special case when the efficiency is fixed a priori. In the general case, the expected

efficiency of the engine is given by Eq. (4.44), so it is reasonable to take this value of efficiency in Eq. (4.54) while making the above comparison. As shown in Fig. 3, the work in the general case is always less than the work in the special case and their ratio approaches the value of 3/4 as the temperature gradient goes to zero ($\theta \to 1$).

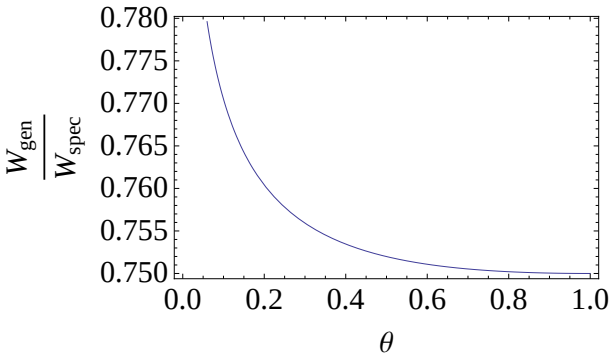

Figure 4.2: Expected work in the general case, is less than the expected work in the special case for which the efficiency is fixed a priori. Both expressions for work are calculated at the same efficiency as given by Eq. (4.44). As $\theta \to 1$, the ratio approaches a constant value 3/4.

4.7 Application of Bayes theorem

Consider a spin-1/2 particle with an unknown level spacing a, attached to a bath of temperature T. So we assign a prior distribution $P(a)$ for this unknown quantity. Now consider a measurement done on the particle such that the measurement outcome is either ground ($\downarrow$) or excited ($\uparrow$) state. The prior can be updated based on the new data using Bayes theorem. Suppose the measurement outcome is $\uparrow$, then we have

$$P(a|\uparrow)da = \frac{P(\uparrow|a)P(a)da}{\int_{a_{\min}}^{a_{\max}} P(\uparrow|a)P(a)da}. \tag{4.55}$$

But we know that our system is in equilibrium with bath. So from Boltzmann distribution we have the conditional probability as

$$P(\uparrow|a) = \frac{1}{(1+e^{a/T})}. \tag{4.56}$$

The posterior distribution in Eq. (4.55) act as the prior hereafter. Suppose in the second measurement, we obtain the result $\downarrow$, then the posterior probability of a is given as

$$P(a|\downarrow,\uparrow)da = \frac{P(\downarrow|a)P(\uparrow|a)P(a)da}{\int_{a_{\min}}^{a_{\max}} P(\downarrow|a)P(\uparrow|a)P(a)da} \tag{4.57}$$

Suppose the actual value of a is a^* and we do N measurements, where we get the outcomes $\uparrow$ and $\downarrow$, n and $(N-n)$ times respectively. For large N, we can write

$$n = \frac{N}{(1+e^{a^*/T})}. \tag{4.58}$$

So the probability distribution after N measurements is given as

$$P(a|\downarrow^{(N-n)},\uparrow^n)da = \frac{1}{I_N}\left(\frac{1}{1+e^{-a/T}}\right)^{(N-n)}\left(\frac{1}{1+e^{a/T}}\right)^n P(a)da \tag{4.59}$$

where

$$I_N = \int_{a_{\min}}^{a_{\max}}\left(\frac{1}{1+e^{-a/T}}\right)^{(N-n)}\left(\frac{1}{1+e^{a/T}}\right)^n P(a)da \tag{4.60}$$

Eq. (4.59) is binomial distribution which has a peak at $a = a^*$, when $N \to \infty$.

Now we consider an explicit example to compare the optimal performance of an engine with its expected performances obtained from the prior and the posterior distributions [112]. Similar to the model of quantum Otto cycle mentioned in Section 4.2, a four-stage Otto cycle is discussed in Ref. [69]. In this model, there are two adiabatic branches, the first adiabatic branch involves changing the energy level spacing of the two level system from a_1 to a_2 adiabatically, in other words the energy eigenvalues of the system change from $(0, a_1)$ to $(0, a_2)$, keeping the system in the instantaneous eigenstate of the Hamiltonian. Similarly in the second adiabatic process, energy spacing change from a_2 to a_1. Before the first adiabatic process, the system is in equilibrium with the hot bath at temperature T_1 and before the second adiabatic process, the system is in equilibrium with the cold bath at temperature T_2. Now we consider a measurement of the state of the system before the first adiabatic process. If the system is initially found in $\uparrow$, then the work done by the system during the first adiabatic process is $W_I = a_1 - a_2 = a_1\eta$.

On the other hand, if the system is in down-state, then the work during the adiabatic process is zero. Based on the measurement outcome, the prior can be updated using Bayes' theorem. For an outcome of spin being up, the posterior

distribution function is given in Eq. 4.55. Using this posterior, we find the expected work in the first adiabatic process is

$$W_I = \int_{a_{\min}}^{a_{\max}} a_1 \eta P(a_1|\uparrow_I) da, \tag{4.61}$$

where $\uparrow_I$ represents the measurement outcome (up) before the first adiabatic process. Now we consider the measurement before the second adiabatic process. If the system is found to be in up state, then the work done during the process is given as $-a_1\eta$. So the expected work in the second adiabatic process is estimated as

$$W_{II} = \int_{a_{\min}}^{a_{\max}} -a_1 \eta P(a_1|\uparrow_{II}) da, \tag{4.62}$$

where $\uparrow_{II}$ denotes the measurement outcome (up) before the second adiabatic process. So the total expected work estimated by averaging over the posterior is $W_{\text{pos}} = W_I + W_{II}$.

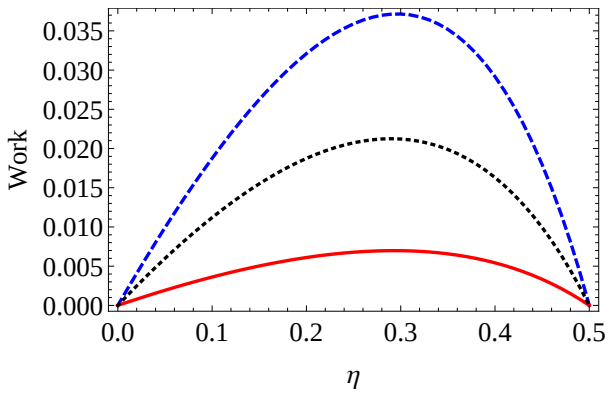

Figure 4.3: The work versus efficiency plot. The expected work obtained by averaging over prior (using Eq. (4.52)) and posterior distribution is shown with normal and dotted curve respectively. The dashed curve shows the maximum work obtained at a given efficiency, when there is no uncertainty of energy level spacings. Here we use $T_1 = 1$, $T_2 = 0.5$, $a_{\min} = 0.01$ and $a_{\max} = 50$ [112].

In Fig. 4.3, the expected work obtained by averaging over the prior and the posterior distributions at a given efficiency, is plotted. This expected work is compared with the maximum work of the heat engine at the given efficiency. It is interesting to note that the efficiency at maximum work of all the three curves lies very close

to each other. The expected work by averaging over the posterior is higher than the expected work obtained from the prior distribution and it lies closer to the maximum work obtained from the engine.

4.8 Conclusions

We considered a model of quantum Otto engine with uncertain control parameters. We posed the following question: What is the expected performance of this engine under this uncertainty and how can it be deduced from the prior information? Based on certain simple assumptions we derived the prior for the uncertain parameters. In the absence of data from observations, in our opinion, the initial prior so assigned has to be used to make inferences about physical quantities. The estimates for these quantities have been defined as the average value over the chosen prior. Further considerations lead us to investigate a particular asymptotic limit, because to maintain consistency, the observers A and B should arrive at similar estimates for a given quantity, if each is in an equivalent state of knowledge. It is in this limit, we observe classical thermodynamic features for the estimated quantities of our quantum heat engine. In particular, the expected mean energies of the two-level systems become proportional to their temperature, with the expected heat capacity $\overline{C}$ becoming independent of the temperature. It is also interesting to observe that the factor $\ln(a_{\max}/a_{\min})$ occurring in the normalisation of the prior can be expressed in terms of the expected heat capacity of the system. Further we consider measurements carried out on the system. The data obtained from the outcome of measurement changes the state of knowledge of the observer and hence the prior is updated in the light of new data using Bayes theorem. We also compare the the expected performance inferred from prior and posterior distributions.

Chapter 5

Efficiency of heat engines and information

5.1 Introduction

The quantities such as the work obtained or power output per cycle and the efficiency are the major factors which characterize the performance of a heat engine. The maximum achievable efficiency for an engine working between two reservoirs with temperature T_1 and T_2 ($T_1 > T_2$) is the Carnot efficiency, which is given as

$$\eta_c = 1 - \frac{T_2}{T_1}. \tag{5.1}$$

This is one of the central results of classical thermodynamics. In a reversible cycle, the total entropy change (system+bath) is zero. Therefore, to attain this efficiency, the engine should be driven in a quasi-static manner. Hence the power delivered by these thermodynamic cycles is vanishingly small. Practically, an engine is driven in a finite time to extract finite power. In a seminal paper [36], Curzon and Ahlborn showed that the efficiency at maximum power of a finite-time Carnot heat engine is given as

$$\eta_{\mathrm{CA}} = 1 - \sqrt{\frac{T_2}{T_1}}. \tag{5.2}$$

In this paper, a four-staged cycle consisting of two isothermal and two adiabatic processes is considered. During an isothermal process, the working substance maintains a temperature T_i' while it is in contact with the bath T_i as shown in Fig. 5.1, where $i = 1, 2$ indicates the first and the second isothermal processes. The heat flow

into or out of the working substance is assumed to be proportional to the temperature gradient $|T_i' - T_i|$. Both the adiabatic processes are considered as completely reversible. The efficiency obtained by this engine at maximum power is given in Eq. (5.2). Interestingly, some of the examples of real heat engines working near this efficiency are shown in Ref. [36]. Because of the appearance of this efficiency

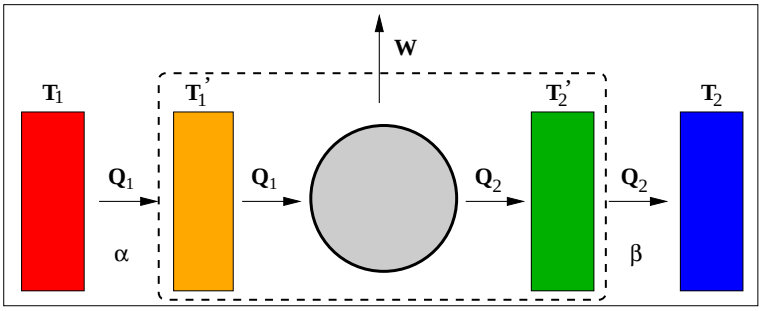

Figure 5.1: Finite-time Carnot cycle: Curzon-Ahlborn model. The efficiency at maximum power of this cycle is given in Eq. 5.2

at optimum performance of many models, the possible universal character of this efficiency attracted the attention of many researchers [81, 78]. Using the arguments of irreversible thermodynamics, CA efficiency is shown as an upper bound of the efficiency of a heat engines which extract maximum power [120]. The Curzon-Ahlborn (CA) efficiency can be expanded in terms of Carnot efficiency in the near equilibrium limit ($\eta_c \to 0$) as

$$\eta_{ca} = \frac{\eta_c}{2} + \frac{\eta_c^2}{8} + O[\eta_c^3]. \tag{5.3}$$

Further many studies were carried out showing the universality of the first two terms. The universal coefficients, 1/2 and 1/8 are displayed in the efficiency at maximum power for the engine characterized by left-right symmetry and strong coupling between particle and heat flow [40].

In this chapter, we show two classes of efficiency, obtained from Bayesian approach to uncertain parameters. Apart from quantum model, we also discuss a stochastic model of heat engine.

5.2 Bayesian statistics and CA efficiency

We have observed that, quite surprisingly, through Bayesian statistics, CA efficiency is recovered from a four-staged quantum Otto cycle [69]. In this model, efficiency is given a priori, but energy level spacing a of the two level system is unknown. Since the efficiency is given, the problem reduces to single uncertain parameter. The prior for this uncertain parameter is taken as proportional to $1/a$. Analogous to this cycle, we have considered a two-stage Otto cycle using two spin-1/2 systems [115] as discussed in Section 4.6. The expression for the work in the asymptotic limit is given in Eq. (4.54),

$$\overline{W} \approx \overline{C}\eta \left(T_1 - \frac{T_2}{(1-\eta)} \right). \tag{5.4}$$

Thus the efficiency at maximum expected work is the CA value.

An analogous heat engine with two internal energy scales is the Feynman's ratchet. When working as an engine, this device has the efficiency which is closely similar to the efficiency of an Otto engine. In the following section, we discuss the performance of Feynman's ratchet as a heat engine and also as a refrigerator. We consider a situation where the energy scales of the system are uncertain, but the efficiency for heat engine or the coefficient of performance (COP) of the refrigerator is given. Based on the Bayesian approach to an uncertain parameter, we assign a prior probability distribution for the uncertain parameter. In our discussion, the prior discussed has the same functional form as the Jeffreys prior. Later, we compare our result with the expected performance obtained from a uniform distribution.

5.3 Feynman's ratchet

Feynman showed a simple and profound mechanism using a ratchet and a pawl to convert heat into work [44]. Even though the model was introduced for pedagogical purposes, it attracted attention as heat engine [118, 63], refrigerator [88, 110] and to study the mechanism of motor proteins [19]. The model of Feynman's ratchet as a heat engine consists of two heat baths with temperatures T_1 and T_2 ($T_1 > T_2$). A vane is immersed in the hot bath. The vane is connected through an axle with a ratchet which is in contact with the cold bath. The rotation of the ratchet is restricted in one direction due to a pawl which in turn is connected to a spring.

The axle passes through the center of a wheel from which hangs a weight. So the directed motion of the ratchet rotates the wheel, thereby lifting the weight. To raise the pawl, the system needs ϵ_2 amount of energy to overcome the elastic energy of the spring. Suppose in each step, the wheel rotates an angle δ and the torque induced by the weight is Z. Then the system requires a minimum of $\epsilon_1 = \epsilon_2 + Z\delta$ energy to lift the weight. Hence the rate of forward jumps for lifting the weight is given as

$$R_{\rm F} = r_0 e^{-\epsilon_1/T_1}, \tag{5.5}$$

where r_0 is a constant with the dimension of rate (s^{-1}).

The statistical fluctuations can produce a directed motion at a finite rate, only if the ratchet-pawl system is microscopic. Hence the pawl can undergo a Brownian motion by bouncing up and down as it is immersed in a finite temperature bath. This turns the wheel in backward direction and lowers the position of the weight. This is the reason that the system cannot work as an engine if $T_1 = T_2$. The rate of the backward jumps is

$$R_{\rm B} = r_0 e^{-\epsilon_2/T_2}. \tag{5.6}$$

Therefore, $Z\delta$ and $-Z\delta$ are the work done by and on the system, respectively. In an infinitesimally small time Δt, the work done by the system is given as

$$\begin{aligned} W &= (\epsilon_1 - \epsilon_2)(R_{\rm F} - R_{\rm B})\Delta t, \\ &= r_0(\epsilon_1 - \epsilon_2)\left(e^{-\epsilon_1/T_1} - e^{-\epsilon_2/T_2}\right)\Delta t. \end{aligned} \tag{5.7}$$

Similarly, the heat absorbed in this interval from the hot reservoir is given as

$$Q_h = r_0\epsilon_1\left(e^{-\epsilon_1/T_1} - e^{-\epsilon_2/T_2}\right)\Delta t. \tag{5.8}$$

So the efficiency of the engine is given as

$$\eta = \frac{W}{Q_h} = 1 - \frac{\epsilon_2}{\epsilon_1}. \tag{5.9}$$

Power of the engine is defined as

$$P = \frac{W}{\Delta t} = r_0(\epsilon_1 - \epsilon_2)\left(e^{-\epsilon_1/T_1} - e^{-\epsilon_2/T_2}\right). \tag{5.10}$$

Using $\epsilon_1 = \epsilon_2/(1-\eta)$, we can write the expression for power as

$$P(\eta, \epsilon_2) = r_0\frac{\epsilon_2\eta}{(1-\eta)}\left(e^{-\epsilon_2/(1-\eta)T_1} - e^{-\epsilon_2/T_2}\right). \tag{5.11}$$

5.3.1 Optimal performance as a heat engine

In [118], the power is optimized with respect to the load Z and internal parameter ϵ_2 or in other words optimizing over the energy scales ϵ_1 and ϵ_2 we get the optimum power as

$$P^* = \frac{r_0 T_1 \eta_c^2}{e(1-\eta_c)^{(1-\eta_c^{-1})}}. \tag{5.12}$$

The corresponding efficiency at maximum power is

$$\tilde{\eta} = \frac{\eta_c^2}{\eta_c - (1-\eta_c)\ln(1-\eta_c)}. \tag{5.13}$$

Bayesian approach

We consider the following situation where η of the engine is given but the energy scales (ϵ_1, ϵ_2) are uncertain in the range $[\epsilon_{\min}, \epsilon_{\max}]$ [116]. Since η is known, the problem is reduced to single uncertain parameter. Here we assign a prior distribution to ϵ_2 in the range $[\epsilon_{\min}, \epsilon_{\max}]$. We take a finite-range for assigning a normalized prior. Later we consider the maximum ignorance about the uncertain parameter by setting the limit, $\epsilon_{\min} \to 0$ and $\epsilon_{\max} \to \infty$. Based on arguments similar to those put forward in Section 4.6, the functional form of the prior is found to be $\Pi(\epsilon_2) \propto 1/\epsilon_2$. Therefore we can estimate the expected value of the power as

$$\begin{aligned} \overline{P}(\eta) &= \int_{\epsilon_{\min}}^{\epsilon_{\max}} P(\eta, \epsilon_2)\Pi(\epsilon_2) d\epsilon_2 \\ &= \frac{C\eta}{(1-\eta)} \int_{\epsilon_{\min}}^{\epsilon_{\max}} \left(e^{-\epsilon_2/(1-\eta)T_1} - e^{-\epsilon_2/T_2} \right) d\epsilon_2, \end{aligned} \tag{5.14}$$

where $C = r_0/\ln(\epsilon_{\max}/\epsilon_{\min})$. Upon integrating, we get

$$\begin{aligned} \overline{P}(\eta) &= CT_1\eta \left(e^{-\epsilon_{\min}/(1-\eta)T_1} - e^{-\epsilon_{\max}/(1-\eta)T_1} \right) \\ &\quad + \frac{CT_2\eta}{(1-\eta)} \left(e^{-\epsilon_{\max}/T_2} - e^{-\epsilon_{\min}/T_2} \right). \end{aligned} \tag{5.15}$$

We are interested in the efficiency at maximum of expected power. Hence, on maximizing $\overline{P}(\eta)$ with respect to η, we get

$$\begin{aligned} \frac{\partial \overline{P}}{\partial \eta} &\equiv T_1 \left(e^{-\epsilon_{\min}/(1-\eta)T_1} - e^{-\epsilon_{\max}/(1-\eta)T_1} \right) \\ &\quad - \frac{\eta}{(1-\eta)^2} \left(\epsilon_{\min} e^{-\epsilon_{\min}/(1-\eta)T_1} - \epsilon_{\max} e^{-\epsilon_{\max}/(1-\eta)T_1} \right) \\ &\quad + \frac{T_2}{(1-\eta)^2} \left(e^{-\epsilon_{\max}/T_2} - e^{-\epsilon_{\min}/T_2} \right) = 0. \end{aligned} \tag{5.16}$$

Considering the limit $\epsilon_{\max} \to \infty$ and $\epsilon_{\min} \to 0$, the above expression can be written as

$$T_1 - \frac{T_2}{(1-\eta)^2} = 0. \tag{5.17}$$

Solving the above equation, we get the efficiency which maximizes the expected power as

$$\eta^* = 1 - \sqrt{\theta} = \eta_{CA}, \tag{5.18}$$

where $\theta = T_2/T_1$. On the other hand, if a uniform prior $1/(\epsilon_{\max} - \epsilon_{\min})$ is assigned for the uncertain parameter, then the efficiency at maximum expected power is given as $\eta_u = (5K_1 - K_1^2 - 1)/6K_1$, where $K_1 = (1 + 54\theta^2 + 6\sqrt{3}\theta\sqrt{1+27\theta^2})^{1/3}$ (see Fig. 5.2).

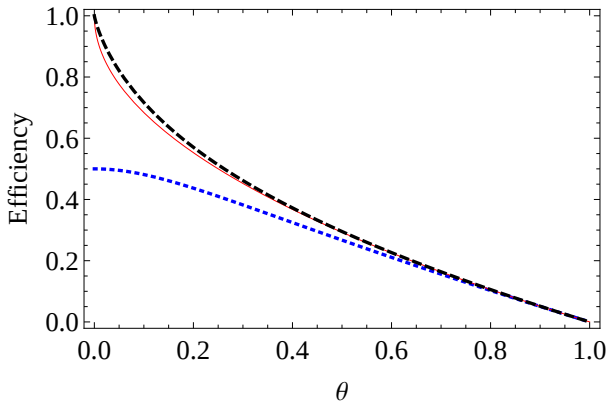

Figure 5.2: The normal curve shows the CA value for Feynman's ratchet as a heat engine which is also obtained when Jeffreys prior is assigned for the uncertain parameter. The dotted curve is the corresponding efficiency when a uniform prior is used. The dashed curve represents the efficiency at optimal power $\tilde{\eta}$.

Now we compare the efficiencies near equilibrium, obtained from $1/\epsilon_2$ prior and uniform prior, with the efficiency $(\tilde{\eta})$ at maximum power when there is no uncertainty.

$$\tilde{\eta} = \frac{\eta_c}{2} + \frac{\eta_c^2}{8} + \frac{7\eta_c^3}{96} + O[\eta_c^4] \quad \text{(optimal value)} \tag{5.19}$$

$$\eta = \frac{\eta_c}{2} + \frac{\eta_c^2}{8} + \frac{6\eta_c^3}{96} + O[\eta_c^4] \quad \text{(CA value from } 1/\epsilon_2 \text{ prior)} \tag{5.20}$$

$$\eta_u = \frac{\eta_c}{2} + \frac{\eta_c^2}{16} + \frac{\eta_c^3}{64} + O[\eta_c^4]. \quad \text{(with uniform prior)} \tag{5.21}$$

Interestingly, with the appropriate choice of prior $(1/\epsilon_2)$, the first two terms of the efficiency at maximum power are reproduced.

5.3.2 Optimal performance as a refrigerator

Maximum of power is a good criterion to study the optimal performance of finite-time heat engines as seen in a variety of models such as finite-time Carnot cycle [36], stochastic heat engine [20] and Feynman's ratchet [118]. In the case of the refrigerator, many optimization criterion have been tried [125, 121, 119]. Further, there is a complementarity between cooling rate and the coefficient of performance of the refrigerator [125, 9]. When one is maximized, the other is nullified and vice versa. To give equal attention to both the quantities, the product of COP and cooling rate is regarded as an objective function [125]. In Ref. [37], a unified criterion applicable for both Carnot heat engine and refrigerators is proposed. In both the cases, χ-criterion, which is defined as the product of energy conversion efficiency and the heat absorbed per unit time, is to be optimized. So for the heat engine, the quantity to be optimized is the product of efficiency η and the rate of heat absorbed from the hot bath $\dot{Q}_h$, which is the power and hence the CA efficiency is recovered at optimal performance. For refrigerator, the χ-criterion is defined as the product of coefficient of performance ζ and rate of heat exchange with cold bath $\dot{Q}_c$. Further with this criterion, the counterpart of CA efficiency for refrigerator $\zeta_{CA} = 1/\sqrt{1-\theta} - 1$ [125] is also obtained.

Feynman's ratchet is also studied as a refrigerator [88, 110, 4, 83]. It can also be regarded as Büttiker-Landauer model [32, 77] as discussed in [110]. By optimizing the χ-criterion for Feynman's ratchet as a refrigerator, the COP at optimal performance $\tilde{\zeta}$ satisfy the following transcendental equation [110]

$$\frac{\zeta_c - \tilde{\zeta}}{\zeta_c + 1}\left(\frac{2}{\tilde{\zeta}} - \frac{1}{\zeta_c}\right) = \ln\left[\frac{(2+\tilde{\zeta})\zeta_c}{\tilde{\zeta}(\zeta_c+1)}\right], \tag{5.22}$$

where $\tilde{\zeta}$ is the COP at optimal performance and $\zeta_c = T_2/(T_1 - T_2)$, the Carnot bound for the refrigerator. Since the analytical solution for the above equation is not possible, using an interpolation formula, the approximate solution is found to be

$$\tilde{\zeta} = \sqrt{\zeta_c + (0.954)^2} - 0.954 \tag{5.23}$$

This approximate solution is verified with asymptotic solutions obtained for small and large temperature differences.

Bayesian approach

As we have seen in the earlier discussions, with a Bayesian analysis we obtained CA value in the case of Feynman's ratchet as a heat engine. Now we show that from Bayesian approach, the corresponding CA value of refrigeration cycle can also be obtained from the model of Feynman's ratchet [116].

The χ-criterion is defined as

$$\chi = \zeta \dot{Q}_2, \tag{5.24}$$

where

$$\begin{aligned} \zeta &= \frac{Q_2}{W} = \frac{\epsilon_2}{(\epsilon_1 - \epsilon_2)} && (5.25) \\ \dot{Q}_2 &= r_0 \epsilon_2 \left(e^{-\epsilon_2/T_2} - e^{-\epsilon_1/T_1} \right). && (5.26) \end{aligned}$$

Substituting $\epsilon_1 = \epsilon_2(1+\zeta)/\zeta$ in the above equations, we get

$$\chi(\zeta, \epsilon_2) = \zeta r_0 \epsilon_2 \left(e^{-\epsilon_2/T_2} - e^{-\epsilon_2(1+\zeta)/\zeta T_1} \right). \tag{5.27}$$

If ζ is given and ϵ_2 is uncertain in the range $[\epsilon_{\min}, \epsilon_{\max}]$, then we can assign a prior for ϵ_2 based on the prior information. One can argue that an appropriate prior has the form

$$\Pi(\epsilon_2) = \frac{1}{\ln\left[\frac{\epsilon_{\max}}{\epsilon_{\min}}\right]} \frac{1}{\epsilon_2}. \tag{5.28}$$

Now we can define the expected value of χ as

$$\begin{aligned} \overline{\chi}(\zeta) &= \int_{\epsilon_{\min}}^{\epsilon_{\max}} \chi(\zeta, \epsilon_2) \Pi(\epsilon_2) d\epsilon_2 && (5.29) \\ &= C \int_{\epsilon_{\min}}^{\epsilon_{\max}} \zeta \left(e^{-\epsilon_2/T_2} - e^{-\epsilon_2(1+\zeta)/\zeta T_1} \right) d\epsilon_2, && (5.30) \end{aligned}$$

where $C = r_0 / \ln(\epsilon_{\max}/\epsilon_{\min})$. Upon integrating the above equation, we get

$$\begin{aligned} \overline{\chi}(\zeta) &= C\zeta T_2 \left(e^{-\epsilon_{\min}/T_2} - e^{-\epsilon_{\max}/T_2} \right) \\ &\quad + \frac{C\zeta^2 T_1}{(1+\zeta)} \left(e^{-\epsilon_{\max}(1+\zeta)/\zeta T_1} - e^{-\epsilon_{\min}(1+\zeta)/\zeta T_1} \right). && (5.31) \end{aligned}$$

Now maximizing $\overline{\chi}$ with respect to ζ, we get

$$\begin{aligned} \frac{\partial \overline{\chi}}{\partial \zeta} &\equiv T_2 \left(e^{-\epsilon_{\min}/T_2} - e^{-\epsilon_{\max}/T_2} \right) \\ &\quad + \frac{\zeta(\zeta+2) T_1}{(1+\zeta)^2} \left(e^{-\epsilon_{\max}(1+\zeta)/\zeta T_1} - e^{-\epsilon_{\min}(1+\zeta)/\zeta T_1} \right) \\ &\quad + \frac{1}{(1+\zeta)} \left(\epsilon_{\max} e^{-\epsilon_{\max}(1+\zeta)/\zeta T_1} - \epsilon_{\min} e^{-\epsilon_{\min}(1+\zeta)/\zeta T_1} \right) = 0. && (5.32) \end{aligned}$$

Considering the limit $\epsilon_{\max} \to \infty$ and $\epsilon_{\min} \to 0$, the above expression reduces to

$$\frac{\zeta(\zeta+2)}{(1+\zeta)^2} - \theta = 0. \tag{5.33}$$

So the possible solution for ζ which maximizes $\overline{\chi}$ is given as

$$\zeta^* = \frac{1}{\sqrt{(1-\theta)}} - 1 = \zeta_{\rm CA}. \tag{5.34}$$

In Fig. 5.3, $\zeta_{\rm CA}$ is compared with COP at optimal performance $\tilde{\zeta}$. Interestingly, $\zeta_{\rm CA}$ is very close to the optimal solution.

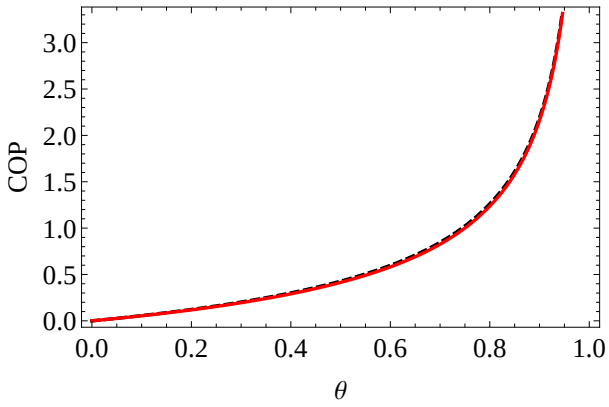

Figure 5.3: The coefficient of performance of Feynman's ratchet is plotted versus θ. The normal curve shows the CA value for refrigerator which is the COP at optimal performance of the refrigerator when Jeffreys prior is assigned for the uncertain parameter. The dashed line represents the interpolation formula for COP corresponding to optimal values of χ-criterion [110].

5.4 A different class of efficiency

We have seen the importance of CA efficiency in the optimal behavior of heat engines and also the universal behavior of the leading terms of this efficiency. Such efficiencies are also obtained from a Bayesian analysis. On the other hand, we came across a model of Brownian heat engine [128] in which the efficiency at maximum power near equilibrium limit approaches one third of Carnot efficiency. Another example showing this behavior is observed in the case of a Maxwell's demon [20]. Remarkably, we achieved similar efficiencies from the Bayesian approach [115, 113].

Recent work [70] showed that the one-third of Carnot value appears due to the label uncertainty when the problem of inference is applied to maximum work extraction process. In the following sections, we discuss such efficiencies in detail.

5.4.1 Efficiency of a Brownian heat engine

We consider a thermally driven model of Brownian heat engine discussed in [128]. In this model, the Brownian particle is moving through a periodic and asymmetric potential (ratchet) with a load f as shown in Fig. 5.4. The energy needed for forward and backward jumps is $E - fL_1$ and $E + fL_2$ respectively where L_1 and L_2 are the lengths of the left and the right sides of the ratchet and E is the barrier height. The temperatures of hot and cold reservoirs are T_H and T_C respectively. The power output of this engine [128] is given as

$$\dot{W} = \frac{k_B T_H x}{t}\left(e^{-(\epsilon + x\mu)} - e^{-(\epsilon - x + x\mu)/\theta}\right), \tag{5.35}$$

where $x = fL/k_B T_H$ (dimensionless load), $\mu = L_1/L$, $\theta = T_C/T_H$, $L = L_1 + L_2$ and $\epsilon = E/k_B T_H$ (dimensionless barrier height). Here 't' is a constant with dimensions of time. We maximize the power output with respect to the barrier height and the

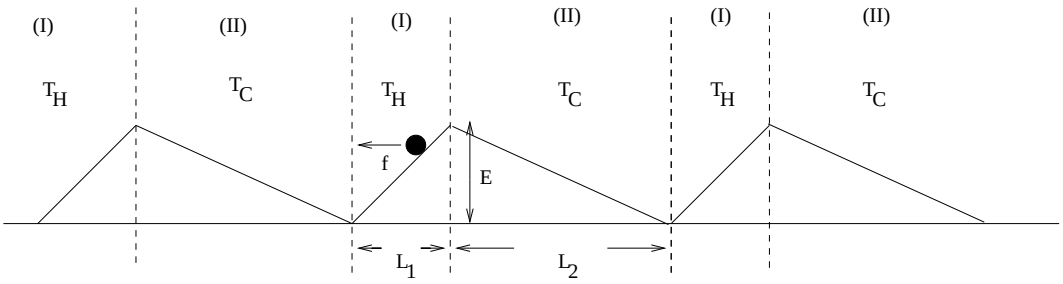

Figure 5.4: A Brownian particle in a periodic and asymmetric potential.

load by taking

$$\frac{\partial \dot{W}}{\partial \epsilon} = 0 \qquad \text{and} \qquad \frac{\partial \dot{W}}{\partial x} = 0. \tag{5.36}$$

Solving the above equations we get,

$$x = \eta_c, \tag{5.37}$$

$$\epsilon = 1 - \frac{(1-\eta_c)\ln(1-\eta_c)}{\eta_c} - \mu\eta_c. \tag{5.38}$$

The efficiency of the engine at maximum power is given as

$$\eta^* = \frac{2\eta_c^2}{3 - 2(1-\eta_c)(1+\ln(1-\eta_c)) - (1-\eta_c)^2}. \tag{5.39}$$

The near-equilibrium expansion ($\eta_c \approx 0$) of this efficiency is

$$\eta^* \approx \frac{\eta_c}{3} + \frac{\eta_c^2}{9} + \frac{\eta_c^3}{18} + O[\eta_c^4]. \tag{5.40}$$

5.4.2 Efficiency of a quantum heat engine from Bayesian statistics

Now we take a specific example discussed in the previous chapter. When a_1 and a_2 are unknown, we derived the prior for these parameters based on some simple assumptions as

$$\Pi(a_1, a_2) = \frac{K}{a_1 a_2}, \tag{5.41}$$

where $K = [\ln(1/\theta) \ln(a_{\max}/a_{\min})]^{-1}$ Using this prior, we derived the efficiency at which the engine is expected to operate for a given θ as shown in Eq. (4.44). The above expression is a function only of the ratio of the reservoir temperatures. The near equilibrium expansion of this efficiency is

$$\eta \approx \frac{\eta_c}{3} + \frac{\eta_c^2}{9} + \frac{8\eta_c^3}{135} + O[\eta_c^4]. \tag{5.42}$$

Again, the leading term is one-third of Carnot efficiency. It is interesting to note that the same efficiency is also obtained in a classical model, where the intermediate temperature is an uncertain quantity [113]. Surprisingly, the efficiencies given in Eqs. (5.40) and (5.42) agree up to the second order. These efficiencies are plotted in Fig. 5.5.

Obviously, the above efficiency does not belong to the universality class of efficiency as we discussed in the case of CA efficiency, where the leading term is $\eta_c/2$. So we point out the possibility of a new universality class of the efficiency where the first order term in the near equilibrium expansion is one-third of η_c.

5.5 Efficiency at maximum work when one of the energy scales is given

Here we consider a model of heat engine which extracts work as described in Section 4.2. In this set up, the value of either a_1 or a_2 is given and the other parameter is uncertain. So our task is to derive a suitable prior for the uncertain parameter

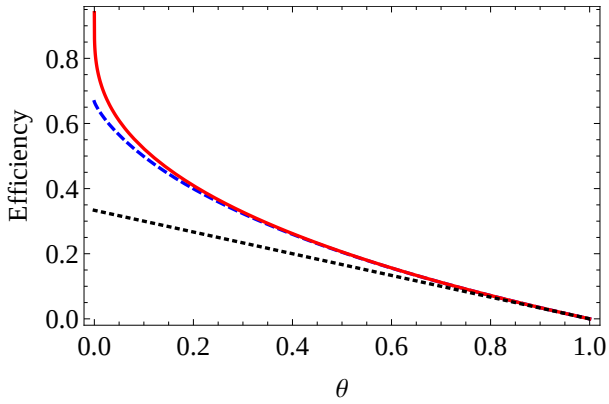

Figure 5.5: The efficiency in Eqs. (4.44) and (5.39) are plotted versus θ. The dashed curve is the efficiency at maximum power for the Brownian heat engine. The upper curve is the efficiency obtained in the asymptotic limit of the quantum model when two intrinsic energy scales of the working medium are uncertain. The dotted line corresponds to $(1-\theta)/3$.

and estimate the expected performance of the engine. Then we discuss expected efficiency at maximum work and its near equilibrium expansion.

5.5.1 Choice of prior

In this model, we consider that one of the energy scales of the working medium, say a_1 is given. Since our system is working as an engine, the immediate question is: What would be the prior distribution for a_2, which can vary only in the range $[a_1\theta, a_1]$? When there is no uncertainty in the energy scales, the efficiency is given by $\eta = 1 - a_2/a_1$. Suppose π is an arbitrary normalized distribution function and $\tilde{a}_2 = a_2/T_2$, then we demand that

$$\pi(\tilde{a}_2)d\tilde{a}_2 = \pi(\nu)d\nu, \tag{5.43}$$

where $\nu = 1 - \eta$. Substituting $\tilde{a}_2 = \nu a_1/T_2$, we get the form of π as $\pi(\nu) \propto 1/\nu$. The condition for the positive work done by the engine defines the range of the parameter ν as $[\theta, 1]$. Alternately we can consider the next case where a_2 is given instead of a_1. As in the previous case, for an arbitrary distribution function π', we demand

$$\pi'(\tilde{a}_1)d\tilde{a}_1 = \pi'(\nu)d\nu, \tag{5.44}$$

where $\tilde{a}_1 = a_1/T_1$. Substituting $\tilde{a}_1 = a_2/T_1\nu$, we get

$$\pi'\left(\frac{a_2}{T_1\nu}\right)\frac{a_2}{T_1\nu^2} = \pi'(\nu). \tag{5.45}$$

So the form of our distribution function is $\pi'(\nu) \propto 1/\nu$ where ν has the range $[\theta, 1]$. With the prior for the unknown quantity, we can find the expected behavior of the system. But here we are interested in the optimum behavior of the system, i.e. when the expected work is maximum for given information.

5.5.2 Expected maximum work for given a_1

As we discussed in the last chapter, the work extracted from the quantum model of heat engine is given as

$$W(a_1, \nu) = a_1(1-\nu)\left[\frac{1}{(1+e^{a_1/T_1})} - \frac{1}{(1+e^{a_1\nu/T_2})}\right]. \tag{5.46}$$

We have the expression for expected work

$$\overline{W} = \frac{a_1}{\ln(1/\theta)}\int_\theta^1 \frac{(1-\nu)}{\nu}\left(\frac{1}{(1+e^{a_1/T_1})} - \frac{1}{(1+e^{a_1\nu/T_1\theta})}\right)d\nu. \tag{5.47}$$

Similarly the expected heat absorbed by the system is

$$\overline{Q} = \frac{a_1}{\ln(1/\theta)}\int_\theta^1 \frac{1}{\nu}\left(\frac{1}{(1+e^{a_1/T_1})} - \frac{1}{(1+e^{a_1\nu/T_1\theta})}\right)d\nu. \tag{5.48}$$

Now we maximize the expected work with respect to a_1. Setting $\partial\overline{W}/\partial a_1 = 0$, we get

$$\frac{a_1 e^{a_1/T_1}[1-\theta+\ln(\theta)]}{T_1(1+e^{a_1/T_1})^2} - \frac{\ln\theta}{(1+e^{a_1/T_1})} = \int_\theta^1 \frac{d\nu}{\nu(1+e^{a_1\nu/T_1\theta})}. \tag{5.49}$$

The integral in the right hand side is not solvable. Let us take $x = a_1/T_1$ and $\theta = (1-\eta_c)$. So Eq. (5.49) takes the form

$$\frac{xe^x[\eta_c + \ln(1-\eta_c)]}{(1+e^x)^2} - \frac{\ln(1-\eta_c)}{(1+e^x)} = \int_{(1-\eta_c)}^1 \frac{d\nu}{\nu(1+e^{x\nu/(1-\eta_c)})}. \tag{5.50}$$

This integral appears in the expression of work shown in Eq. (5.47). Substituting the condition (Eq. 5.50) in Eq. (5.47), we get the expression for expected maximum work as

$$\begin{aligned}\overline{W}_{max} &= \frac{T_1 x}{\ln\left(\frac{1}{(1-\eta_c)}\right)}\left[\frac{e^x}{(1+e^x)}\eta_c\right] \\ &+ \frac{T_1 x}{\ln\left(\frac{1}{(1-\eta_c)}\right)}\left[\ln\left[\frac{1+e^x}{1+e^{\frac{x}{(1-\eta_c)}}}\right]\frac{(1-\eta_c)}{x} - \frac{xe^x(\eta_c+\ln(1-\eta_c))}{(1+e^x)^2}\right].\end{aligned} \tag{5.51}$$

In general, the value of x depends on θ and it has to be found out using the condition given in Eq.(5.50). Similarly the heat absorbed from hot bath in the case of expected maximum work is given as

$$\overline{Q} = \frac{T_1 x}{\ln\left(\frac{1}{(1-\eta_c)}\right)}\left[-\frac{xe^x(\eta_c + \ln(1-\eta_c))}{(1+e^x)^2}\right]. \tag{5.52}$$

So the efficiency at expected maximum work is given as

$$\overline{\eta}_1 = \frac{\overline{W}_{max}}{\overline{Q}} = 1 - \frac{\left(\frac{1+e^x}{x}\right)\eta_c + \left(\frac{(1+e^x)^2}{e^x x^2}\right)\ln\left[\frac{1+e^x}{1+e^{\frac{x}{(1-\eta_c)}}}\right](1-\eta_c)}{\ln(1-\eta_c)+\eta_c}. \tag{5.53}$$

5.5.3 Efficiency in near-equilibrium limit

Now, we wish to estimate the efficiency at maximum expected work near equilibrium regime ($\theta \approx 1$ or $\eta_c \approx 0$). So, we need to calculate the value of x in this limit. Hence, we expand both sides of Eq. (5.50), up to the third order, using the following series

$$\ln(1-\eta_c) = -\eta_c - \frac{\eta_c^2}{2} - \frac{\eta_c^3}{3} + O[\eta_c^4], \tag{5.54}$$

and

$$\begin{aligned}\int_{(1-\eta_c)}^{1} \frac{d\nu}{\nu(1+e^{x\nu/(1-\eta_c)})} &= \frac{\eta_c}{1+e^x} + \left[\frac{1}{1+e^x} - \frac{xe^x}{(1+e^x)^2}\right]\frac{\eta_c^2}{2} + \\ &\left[\frac{e^{2x}(x^2-4x+2) - e^x(x^2+4x-4)+2}{(1+e^x)^3}\right]\frac{\eta_c^3}{6} \\ &+O[\eta_c]^4. \end{aligned} \tag{5.55}$$

Substituting Eqs. (5.54) and (5.55) in Eq.(5.50), we get

$$\frac{x}{2}\tanh\left[\frac{x}{2}\right] = 1. \tag{5.56}$$

Now we analyze the efficiency in this limit. Expanding the efficiency given in Eq. (5.53) upto the second order, we get

$$\begin{aligned}\overline{\eta}_1 &= \frac{1}{3}\left(-1 + x\tanh\left[\frac{x}{2}\right]\right)\eta_c \\ &+ \left(\frac{4}{9}x\tanh\left[\frac{x}{2}\right] - \frac{x^2(\cosh x - 2)}{12(\cosh x + 1)} - \frac{5}{18}\right)\eta_c^2 + O[\eta_c^3]\end{aligned} \tag{5.57}$$

Substituting Eq. (5.56) in the above equation and restricting to first order of η_c, we get

$$\overline{\eta}_1 \approx \frac{\eta_c}{3} + \left(\frac{11}{18} - \frac{x^2(\cosh x - 2)}{12(\cosh x + 1)}\right)\eta_c^2 + O[\eta_c^3]. \tag{5.58}$$

So this presents a situation where the leading term of the efficiency in the near equilibrium expansion is one-third of Carnot value. Now consider the second situation, where a_2 is specified. This case is treated in detail in Appendix B.1. In this case, a_1 is uncertain in the range $[a_2, a_2/\theta]$. Following the same procedure as above, the efficiency at expected maximum work is given in Eq. B.6. The near equilibrium expansion of this efficiency is given as

$$\begin{aligned} \overline{\eta}_2 &= \frac{1}{3}\left(-1 + x\tanh\left[\frac{x}{2}\right]\right)\eta_c \\ &\quad + \left(\frac{1}{9}x\tanh\left[\frac{x}{2}\right] - \frac{x^2(\cosh x + 2)}{36(\cosh x + 1)} - \frac{1}{6}\right)\eta_c^2 + O[\eta_c^3]. \end{aligned} \tag{5.59}$$

Substituting the transcendental equation for x, we get

$$\overline{\eta}_2 \approx \frac{\eta_c}{3} + \left(\frac{1}{18} - \frac{x^2(\cosh x + 2)}{36(\cosh x + 1)}\right)\eta_c^2 + O[\eta_c^3]. \tag{5.60}$$

We have estimated the efficiencies in two different cases. According to Laplace's principle of insufficient reason, to infer from two different hypotheses, equal weights can be given to both the hypotheses, if one is not preferred over the other [79]. Here both a_1 and a_2 are energy scales and we are interested in the near equilibrium regime. So it seems reasonable to define the mean efficiency as $\overline{\eta} = (\overline{\eta}_1 + \overline{\eta}_2)/2$ [14, 15]. From Eqs. (5.56), (5.60) and (5.58), we get

$$\overline{\eta} = \frac{1}{3}\eta_c + \frac{1}{9}\eta_c^2 + O[\eta_c^3]. \tag{5.61}$$

Interestingly, the two leading terms also appear in the expansion of the efficiency when both a_1 and a_2 are unknown as shown in Eq.(5.42). The above mentioned approach with uniform prior is analyzed in Appendix B.2.

5.5.4 Numerical results

The efficiency obtained in Section 5.5.2 belongs to a different class, where the leading term is one third of Carnot efficiency in the near equilibrium expansion. In order to understand the behavior of this efficiency away from equilibrium, we numerically simulate the efficiency at maximum expected work for different values θ ($T_1 = 1$). In Fig. 5.6, we plot the efficiency at maximum expected work for given a_1 or a_2 and the mean of the two efficiencies. Further, in Fig. 5.7, we compare the behavior of this mean efficiency with some other known efficiencies whose leading term in the

near equilibrium expansion is one third of Carnot efficiency such as the efficiency of a quantum model discussed in Section 5.4.2 and the efficiency at optimum power of a Brownian heat engine discussed in Section 5.4.1.

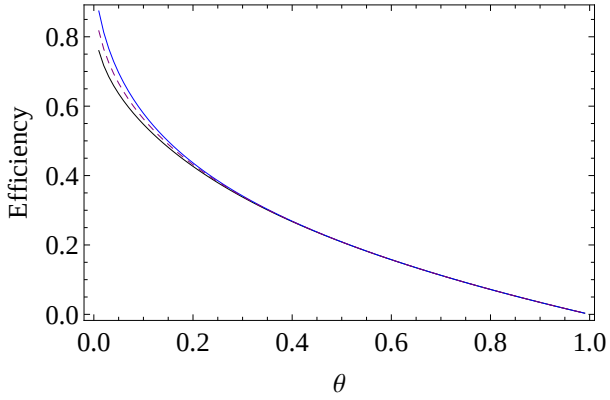

Figure 5.6: The top curve shows the efficiency at maximum work when a_2 is given. The lower curve corresponds to the efficiency at maximum work when a_1 is specified. The middle dashed curve indicates the arithmatic mean of the above mentioned efficiencies.

5.6 Expected performance of Feynman's ratchet when ϵ_1 or ϵ_2 is given

Similar to the quantum model discussed in Section 5.5, one can consider a case of Feynman's ratchet as a heat engine where either ϵ_1 or ϵ_2 is given a *priori*. Suppose ϵ_2 is specified, then the allowed range of ϵ_1 is $[\epsilon_2, \epsilon_2/\theta]$. Here, for simplicity, we assign a uniform distribution $\theta/\epsilon_2(1-\theta)$ for the uncertain parameter. So, the expected power is calculated by averaging the power (Eq. (5.10)) over the prior distribution as

$$\begin{aligned}
\overline{P}_2 &= \frac{\theta}{\epsilon_2(1-\theta)} \int_{\epsilon_2}^{\epsilon_2/\theta} P d\epsilon_1 \\
&= -\frac{r_0 e^{-\epsilon_2/T_1\theta}}{2\epsilon_2\theta\,(1-\theta)} \left(\epsilon_2^2(1-\theta)^2 + 2\epsilon_2 T_1(1-\theta)\theta + 2T_1^2\theta^2\right) \\
&\quad + \frac{r_0 e^{-\epsilon_2/T_1} T_1^2\theta}{\epsilon_2\,(1-\theta)}.
\end{aligned} \tag{5.62}$$

We maximize this power with respect to ϵ_2, by putting the derivative of $\overline{P}_2$ with respect to ϵ_2 as zero. Since we are interested near equilibrium performance, restricting

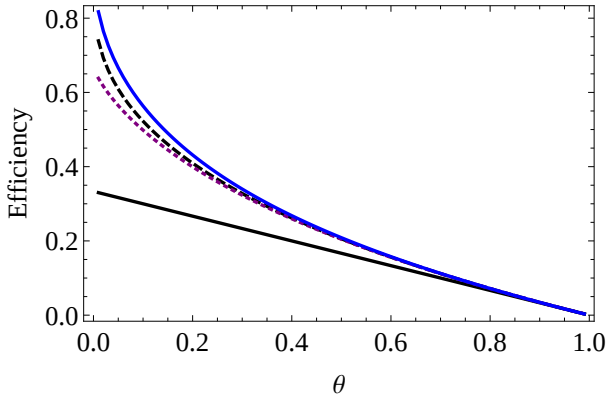

Figure 5.7: The top normal curve shows the mean efficiency ($\overline{\eta}$) estimated for the quantum model. The dashed curve corresponds to the efficiency of the engine when a_1 and a_2 are unknown as given in Eq. (4.44). The dotted curve indicates the efficiency at maximum power of a Brownian heat engine, (see Eq. (5.39)). The lower line shows the one third of Carnot value which is the first order term of all the above mentioned efficiencies near equilibrium.

the derivative upto second order, we get

$$\frac{\partial \overline{P}_2}{\partial \epsilon_2} \approx r_0 \epsilon_2 e^{-\epsilon_2/T_1} \frac{(2T_1 - \epsilon_2)(1-\theta)^2}{6T_1^2} + O[1-\theta]^3. \tag{5.63}$$

Equating the derivative to zero, we get the solution near equilibrium as $\epsilon_2 = 2T_1$. The expected heat absorbed in Δt from hot bath is

$$\begin{aligned} \overline{Q}_h &= \frac{r_0 e^{-\epsilon_2/T_1\theta}}{2\epsilon_2\theta\,(1-\theta)} \Big((\theta^2-1) - 2T_1\theta(T_1\theta+\epsilon_2)\Big)\,\Delta t \\ &\quad + \frac{r_0 e^{-\epsilon_2/T_1} T_1\theta(\epsilon_2+T_1)}{\epsilon_2\,(1-\theta)}\Delta t. \end{aligned} \tag{5.64}$$

Now we define the efficiency as $\overline{\eta}_2 = \overline{W}/\overline{Q}_h$, where $\overline{W} = \overline{P}_2\Delta t$. From Eqs. (5.62, 5.64) and substituting the value, $\epsilon_2 = 2T_1$, we get the efficiency as

$$\overline{\eta}_2 = \frac{\theta^2 e^{2(1-\theta)/\theta} + \theta(2-\theta) - 2}{3\theta^2 e^{2(1-\theta)/\theta} - \theta(2-\theta) - 2}. \tag{5.65}$$

Expanding this efficiency in terms of $\eta_c = 1-\theta$ near equilibrium, we get

$$\overline{\eta}_2 = \frac{1}{3}\eta_c + \frac{1}{6}\eta_c^2 + O[\eta_c^3]. \tag{5.66}$$

In a similar way, one can consider the second case where ϵ_1 is given and ϵ_2 is uncertain in the range $[\epsilon_1\theta, \epsilon_1]$. Following the above procedure, we get the efficiency in the

second case as

$$\overline{\eta}_1 = \frac{e^{2(1-\theta)/\theta}\left[\theta(6-5\theta)-2\right]+\theta^2}{e^{2(1-\theta)/\theta}\left(6\theta-4\right)-2\theta}. \tag{5.67}$$

Near equilibrium expansion of this efficiency is given as

$$\overline{\eta}_1 = \frac{1}{3}\eta_c + \frac{1}{18}\eta_c^2 + O[\eta_c^3]. \tag{5.68}$$

Considering both the inferences with the same preference as argued in Subsection 5.5.3, we assign equal weight to both the inferences to estimate the mean efficiency as $\overline{\eta} = (\overline{\eta}_1 + \overline{\eta}_2)/2$ [14, 15].

$$\overline{\eta} \;\; = \;\; \frac{1}{3}\eta_c + \frac{1}{9}\eta_c^2 + O[\eta_c^3]. \tag{5.69}$$

The two leading terms also appear in the expansion of the efficiency of a Brownian heat engine and a quantum model as shown in Eqs. (5.40) and (5.42), respectively.

5.7 Conclusion

In this chapter, we analyzed different efficiencies obtained from prior based estimation and compared it with the efficiencies obtained from the optimal performances of real heat engines. We mainly point out two classes of efficiencies, in the first category, the leading term in the near equilibrium expansion of the efficiency is $\eta_c/2$ and in the second category, the leading term is $\eta_c/3$.

The expression for the expected work of a quantum heat engine when efficiency is specified with one uncertain parameter (one of the energy scales) is identified similar to the expression for the work obtained from a classical Otto cycle. Hence the efficiency at expected maximum work of the quantum heat engine is the CA efficiency [69]. With Bayesian approach, the estimated efficiency at maximum expected work of a Feynman's ratchet as a heat engine is found to be CA efficiency. Surprisingly, the coefficient of performance of Feynman ratchet as a refrigerator is also identified as the corresponding CA value for the refrigerator.

The leading term in the expansion of the efficiency of quantum model with two uncertain parameters is found to be $\eta_c/3$. The expression of this efficiency is identical to the efficiency of a classical model with one uncertain parameter [113]. Another interesting fact is that this efficiency agrees with the efficiency at the maximum

power of a Brownian heat engine up to the second order in near-equilibrium expansion. Further we estimated the performance of the heat engine when one of the energy scales, either a_1 or a_2 is specified. In this case, we proved that the leading term in the near-equilibrium expansion of the efficiency at maximum expected work is one-third of Carnot value. Finally, we estimate the mean efficiency from two different inferences, where in the first case a_1 is given and in the second case a_2 is specified. We also show that when one of the energy scales is specified, the efficiency at expected maximum power of a Feynman's ratchet yields $\eta_c/3$ near equilibrium.

To summarize, the efficiencies obtained through Bayesian approach to uncertain parameter are categorized mainly into two classes. Further we compared these efficiencies with the performance of certain finite-time models of heat engines. This similarity in the efficiencies obtained by two different methods, is striking. The deeper connection between the two approaches needs to be investigated further.

Chapter 6

Conclusions and future directions

The main motivation of this thesis is to understand the thermodynamic properties of quantum systems through quantum heat cycles in particular the quantum Otto cycle. Our study was carried out mainly in three parts. In the first part, two spin-half systems coupled via isotropic Heisenberg interaction is studied as a model of quantum working medium and the performance of Otto cycle is analyzed. In the second part, we analyse the effect of finite-time driving in the adiabatic branches of the cycle, with particular focus on the phenomenon of intrinsic friction. In the third part of the thesis, a different model of quantum Otto engine is considered with uncertain internal energy scales. We address the following question: How can the expected performance of this engine be deduced from the prior information? Thereby, we propose an interesting connection between incomplete information and thermodynamics.

In Chapters 2 and 3, we modeled a quantum Otto cycle where the working medium consists of two spin-1/2 systems with isotropic Heisenberg Hamiltonian. We showed that this engine can outperform an uncoupled model in terms of the efficiency. The work obtained from the engine is shown to be the sum of the local work done by the individual spins. The local behavior of the spins is studied through the reduced density matrix. We have calculated the local effective temperature and shown the criterion for the total system to work as an engine in terms of magnetic field strength and local effective temperatures. We made a significant observation that for a suitable choice of parameters, heat can flow locally from cold bath to hot bath while the total system work as an engine. By analyzing the energy levels and

how the energy level spacings of the system changes during the adiabatic process, we derive an upper bound for the efficiency that the system can attain. This upper bound is shown to be tighter than Carnot bound and consistency with classical thermodynamics is established.

Instead of changing the magnetic field of the total system during the adiabatic process as discussed above, we consider a situation in which only the magnetic field applied on one of the spins is varied. Interestingly, we observed that as the speed of driving increases, the work obtained from the system decreases. This phenomenon is identified as quantum analogue of internal friction which arises due to non-commutativity of the Hamiltonian at different times. This frictional effect is quantified by the increase in energy-entropy. Analytical expression for work in a slow process where the system follows quantum adiabatic theorem, is calculated. At the other extreme, work obtained from a sudden process is also derived. These upper and lower bounds are compared with the work extracted when the engine is driven at a finite speed. We considered a special situation where the magnetic fields associated with both the systems are changed in such way that the difference of the magnetic fields applied on both the spins remain constant. This example shows that non-commutativity of the external and the internal Hamiltonian may not always lead to non-commutativity of the Hamiltonian at different times and thereby friction is absent in this case.

Chapters 4 and 5 of the thesis are devoted to the application of Bayesian reasoning in a model of quantum Otto cycle. Here we consider a two-staged heat engine. But the energy level spacings of the two level systems which constitute the working medium are unknown. With the available information, we derived the form of the prior under certain simplified assumptions. Further this prior is used to estimate the expected behavior of the engine. Then we considered a limiting case, where the minimum value of the energy level spacing is much less than temperature of the cold reservoir and the maximum possible value is much higher than the temperature of the hotter reservoir. In this asymptotic limit, the expected mean energy is found to be proportional to the temperature of the system. The proportionality constant is identified as the expected heat capacity which is also independent of temperature. This behavior is analogous to the behavior of a perfect gas. As a special case, we

also considered a situation where the efficiency of the engine is given a priori. This reduces the problem from two uncertain parameters to one. The form of the prior is similar to the earlier (two parameters) case. Further in the asymptotic limit, the efficiency at the maximum work approaches the CA efficiency. Our analysis shows that when the prior information is quantified as a suitable prior probability distribution, then the expected performance of the system shows classical thermodynamic behavior.

Further we show two different classes of efficiency obtained from the Bayesian approach to uncertain parameters present in different models of heat engines. We showed that, when the efficiency of a quantum heat engine is given a priori, i.e. the system with one unknown parameter, the efficiency at the maximum work is CA efficiency as in a classical heat engine with no uncertain parameter. We have also considered Feynman's ratchet both as a heat engine and a refrigerator. For heat engine, the power (χ-criterion for heat engine) and for the refrigerator, the product of COP and cooling rate (χ-criterion for refrigerator) are optimized. Based on the Bayesian analysis, for both the cases, we obtained the corresponding CA value.

When both the energy scales of the quantum model are unknown, we define the expected efficiency as the ratio of expected work to the expected heat absorbed by the system. This efficiency in near-equilibrium limit approaches one third of Carnot efficiency. A similar behavior of the efficiency is observed in a Brownian heat engine operating at maximum power. Here the power is maximized with the load and the energy barrier height. Surprisingly, the agreement of these two efficiencies is up to the the second order in the near-equilibrium expansion. Furthermore we consider a case in which one of the energy scales is given. We also show under certain prior information, the efficiency of the Feynman's ratchet near equilibrium approaches one-third of Carnot value.

In the first part of the thesis, two coupled spins via isotropic Heisenberg interaction is studied as heat engine. This can be generalized to arbitrary number of spins and for different interaction models. In the friction model, the possibility of quantum lubrication [42] can be investigated. Moreover physical realization of these models is a very interesting prospect. Ion trap [101], cavity QED [107, 108, 38] and NMR [87] are potential scenarios to physically realize the quantum heat engines. We have

seen that when the prior information is quantified as prior probability distribution in a systematic manner, quantum heat engine shows certain classical thermodynamic features. How much one can learn about a system with the given incomplete information is an interesting but subtle question. The approach has to be further explored to understand this connection between information and thermodynamics as shown here using quantum heat engines.

Appendix A

Coupled quantum Otto cycle

A.1 Heisenberg spin chain as working medium

This is a program to find the work, heat exchanged and efficiency of an Otto cycle in which the working medium is n-spin, 1D Heisenberg chain. Depending upon the values assigned to J_x, J_y and J_z, both isotropic and anisotropic models can be simulated. In the first part, density matrix is taken to be unchanged during the driving. We also discuss a general case where inhomogeneous magnetic field can also be assigned. If inhomogeneous magnetic field is considered during the driving, then frictional effect is observed in the adiabatic branch. So one has to use the subroutine given in Section A.2 to find the density matrix at the end of the adiabatic branch.

A.1.1 Mathematica code

Lists, Z_1 and Z_2 consist the values of magnetic fields associated with individual systems, when it is attached to hot bath and cold bath respectively.

$$\begin{aligned} J_x &= J_1; J_y = J_2; J_z = J_3; \\ Z_1 &= \text{List}[B_1, B_2, B_3, B_4, ...] \\ Z_2 &= \text{List}[B_1', B_2', B_3', B_4', ...] \\ T_h &= \text{Hot bath temperature} \\ T_c &= \text{Cold bath Temperature} \\ n &= \text{Number of particles} \end{aligned}$$

The Pauli matrices:

$$\begin{aligned}\sigma_x &= \{\{0,1\},\{1,0\}\}\\ \sigma_y &= \{\{0,-I\},\{I,0\}\}\\ \sigma_z &= \{\{1,0\},\{0,-1\}\}\end{aligned}$$

Setting the initial values:

$$\begin{aligned}S &= \text{IdentityMatrix}[2^n] - \text{IdentityMatrix}[2^n]\\ S_1 &= S; S_2 = S; L_5 = S; L_5' = S\end{aligned}$$

To calculate $\sum_i J_x(\sigma_x^i.\sigma_x^{(i+1)})$ for the chain:

$$\begin{aligned}i &= 1;\\ \text{While} &\quad [i \leq n-1,\\ &\quad H = \text{KroneckerProduct}[J_x, \text{IdentityMatrix}[2^{(i-1)}], \sigma_x,\\ &\quad \text{IdentityMatrix}[2^{(n-i)}]].\text{KroneckerProduct}[\text{IdentityMatrix}[2^i],\\ &\quad \sigma_x, \text{IdentityMatrix}[2^{n-(i+1)}]];\\ &\quad S = S + H; i++];\\ K &= \text{KroneckerProduct}[J_x, \text{IdentityMatrix}[2^{(n-1)}],\\ &\quad \sigma_x].\text{KroneckerProduct}[\sigma_x, \text{IdentityMatrix}[2^{(n-1)}]];\\ L &= S + K;\end{aligned}$$

To calculate $\sum_i J_y(\sigma_y^i.\sigma_y^{(i+1)})$ for the chain:

$$\begin{aligned}i &= 1;\\ \text{While} &\quad [i \leq n-1,\\ &\quad H_1 = \text{KroneckerProduct}[J_y, \text{IdentityMatrix}[2^{(i-1)}], \sigma_y,\\ &\quad \text{IdentityMatrix}[2^{(n-i)}]].\text{KroneckerProduct}[\text{IdentityMatrix}[2^i],\\ &\quad \sigma_y, \text{IdentityMatrix}[2^{n-(i+1)}]]; S_1 = S_1 + H_1; i++]\\ K_1 &= \text{KroneckerProduct}[J_y, \text{IdentityMatrix}[2^{(n-1)}],\\ &\quad \sigma_y].\text{KroneckerProduct}[\sigma_y, \text{IdentityMatrix}[2^{(n-1)}]];\\ L_1 &= S_1 + K_1;\end{aligned}$$

To calculate $\sum_i J_z(\sigma_z^i.\sigma_z^{(i+1)})$ for the chain:

$$\begin{aligned}
i &= 1; \\
\text{While} \quad & [i \leq n-1, \\
& H_2 = \text{KroneckerProduct}[J_z, \text{IdentityMatrix}[2^{(i-1)}], \sigma_z, \\
& \text{IdentityMatrix}[2^{(n-i)}]].\text{KroneckerProduct}[\text{IdentityMatrix}[2^i], \\
& \sigma_z, \text{IdentityMatrix}[2^{(n-i+1)}]]; S_2 = S_2 + H_2; i++] \\
K_2 &= \text{KroneckerProduct}[J_z, \text{IdentityMatrix}[2^{(n-1)}], \\
& \sigma_z].\text{KroneckerProduct}[\sigma_z, \text{IdentityMatrix}[2^{(n-1)}]]; \\
L_2 &= S_2 + K_2;
\end{aligned}$$

$$H_{\text{int}} = L + L_1 + L_2$$

To Calculate the external Hamiltonian, when the system is attached with hot bath:

$$\begin{aligned}
i &= 1; \\
\text{While} \quad & [i \leq n-1, \\
& L_4 = \text{KroneckerProduct}[\text{Part}[Z_1, i], \text{IdentityMatrix}[2^{(i-1)}], \sigma_z, \\
& \text{IdentityMatrix}[2^{(n-i)}]]; L_5 = L_5 + L_4; i++] \\
L_6 &= \text{KroneckerProduct}[\text{Part}[Z_1, n], \text{IdentityMatrix}[2^{(n-1)}], \sigma_z]; \\
H_{\text{ext}} &= L_5 + L_6;
\end{aligned}$$

The total Hamiltonian and the density matrix when the system is in equilibrium with hot bath:

$$\begin{aligned}
H_h &= H_{\text{int}} + H_{\text{ext}} \\
\rho_h &= \text{MatrixExp}[-H_h/T_h]/\text{Tr}[\text{MatrixExp}[-H_h/T_h]]
\end{aligned}$$

To Calculate the external Hamiltonian, when the system is attached with cold bath:

$$\begin{aligned}
i &= 1; \\
\text{While} \quad & [i \leq n-1, \\
& L_4' = \text{KroneckerProduct}[\text{Part}[Z_2, i], \text{IdentityMatrix}[2^{(i-1)}], \sigma_z, \\
& \text{IdentityMatrix}[2^{(n-i)}]]; L_5' = L_5' + L_4'; i++]; \\
L_6' &= \text{KroneckerProduct}[\text{Part}[Z_2, n], \text{IdentityMatrix}[2^{(n-1)}], \sigma_z]; \\
H_{\text{ext}}' &= L_5' + L_6';
\end{aligned}$$

Total Hamiltonian and the density matrix when the system is in equilibrium with cold bath:

$$\begin{aligned} H_c &= H'_{\text{ext}} + H_{\text{int}} \\ \rho_c &= \text{MatrixExp}[-H_c/T_c]/\text{Tr}[\text{MatrixExp}[-H_c/T_c]] \end{aligned}$$

Heat, work and efficiency of Otto cycle:

$$\begin{aligned} Q_c &= \text{Tr}[H.\rho_h] - \text{Tr}[H.\rho_c] \\ Q_h &= \text{Tr}[H'.\rho_c] - \text{Tr}[H'.\rho_h] \\ W &= Q_h + Q_c \\ \eta &= W/Q_c \end{aligned}$$

A.2 Friction in adiabatic branch

This program calculates the final density matrix at the end of an adiabatic branch. Consider H_h and ρ_h are functions of B_1, $B_2 ... B_n$. Let the jth spin is driven so that the magnetic field changes from b_j to b'_j in a time interval $\tau/2$ due to a time varying magnetic field, $B_j = (b_j + (b'_j - b_j)\text{Sin}[\pi t/\tau])$ applied over the spin. Here the integration of Liouville-von Neumann equation is carried out using fourth order Runge Kutta method.

$$\begin{aligned} H(t) &= H_h; \\ B_1 &= b_1; \\ B_2 &= b_2; \\ &\vdots \\ B_n &= b_n; \\ H_0 &= H_h; \\ \rho_0 &= \rho = \rho_h; \\ t &= 0; \\ h &= dt; \\ \text{While} &\quad [t \leq \tau/2, t' = t; B_j = (b_j + (b'_j - b_j)\text{Sin}[\pi t/\tau]); \end{aligned}$$

$$\rho_t = \rho;$$

$$k_1 = I(\rho.H(t) - H(t).\rho)dt;$$

$$t = t' + h/2;$$

$$\rho = \rho_t + k_1/2;$$

$$B_j = (b_j + (b'_j - b_j)\mathrm{Sin}[\pi t/\tau]);$$

$$k_2 = I(\rho.H(t) - H(t).\rho)dt;$$

$$t = t' + h/2;$$

$$\rho = \rho_t + k_2/2;$$

$$B_j = (b_j + (b'_j - b_j)\mathrm{Sin}[\pi t/\tau]);$$

$$k_3 = I(\rho.H(t) - H(t).\rho)dt;$$

$$t = t' + h;$$

$$\rho = \rho_t + k_3;$$

$$B_j = (b_j + (b'_j - b_j)\mathrm{Sin}[\pi t/\tau]);$$

$$k_4 = I(\rho.H(t) - H(t).\rho)dt;$$

$$\rho = \rho_t + (k_1 + 2 * k_2 + 2 * k_3 + k_4) * (1/6)];$$

The work done in the adiabatic branch is $\mathrm{Tr}[H_0.\rho_0] - \mathrm{Tr}[H(t).\rho]$. A similar program can be developed for the adiabatic branch followed by thermalization of the system with cold bath.

Appendix B

Expected performance at optimal work

B.1 Expected behavior when energy scale of the second spin is given

As discussed earlier Section 5.5.1, the choice of the suitable prior for this case comes out to be $\pi'(\nu) \propto 1/\nu$. The expected work is given as

$$\overline{W} = \frac{a_2}{\ln[1/(1-\eta_c)]} \int_{(1-\eta_c)}^{1} \frac{(1-\nu)}{\nu^2} \left(\frac{1}{1+e^{a_2(1-\eta_c)/T_2\nu}} - \frac{1}{1+e^{a_2/T_2}} \right) d\nu. \tag{B.1}$$

Maximizing the work with respect to a_2, we get the condition for the maximum expected work as

$$\frac{ye^y[\frac{\eta_c}{1-\eta_c} + \ln(1-\eta_c)]}{(1+e^y)^2} - \frac{\ln(1-\eta_c)}{(1+e^y)} = \int_{(1-\eta_c)}^{1} \frac{d\nu}{\nu(1+e^{y(1-\eta_c)/\nu})}, \tag{B.2}$$

where $y = a_2/T_2$. The expected maximum work is obtained by substituting Eq. (B.2) in Eq. (B.1), we get

$$\begin{aligned} \overline{W}_{max} &= \left[\frac{T_2 y}{(1-\eta_c)\ln(1/(1-\eta_c))} \right] \\ &\quad \left[\frac{\eta_c e^y}{(1+e^y)} + \left(\frac{1}{y}\right) \ln\left[\frac{1+e^{y(1-\eta_c)}}{1+e^y} \right] - \frac{ye^y(\eta_c + (1-\eta_c)\ln(1-\eta_c))}{(1+e^y)^2} \right]. \end{aligned} \tag{B.3}$$

Similarly, the expected heat absorbed by the system is

$$\overline{Q} = \frac{T_2 y}{\ln[1/(1-\eta_c)]} \int_{(1-\eta_c)}^{1} \frac{1}{\nu^2} \left(\frac{1}{1+e^{y(1-\eta_c)/\nu}} - \frac{1}{1+e^y} \right) d\nu. \tag{B.4}$$

Upon integrating we get

$$\overline{Q} = \left[\frac{T_2 y}{(1-\eta_c)\ln(1/(1-\eta_c))}\right]\left[\frac{\eta_c e^y}{(1+e^y)} + \left(\frac{1}{y}\right)\ln\left[\frac{1+e^{y(1-\eta_c)}}{1+e^y}\right]\right]. \tag{B.5}$$

The efficiency $\eta_2 = \overline{W}_{max}/\overline{Q}$, is given as

$$\overline{\eta}_2 = 1 - \frac{y e^y(\eta_c + (1-\eta_c)\ln(1-\eta_c)}{(1+e^y)^2\left(\frac{\eta_c e^y}{(1+e^y)} + \left(\frac{1}{y}\right)\ln\left[\frac{1+e^{y(1-\eta_c)}}{1+e^y}\right]\right)}. \tag{B.6}$$

In Eq. (B.2), the general solution for y depends on $(1-\eta_c)$. Expanding both sides of this equation upto the third order in near equilibrium, we get a transcendental equation $(y/2)\tanh(y/2) = 1$.

B.2 Expected maximum work with uniform prior

We derive the expression for expected maximum work with uniform prior distribution when a_1 is given. In this case, the expression for expected work is

$$\overline{W} = \frac{a_1}{(1-\theta)}\int_\theta^1 (1-\nu)\left(\frac{1}{1+e^{a_1/T_1}} - \frac{1}{1+e^{a_1\nu/T_1\theta}}\right)d\nu. \tag{B.7}$$

Now we maximize the work by setting $\partial\overline{W}/\partial a_1 = 0$, we get

$$\begin{aligned}
&\left(\frac{1}{(1+e^{a_1/T_1})} - \frac{a_1}{T_1}\frac{e^{a_1/T_1}}{(1+e^{a_1/T_1})^2}\right)\int_\theta^1 (1-\nu)d\nu \\
&- \int_\theta^1 (1-\nu)\left(\frac{1}{1+e^{a_1\nu/T_1\theta}}\right)d\nu \\
&+ \int_\theta^1 (\nu-\nu^2)\left(\frac{a_1\nu}{T_1\theta}\frac{e^{a_1/T_1\theta}}{(1+e^{a_1\nu/T_1\theta})^2}\right)d\nu = 0.
\end{aligned} \tag{B.8}$$

Further integrating some of the terms we can write

$$\begin{aligned}
-\int_\theta^1 \left(\frac{\nu}{1+e^{a_1\nu/T_1\theta}}\right)d\nu &= \left(\frac{1}{1+e^{a_1/T_1}} - \frac{a_1}{T_1}\frac{e^{a_1/T_1}}{(1+e^{a_1/T_1})^2}\right)\left(1-\theta-\frac{1-\theta^2}{2}\right) \\
&+ \left[\frac{2T_1\theta\nu}{a_1}\ln\left(1+e^{a_1\nu/T_1\theta}\right)\right]_{\nu=\theta}^{\nu=1} \\
&+ \left[\frac{2(T_1\theta)^2}{a_1^2}\text{polylog}[2,-e^{a_1\nu/T_1\theta)}]\right]_{\nu=\theta}^{\nu=1} \\
&+ \left[\frac{(\nu-1)\nu}{1+e^{a_1\nu/T_1\theta}} - \nu^2\right]_{\nu=\theta}^{\nu=1}.
\end{aligned} \tag{B.9}$$

But we know that

$$-2\int_{\theta}^{1}\left(\frac{\nu}{1+e^{a_1\nu/T_1\theta}}\right)d\nu = \left[-\nu^2+\frac{2T_1\theta\nu}{a_1}\ln\left(1+e^{a_1\nu/T_1\theta}\right)\right]_{\nu=\theta}^{\nu=1} + \left[\frac{2(T_1\theta)^2}{a_1^2}\text{polylog}[2,-e^{a_1\nu/T_1\theta}]\right]_{\nu=\theta}^{\nu=1}. \quad \text{(B.10)}$$

Substituting Eq. (B.10) in Eq. (B.9), we get the condition for maximum work as

$$\int_{\theta}^{1}\left(\frac{\nu}{1+e^{a_1\nu/T_1\theta}}\right)d\nu = \frac{(1-\theta^2)}{2(1+e^{a_1/T_1})} - \left(\frac{a_1}{T_1}\frac{e^{a_1/T_1}}{(1+e^{a_1/T_1})^2}\right)\left((1-\theta)-\frac{(1-\theta^2)}{2}\right). \quad \text{(B.11)}$$

Substituting $\eta_c = 1-\theta$ and $x = a_1/T_1$, we get

$$\int_{(1-\eta_c)}^{1}\left(\frac{\nu}{1+e^{x\nu/(1-\eta_c)}}\right)d\nu = \frac{(1-(1-\eta_c)^2)}{2(1+e^x)} - \left(\frac{e^x x}{(1+e^x)^2}\right)\left(\eta_c-\frac{(1-(1-\eta_c)^2)}{2}\right). \quad \text{(B.12)}$$

We are interested in the solution of this equation in the near equilibrium ($\eta_c \to 0$). Expanding the both sides to the third order of η_c we get

$$\frac{x}{2}\tanh\left(\frac{x}{2}\right) = 1. \quad \text{(B.13)}$$

Substituting Eq. (B.12) in Eq. (B.7), we get the expected maximum work when the uniform prior is used for quantifying the information. So the expression for work is

$$\overline{W}_{max} = \frac{T_1 x}{\eta_c}\left[\frac{-e^x\eta_c}{(1+e^x)}-\ln\left[\frac{1+e^x}{1+e^{\frac{x}{(1-\eta_c)}}}\right]\frac{(1-\eta_c)}{x}\right] - \frac{T_1 x}{\eta_c}\left[\left(\frac{e^x x}{(1+e^x)^2}\right)\left(\eta_c-\frac{(1-(1-\eta_c)^2)}{2}\right)\right]. \quad \text{(B.14)}$$

Similarly the expected value of heat absorbed at maximum expected work is given as

$$\overline{Q} = \frac{T_1 x}{\eta_c}\left[\frac{-e^x\eta_c}{(1+e^x)}-\ln\left[\frac{1+e^x}{1+e^{\frac{x}{(1-\eta_c)}}}\right]\frac{(1-\eta_c)}{x}\right]. \quad \text{(B.15)}$$

So the efficiency at maximum expected work is given as

$$\overline{\eta}_1 = 1+\frac{\left(\frac{e^x x}{(1+e^x)^2}\right)\left(\eta_c-\frac{(1-(1-\eta_c)^2)}{2}\right)}{\frac{e^x\eta_c}{(1+e^x)}+\ln\left[\frac{1+e^x}{1+e^{\frac{x}{(1-\eta_c)}}}\right]\frac{(1-\eta_c)}{x}}. \quad \text{(B.16)}$$

This efficiency can be expanded up to the third order of η_c and substituting the expression for x Eq. (B.13) in the near equilibrium limit, we get the first order term in the expansion as one third of Carnot efficiency.

Bibliography

[1] S. Abe and S. Okuyama. Similarity between quantum mechanics and thermodynamics: Entropy, temperature, and carnot cycle. *Phys. Rev. E*, 83:021121, Feb 2011.

[2] G. S. Agarwal. Brownian motion of a quantum oscillator. *Phys. Rev. A*, 4:739–747, Aug 1971.

[3] G. S. Agarwal and S. Chaturvedi. Quantum dynamical framework for Brownian heat engines. *Phys. Rev. E*, 88:012130, Jul 2013.

[4] B.-Q. Ai, L. Wang, and L.-G. Liu. Brownian micro-engines and refrigerators in a spatially periodic temperature field: Heat flow and performances. *Physics Letters A*, 352(4–5):286 – 290, 2006.

[5] E. Albayrak. Thermal entanglement in the anisotropic Heisenberg model with Dzyaloshinskii-Moriya interaction in an inhomogeneous magnetic field. *The European Physical Journal B*, 72:491, 2009.

[6] Y. Alhassid and R. D. Levine. Connection between the maximal entropy and the scattering theoretic analyses of collision processes. *Phys. Rev. A*, 18:89–116, Jul 1978.

[7] R. Alicki. The quantum open system as a model of the heat engine. *Journal of Physics A: Mathematical and General*, 12(5):L103, 1979.

[8] A. E. Allahverdyan, R. Balian, and T. M. Nieuwenhuizen. Quantum thermodynamics: Thermodynamics at the nanoscale. *J. Mod. Opt.*, 51:2703, 2004.

[9] A. E. Allahverdyan, K. Hovhannisyan, and G. Mahler. Optimal refrigerator. *Phys. Rev. E*, 81:051129, May 2010.

[10] A. E. Allahverdyan, R. S. Johal, and G. Mahler. Work extremum principle: Structure and function of quantum heat engines. *Phys. Rev. E*, 77:041118, Apr 2008.

[11] A. E. Allahverdyan and T. M. Nieuwenhuizen. Adiabatic processes need not correspond to optimal work. *Physica E: Low-dimensional Systems and Nanostructures*, 29(1–2):74 – 81, 2005. Frontiers of Quantum Proceedings of the International Conference Frontiers of Quantum and Mesoscopic Thermodynamics.

[12] A. E. Allahverdyan and T. M. Nieuwenhuizen. Minimal work principle: Proof and counterexamples. *Phys. Rev. E*, 71:046107, Apr 2005.

[13] B. Andresen, P. Salamon, and R. S. Berry. Thermodynamics in finite time: extremals for imperfect heat engines. *The Journal of Chemical Physics*, 66(4), 1977.

[14] P. Aneja and R. S. Johal. Prior information and inference of optimality in thermodynamic processes. *Journal of Physics A: Mathematical and Theoretical*, 46(36):365002, 2013.

[15] P. Aneja and R. S. Johal. On the form of prior for constrained thermodynamic processes with uncertainty. *arXiv:1404.0460 [cond-mat.stat-mech]*, Apr. 2014.

[16] M. Annis, W. Cheston, and H. Primakoff. On statistical estimation in physics. *Rev. Mod. Phys.*, 25:818–830, Oct 1953.

[17] M. C. Arnesen, S. Bose, and V. Vedral. Natural thermal and magnetic entanglement in the 1d Heisenberg model. *Phys. Rev. Lett.*, 87:017901, Jun 2001.

[18] M. Asoudeh and V. Karimipour. Thermal entanglement of spins in an inhomogeneous magnetic field. *Phys. Rev. A*, 71:022308, Feb 2005.

[19] R. D. Astumian and M. Bier. Fluctuation driven ratchets: Molecular motors. *Phys. Rev. Lett.*, 72:1766–1769, Mar 1994.

[20] A. C. Barato and U. Seifert. An autonomous and reversible Maxwell's demon. *EPL (Europhysics Letters)*, 101(6):60001, 2013.

[21] T. Bayes and R. Price. An Essay towards Solving a Problem in the Doctrine of Chance. by the late Rev. Mr. Bayes, communicated by Mr. Price, in a letter to John Canton, A. M. F. R. S. *Philosophical Transactions of the Royal Society of London*, 53:370–418, 1763.

[22] J. D. Bekenstein. Black holes and entropy. *Phys. Rev. D*, 7:2333–2346, Apr 1973.

[23] C. H. Bennett, H. J. Bernstein, S. Popescu, and B. Schumacher. Concentrating partial entanglement by local operations. *Phys. Rev. A*, 53:2046–2052, Apr 1996.

[24] C. H. Bennett, D. P. DiVincenzo, J. A. Smolin, and W. K. Wootters. Mixed-state entanglement and quantum error correction. *Phys. Rev. A*, 54:3824–3851, Nov 1996.

[25] R. Bhatia. *Matrix analysis*. Springer-Verlag, New York, 1997.

[26] J. a. P. S. Bizarro. Entropy production in irreversible processes with friction. *Phys. Rev. E*, 78:021137, Aug 2008.

[27] J. P. S. Bizarro. The thermodynamic efficiency of heat engines with friction. *American Journal of Physics*, 80(4), 2012.

[28] M. Born and V. Fock. Beweis des adiabatensatzes. *Z. Phys.*, 51:165, 1928.

[29] J.-P. Brantut, C. Grenier, J. Meineke, D. Stadler, S. Krinner, C. Kollath, T. Esslinger, and A. Georges. A thermoelectric heat engine with ultracold atoms. *Science*, 342(6159):713–715, 2013.

[30] H.-P. Breuer and F. Petruccione. *The Theory of Open Quantum Systems*. Oxford University Press, 2007.

[31] H. Buchdahl. *The Concepts of Classical Thermodynamics*. Cambridge Monographs on Physics. Cambridge University Press, 2009.

[32] M. Büttiker. Transport as a consequence of state-dependent diffusion. *Zeitschrift für Physik B Condensed Matter*, 68(2-3):161–167, 1987.

[33] H. B. Callen. *Thermodynamics and an Introduction to Thermostatistics, 2nd ed.* John Wiley, New York, 1985.

[34] C. M. Caves, C. A. Fuchs, and R. Schack. Quantum probabilities as Bayesian probabilities. *Phys. Rev. A*, 65:022305, Jan 2002.

[35] C. M. Caves, C. A. Fuchs, and R. Schack. Subjective probability and quantum certainty. *Studies in History and Philosophy of Science Part B: Studies in History and Philosophy of Modern Physics*, 38(2):255 – 274, 2007. Probabilities in quantum mechanics.

[36] F. L. Curzon and B. Ahlborn. Efficiency of a Carnot engine at maximum power output. *Am. J. Phys.*, 43:22, 1975.

[37] C. de Tomás, A. C. Hernández, and J. M. M. Roco. Optimal low symmetric dissipation Carnot engines and refrigerators. *Phys. Rev. E*, 85:010104, Jan 2012.

[38] R. Dillenschneider and E. Lutz. Energetics of quantum correlations. *EPL (Europhysics Letters)*, 88(5):50003, 2009.

[39] V. Dose. Bayesian inference in physics: case studies. *Reports on Progress in Physics*, 66(9):1421, 2003.

[40] M. Esposito, K. Lindenberg, and C. Van den Broeck. Universality of efficiency at maximum power. *Phys. Rev. Lett.*, 102:130602, Apr 2009.

[41] T. Feldmann and R. Kosloff. Quantum four-stroke heat engine: Thermodynamic observables in a model with intrinsic friction. *Phys. Rev. E*, 68:016101, Jul 2003.

[42] T. Feldmann and R. Kosloff. Quantum lubrication: Suppression of friction in a first-principles four-stroke heat engine. *Phys. Rev. E*, 73:025107, Feb 2006.

[43] E. Fermi. *Thermodynamics*. Dover books in physics and mathematical physics. Dover Publications, 1956.

[44] R. P. Feynman, R. B. Leighton, and M. Sands. *The Feynman Lectures on Physics*. Addison-Wesley, Reading, MA, 1966.

[45] A. Galindo and M. A. Martín-Delgado. Information and computation: Classical and quantum aspects. *Rev. Mod. Phys.*, 74:347–423, May 2002.

[46] A. García-Saez, A. Ferraro, and A. Acín. Local temperature in quantum thermal states. *Phys. Rev. A*, 79:052340, May 2009.

[47] J. Gemmer, M. Michel, and G. Mahler. *Quantum Thermodynamics*. Springer, Berlin, 2004.

[48] D. Giulio. Teaching statistics in the physics curriculum: Unifying and clarifying role of subjective probability. *Am. J. Phys.*, 67:1260, December 1999.

[49] S. Goldstein, J. L. Lebowitz, R. Tumulka, and N. Zanghì. Canonical typicality. *Phys. Rev. Lett.*, 96:050403, Feb 2006.

[50] V. Gorini, A. Kossakowski, and E. Sudarshan. Completely positive dynamical semigroups of n-level systems. *J. Math. Phys.*, 17:821, 1976.

[51] D. J. Griffiths. *Introduction to Quantum Mechanics*. Pearson Prentice Hall, 2005.

[52] M. Hartmann. Minimal length scales for the existence of local temperature. *Contemp. Phys.*, 47:89, 2006.

[53] G. N. Hatsopoulos and E. P. Gyftopoulos. A unified quantum theory of mechanics and thermodynamics. part IIa: Available energy. *Found. Phys.*, 6:127, 1976.

[54] D. Haynie. *Biological Thermodynamics*. Cambridge University Press, Cambridge, 2001.

[55] X. He, J. He, and J. Zheng. Thermal entangled quantum heat engine. *Physica A: Statistical Mechanics and its Applications*, 391(24):6594 – 6600, 2012.

[56] M. J. Henrich, M. Michel, and G. Mahler. Small quantum networks operating as quantum thermodynamic machines. *EPL (Europhysics Letters)*, 76(6):1057, 2006.

[57] J. M. Hofman and C. H. Wiggins. Bayesian approach to network modularity. *Phys. Rev. Lett.*, 100:258701, Jun 2008.

[58] M. Horodecki and J. Oppenheim. Fundamental limitations for quantum and nanoscale thermodynamics. *Nat. Commun.*, 4, Jun 2013.

[59] X. Hu, R. de Sousa, and S. Das Sarma. Interplay between zeeman coupling and swap action in spin-based quantum computer models: Error correction in inhomogeneous magnetic fields. *Phys. Rev. Lett.*, 86:918–921, Jan 2001.

[60] X. Huang, Y. Liu, Z. Wang, and X. Niu. Special coupled quantum otto cycles. *The European Physical Journal Plus*, 129(1):1–8, 2014.

[61] X. L. Huang, L. C. Wang, and X. X. Yi. Quantum Brayton cycle with coupled systems as working substance. *Phys. Rev. E*, 87:012144, Jan 2013.

[62] D. Hume. Enquiry concerning human understanding. *electronic version at http://www.iep.utm.edu/hume/*, 1748.

[63] C. Jarzynski and O. Mazonka. Feynman's ratchet and pawl: An exactly solvable model. *Phys. Rev. E*, 59:6448–6459, Jun 1999.

[64] E. Jaynes. Prior probabilities. *IEEE Trans. Syst. Sci. Cybernet.*, 4:227, 1968.

[65] E. T. Jaynes. Information theory and statistical mechanics. *Phys. Rev.*, 106:620–630, May 1957.

[66] E. T. Jaynes. Information theory and statistical mechanics. ii. *Phys. Rev.*, 108:171–190, Oct 1957.

[67] E. T. Jaynes and G. L. Bretthorst. *Probability Theory: The Logic of Science*. Cambridge University Press, 2003.

[68] H. Jeffreys. *Theory of Probability*. Clarendon Press, Oxford, 1939.

[69] R. S. Johal. Universal efficiency at optimal work with Bayesian statistics. *Phys. Rev. E*, 82:061113, Dec 2010.

[70] R. S. Johal, R. Rai, and G. Mahler. Reversible heat engines: Bounds on estimated efficiency from inference. Accepted for Foundations of Physics (2014). See also arXiv:1305.6278 [cond-mat.stat-mech].

[71] T. Kato. On the adiabatic theorem of quantum mechanics. *Journal of the Physical Society of Japan*, 5(6):435–439, 1950.

[72] J. Keeler. *Understanding NMR Spectroscopy*. Wiley, 2010.

[73] T. D. Kieu. The second law, Maxwell's demon, and work derivable from quantum heat engines. *Phys. Rev. Lett.*, 93:140403, Sep 2004.

[74] R. Kosloff. Quantum thermodynamics: A dynamical viewpoint. *Entropy*, 15(6):2100–2128, 2013.

[75] R. Kosloff and T. Feldmann. Discrete four-stroke quantum heat engine exploring the origin of friction. *Phys. Rev. E*, 65:055102, May 2002.

[76] R. Landauer. Irreversibility and heat generation in the computing process. *IBM J. Res. Dev.*, 5(3):183, 1961.

[77] R. Landauer. Motion out of noisy states. *Journal of Statistical Physics*, 53(1-2):233–248, 1988.

[78] P. T. Landsberg and H. S. Leff. Thermodynamic cycles with nearly universal maximum-work efficiencies. *Journal of Physics A: Mathematical and General*, 22(18):4019, 1989.

[79] P. S. Laplace. Memoir on the probability of the causes of events. *Statistical Science*, 1(3):364–378, 08 1986.

[80] H. Leff and A. F. Rex. *Maxwell's Demon 2: Entropy, Classical and Quantum Information, Computing*. Institute of Physics, Bristol, 2003.

[81] H. S. Leff. Thermal efficiency at maximum work output: New results for old heat engines. *Am. J. Phys.*, 55:602, 1987.

[82] M. S. Leifer and R. W. Spekkens. Towards a formulation of quantum theory as a causally neutral theory of Bayesian inference. *Phys. Rev. A*, 88:052130, Nov 2013.

[83] B. Lin and J. Chen. Performance characteristics and parametric optimum criteria of a brownian micro-refrigerator in a spatially periodic temperature field. *Journal of Physics A: Mathematical and Theoretical*, 42(7):075006, 2009.

[84] G. Lindblad. On the generators of quantum dynamical semigroups. *Comm. Math. Phys.*, 48:119, 1976.

[85] N. Linden, S. Popescu, A. J. Short, and A. Winter. Quantum mechanical evolution towards thermal equilibrium. *Phys. Rev. E*, 79:061103, Jun 2009.

[86] N. Linden, S. Popescu, and P. Skrzypczyk. How small can thermal machines be? The smallest possible refrigerator. *Phys. Rev. Lett.*, 105:130401, Sep 2010.

[87] S. Lloyd. Quantum-mechanical Maxwell's demon. *Phys. Rev. A*, 56:3374–3382, Nov 1997.

[88] X. G. Luo, N. Liu, and J. Z. He. Optimum analysis of a Brownian refrigerator. *Phys. Rev. E*, 87:022139, Feb 2013.

[89] K. Maruyama, F. Nori, and V. Vedral. *Colloquium* : The physics of Maxwell's demon and information. *Rev. Mod. Phys.*, 81:1–23, Jan 2009.

[90] M. Nielsen and I. Chuang. *Quantum Computation and Quantum Information*. Cambridge University Press, Cambridge, 2000.

[91] M. A. Nielsen. Conditions for a class of entanglement transformations. *Phys. Rev. Lett.*, 83:436–439, Jul 1999.

[92] M. Peskin and D. Schroeder. *An Introduction to Quantum Field Theory*. Westview Press, 1995.

[93] S. Popescu and D. Rohrlich. Thermodynamics and the measure of entanglement. *Phys. Rev. A*, 56:R3319–R3321, Nov 1997.

[94] S. Popescu, A. J. Short, and A. Winter. Entanglement and the foundations of statistical mechanics. *Nature Physics*, 2:754, 2006.

[95] H. T. Quan. Quantum thermodynamic cycles and quantum heat engines. II. *Phys. Rev. E*, 79:041129, Apr 2009.

[96] H. T. Quan, Y.-x. Liu, C. P. Sun, and F. Nori. Quantum thermodynamic cycles and quantum heat engines. *Phys. Rev. E*, 76:031105, Sep 2007.

[97] H. T. Quan, P. Zhang, and C. P. Sun. Quantum heat engine with multilevel quantum systems. *Phys. Rev. E*, 72:056110, Nov 2005.

[98] D. E. Raeside. A physicist's introduction to Bayesian statistics. *American Journal of Physics*, 40(5), 1972.

[99] Y. Rezek. Reflections on friction in quantum mechanics. *Entropy*, 12(8):1885–1901, 2010.

[100] C. Robert. *The Bayesian Choice: From Decision-Theoretic Foundations to Computational Implementation*. Springer Texts in Statistics. Springer, 2007.

[101] J. Roßnagel, O. Abah, F. Schmidt-Kaler, K. Singer, and E. Lutz. Nanoscale heat engine beyond the Carnot limit. *Phys. Rev. Lett.*, 112:030602, Jan 2014.

[102] T. Sagawa and M. Ueda. Minimal energy cost for thermodynamic information processing: Measurement and information erasure. *Phys. Rev. Lett.*, 102:250602, Jun 2009.

[103] J. J. Sakurai and S. F. Tuan. *Modern Quantum Mechanics*. Pearson Education, 1994.

[104] N. Sangouard, X. Lacour, S. Guérin, and H. R. Jauslin. Fast SWAP gate by adiabatic passage. *Phys. Rev. A*, 72:062309, Dec 2005.

[105] E. Schroedinger. *What Is Life?* Cambridge University Press, Cambridge, England, 1945.

[106] H. E. D. Scovil and E. O. Schulz-DuBois. Three-level masers as heat engines. *Phys. Rev. Lett.*, 2:262–263, Mar 1959.

[107] M. O. Scully. Extracting work from a single thermal bath via quantum negentropy. *Phys. Rev. Lett.*, 87:220601, Nov 2001.

[108] M. O. Scully, M. S. Zubairy, G. S. Agarwal, and H. Walther. Extracting work from a single heat bath via vanishing quantum coherence. *Science*, 299(5608):862–864, 2003.

[109] C. E. Shannon. A mathematical theory of communication. *Bell System Technical Journal*, 27:379, 1948.

[110] S. Sheng, P. Yang, and Z. C. Tu. Coefficient of performance at maximum χ-criterion for Feynman ratchet as a refrigerator. *Communications in Theoretical Physics*, 62(4):589, 2014.

[111] P. Skrzypczyk, A. J. Short, and S. Popescu. Work extraction and thermodynamics for individual quantum systems. *Nat. Commun.*, 5, Jun 2014.

[112] G. Thomas, P. Aneja, and R. S. Johal. Incomplete information and expected performance characteristics of heat engines. Research and Reviews : Journal of Statistics, special issue on recent statistical methodologies and applications (in press).

[113] G. Thomas, P. Aneja, and R. S. Johal. Informative priors and the analogy between quantum and classical heat engines. *Physica Scripta*, 2012(T151):014031, 2012.

[114] G. Thomas and R. S. Johal. Coupled quantum Otto cycle. *Phys. Rev. E*, 83:031135, Mar 2011.

[115] G. Thomas and R. S. Johal. Expected behavior of quantum thermodynamic machines with prior information. *Phys. Rev. E*, 85:041146, Apr 2012.

[116] G. Thomas and R. S. Johal. Estimating performance of Feynman's ratchet from limited information. *arXiv:1410.2140 [cond-mat.stat-mech]*, Oct. 2014.

[117] G. Thomas and R. S. Johal. Friction due to inhomogeneous driving of coupled spins in a quantum heat engine. *The European Physical Journal B*, 87(7), 2014.

[118] Z. C. Tu. Efficiency at maximum power of Feynman's ratchet as a heat engine. *Journal of Physics A: Mathematical and Theoretical*, 41(31):312003, 2008.

[119] Y. Ust, B. Sahin, and O. S. Sogut. Performance analysis and optimization of an irreversible dual-cycle based on an ecological coefficient of performance criterion. *Applied Energy*, 82(1):23 – 39, 2005.

[120] C. Van den Broeck. Thermodynamic efficiency at maximum power. *Phys. Rev. Lett.*, 95:190602, Nov 2005.

[121] S. Velasco, J. M. M. Roco, A. Medina, and A. C. Hernández. New performance bounds for a finite-time Carnot refrigerator. *Phys. Rev. Lett.*, 78:3241–3244, Apr 1997.

[122] D. Venturelli, R. Fazio, and V. Giovannetti. Minimal self-contained quantum refrigeration machine based on four quantum dots. *Phys. Rev. Lett.*, 110:256801, Jun 2013.

[123] H. Wang, S. Liu, and J. He. Thermal entanglement in two-atom cavity QED and the entangled quantum otto engine. *Phys. Rev. E*, 79:041113, Apr 2009.

[124] W. K. Wootters. Entanglement of formation of an arbitrary state of two qubits. *Phys. Rev. Lett.*, 80:2245–2248, Mar 1998.

[125] Z. Yan and J. Chen. A class of irreversible Carnot refrigeration cycles with a general heat transfer law. *Journal of Physics D: Applied Physics*, 23(2):136, 1990.

[126] G. F. Zhang. Entangled quantum heat engines based on two two-spin systems with Dzyaloshinski-Moriya anisotropic antisymmetric interaction. *Eur. Phys. J. D*, 49:123, 2008.

[127] T. Zhang, W.-T. Liu, P.-X. Chen, and C.-Z. Li. Four-level entangled quantum heat engines. *Phys. Rev. A*, 75:062102, Jun 2007.

[128] Y. Zhang, B. H. Lin, and J. C. Chen. Performance characteristics of an irreversible thermally driven Brownian microscopic heat engine. *Eur. Phys. J. B*, 53:481, 2006.